

# Rare $K$ decays

Jack L. Ritchie

University of Texas, Austin, Texas 78712

Stanley G. Wojcicki

Stanford University, Stanford, California 94305

This article reviews the current situation in the field of rare  $K$  decays: the relevant phenomenology, the present experimental situation, and prospects for the near future. Study of rare  $K$  decays can make a significant contribution in a number of different frontier areas of research in high-energy physics. In the area of  $CP$  violation, study of such rare decays as  $K_L^0 \rightarrow \pi^0 e^+ e^-$ ,  $K_L^0 \rightarrow \pi^0 \mu^+ \mu^-$ ,  $K_L^0 \rightarrow \pi^0 \nu \bar{\nu}$ , and muon polarization in  $K_L^0 \rightarrow \mu^+ \mu^-$  can provide important complementary information to what has been learned from the decay  $K_L^0 \rightarrow \pi \pi$ . Even though experiments with sufficient accuracy to make a meaningful study of  $CP$  violation are still a few years away, significant progress has been made in this general area during the last decade. A second major area of interest in the field of rare  $K$  decays is the search for processes forbidden in the Standard Model, e.g.,  $K_L^0 \rightarrow \mu e$  and  $K^+ \rightarrow \pi^+ \mu^+ e^-$ . Various extensions of the Standard Model predict that these processes will occur with branching fractions in the range of  $10^{-10}$  to  $10^{-15}$ . Experiments of the last decade have pushed the limits into the  $10^{-10}$  to  $10^{-11}$  range, and further improvements in sensitivity of one to two orders of magnitude can be expected in the next few years.  $K$  decays allow one also to study higher-order weak-interaction processes such as  $K_L^0 \rightarrow \mu^+ \mu^-$ ,  $K_L^0 \rightarrow e^+ e^-$ ,  $K^+ \rightarrow \pi^+ \nu \bar{\nu}$ , which are forbidden to first order in the Standard Model. Because of strong suppression, these decay modes offer potential windows on new physics; in addition, they may offer the most reliable measurement of  $V_{td}$ , one of the elements of the weak mixing matrix in the quark sector. The studies of the  $\mu^+ \mu^-$  channel have achieved data samples of close to 1000 events; the other two modes should be observed for the first time in the next few years. Finally, as a byproduct of these studies, one has been able to look simultaneously for new light particles into which the  $K$  meson could decay. Limits obtained for various hypothetical particles are summarized.

## CONTENTS

I. Introduction	1149
II. $CP$ -Violating Processes	1150
A. $K_L^0 \rightarrow \pi^0 e^+ e^-$	1151
1. General phenomenology	1151
2. Direct $CP$ violation	1151
3. Indirect $CP$ violation	1154
4. $CP$ -conserving amplitude: $K_L^0 \rightarrow \pi^0 \gamma \gamma$	1155
5. Status of the $K_L^0 \rightarrow \pi^0 e^+ e^-$ experiments	1159
6. Future prospects	1161
B. $K \rightarrow \pi \mu^+ \mu^-$ decays	1162
1. Phenomenology	1163
2. Experimental status	1164
C. $K_L^0 \rightarrow \pi^0 \nu \bar{\nu}$	1164
1. Phenomenology	1164
2. Experimental situation	1165
D. $K_L^0 \rightarrow \mu^+ \mu^-$ polarization	1166
1. Phenomenology	1166
2. Experimental prospects	1167
III. Forbidden Decays	1167
A. $K_L^0 \rightarrow \mu e$	1168
1. General phenomenology	1168
2. Status of $K_L^0 \rightarrow \mu e$ experiments	1171
3. Future prospects	1173
B. $K^+ \rightarrow \pi^+ \mu e$	1174
1. Phenomenology	1174
2. Experimental status	1174
3. Future prospects	1176
C. $K^+ \rightarrow \pi^- l^+ l'^+$ and $K_L^0 \rightarrow \pi^- \pi^- l^+ l'^+$	1176
IV. Suppressed Decay Modes	1176
A. $K^+ \rightarrow \pi^+ \nu \bar{\nu}$ decay	1176

1. Phenomenology	1176
2. Experimental status	1180
B. $K_L^0 \rightarrow \mu \mu$	1183
1. Phenomenology	1183
2. Experimental status	1187
3. Future prospects	1188
C. $K_L^0 \rightarrow ee$	1188
1. Phenomenology	1188
2. Experimental considerations and status	1189
3. Future prospects	1190
V. Decays into New Particles	1190
A. Theoretical background	1190
B. Experimental results	1191
Addendum	1194
Acknowledgments	1194
References	1194

## I. INTRODUCTION

Over the past 40 years the study of production and decays of  $K$  mesons has been one of the most productive areas in particle physics from the point of view of producing unexpected and startling discoveries, verifying new hypotheses, and providing stimuli towards the next generation of theoretical ideas. Thus the diversity of the quark spectrum was first indicated by the discovery of the  $K$  meson via observation of  $K^+ \rightarrow \pi^+ \pi^+ \pi^-$  decay (Brown *et al.*, 1949). Some time later the ideas of associated production and strangeness were put forth (Pais, 1952; Gell-Mann, 1953); they were subsequently verified

experimentally by studies of  $\pi p \rightarrow \Lambda K$  and  $\pi p \rightarrow \Sigma K$  channels (Fowler *et al.*, 1954). Quantum-mechanical phenomena predicted for the  $K^0\text{-}\bar{K}^0$  system (Gell-Mann and Pais, 1955; Pais and Piccioni, 1955) were verified by observation (Lande *et al.*, 1956) of  $K_L^0$  decays and later by studies of  $K_S^0$  regeneration (Good, 1957; Good *et al.*, 1961). The discovery of parity violation in weak interactions was stimulated by the “ $\theta$ - $\tau$  puzzle” in the kaon system (Dalitz, 1954), which led to the famous postulate of Lee and Yang (1956). The phenomenon of  $CP$  violation was first observed in the  $K_L^0 \rightarrow 2\pi$  channel (Christenson *et al.*, 1964) and its phenomenological details elucidated by subsequent careful study of the  $K^0\text{-}\bar{K}^0$  system (Kleinknecht, 1976). The experimentally observed suppression of the flavor-changing neutral currents was first studied in the  $K_L^0 \rightarrow \mu\mu$  (Clark *et al.*, 1971; Carithers *et al.*, 1973) and  $K^+ \rightarrow \pi^+ \nu\bar{\nu}$  (Klems *et al.*, 1970) decay modes and led subsequently to the postulate of the GIM mechanism (Glashow, Iliopoulos, and Maiani, 1970). The analysis of the  $K_L^0\text{-}K_S^0$  mass difference in terms of the second-order weak-interaction box diagrams allowed one to predict the approximate mass of the charm quark (Gaillard and Lee, 1974). These are only the highlights of the past  $K$ -meson studies; several other examples can be cited which also played a crucial role in the development of today’s Standard Model.

The past decade has seen a remarkable revival of interest in  $K$ -decay studies. This interest has been partly stimulated by the importance of some physics questions that can be best, or maybe even uniquely, studied by looking at  $K$  decays. But this stimulus has been helped considerably by new advances in technology, especially in the areas of detectors, electronics, and computers, which made possible a much improved new generation of  $K$ -decay experiments. Very roughly, these experiments can be divided into two areas. The first is the area of high-statistics precision studies, exemplified best by the two  $e^+e^-$  experimental programs at CERN and Fermilab. The second includes high-sensitivity experiments searching for as yet unseen processes or studying with high precision channels that yielded only a handful of events before the start of these experimental programs.

It is the second category of processes that is the subject of this review. Specifically, we divide our topics into four broad categories:  $CP$  violation issues, processes forbidden in the Standard Model, processes suppressed to first order in the Standard Model, and new particle searches. Clearly this limitation is arbitrary; it represents to some extent the reviewers’ interest, but also a need to limit this work to a finite size. It also reflects reasonably well the current maturity in the field of rare  $K$  decays.

Under  $CP$  violation processes we shall discuss the decays  $K_L^0 \rightarrow \pi^0 e^+ e^-$ ,  $K_L^0 \rightarrow \pi^0 \mu^+ \mu^-$ ,  $K_L^0 \rightarrow \pi^0 \nu\bar{\nu}$ , and muon polarization in  $K_L^0 \rightarrow \mu^+ \mu^-$ . In the second category we shall focus on searches for  $K_L^0 \rightarrow \mu e$  and  $K^+ \rightarrow \pi^+ \mu^+ e^-$ , and in the third on  $K^+ \rightarrow \pi^+ \nu\bar{\nu}$ ,  $K_L^0 \rightarrow \mu^+ \mu^-$ , and  $K_L^0 \rightarrow e^+ e^-$ . Finally, in the last category we shall summarize the information obtained

from rare decays on possible new particles, such as light Higgs, axions, etc.

This organization does not explicitly identify several channels that have received quite a bit of attention in recent years, decays such as  $K^+ \rightarrow \pi^+ e^+ e^-$ ,  $K_L^0 \rightarrow \pi^0 \gamma \gamma$ , and  $K_L^0 \rightarrow e^+ e^- \gamma$ , among others. These channels are of great interest in their own right, especially in the area of trying to understand the long-distance dynamics. However, to keep this review finite, we limit the discussion of these channels to their experimental status and to those theoretical aspects which impact the primary topics of this review.

This review covers mainly experimental issues and its primary focus is on summarizing the most recent results and describing the work currently in progress. Some space is devoted to discussing the experiments that should be producing physics during the next five years. We do try to summarize briefly the phenomenology that is relevant to the decays discussed, but no pretense is made of presenting a comprehensive review of the substantial amount of theoretical work in the area of  $K$  decays.

## II. $CP$ -VIOLATING PROCESSES

To understand the origin of  $CP$  violation is one of the main challenges of particle physics today. Thus it is not surprising that this question has been attracting a great deal of experimental and theoretical effort ever since the discovery of the  $K_L^0 \rightarrow 2\pi$  decay mode a little over a quarter of a century ago (Christenson *et al.*, 1964). In spite of these efforts, however, the  $K^0$ -decay channels are still the only processes known at the present time that manifest observable  $CP$  violation and can provide us with an opportunity to do quantitative measurements. The vigorous experimental program in this area has resulted in remarkable progress in defining the  $CP$  violation parameters in the  $K^0\text{-}\bar{K}^0$  system. But the ultimate understanding of the source of  $CP$  violation still eludes us. Thus, for example, the superweak theory proposed by Wolfenstein (1964) almost 30 years ago is still consistent with all the known data. Alternatively, the Standard Model can accommodate a small  $CP$  violation by virtue of a phase in the Cabibbo-Kobayashi-Maskawa (CKM) matrix (Kobayashi and Maskawa, 1973), but here also the present experimental situation is still too unclear to either confirm or contradict that particular “explanation” of the  $CP$  violation. This situation has led in the past decade to a number of theoretical investigations of other possible processes that might shed light on the origin of  $CP$  invariance. Other  $K$ -decay channels, and more recently the  $B\text{-}\bar{B}$  system, have been identified as possible sources of new information. Several rare  $K$ -decay modes are among the possible fruitful lines of investigation, and in this section we shall focus on that general physics area. Specifically, we shall discuss the phenomenology and experimental status of the decay channels  $K_L^0 \rightarrow \pi^0 e^+ e^-$ ,

$K_L^0 \rightarrow \pi^0 \mu^+ \mu^-$ ,  $K_L^0 \rightarrow \pi^0 \nu \bar{\nu}$ , and muon polarization in  $K_L^0 \rightarrow \mu^+ \mu^-$ .

A.  $K_L^0 \rightarrow \pi^0 e^+ e^-$

1. General phenomenology

It was observed already in the early 1960s that in the limit of  $CP$  invariance the decay  $K_L^0 \rightarrow \pi^0 e^+ e^-$  cannot proceed via an intermediate one-photon state (Baker and Glashow, 1962; Pais and Treiman, 1968). Thus it appeared promising that this decay mode might provide information on  $CP$  violation complementary to that obtained from the study of  $K \rightarrow 2\pi$  processes (Gaillard and Lee, 1974). The latter channels exhibit  $CP$  violation mainly in the mass matrix of the  $K^0-\bar{K}^0$  system; the “direct”  $CP$  violation in the  $K \rightarrow 2\pi$  channel is small. Experimentally, this is indicated by the fact that the ratio of the two relevant parameters  $\epsilon'/\epsilon$  is  $O(10^{-3})$  (Barr, 1992; see also Burkhardt *et al.*, 1988) and possibly consistent with zero (Patterson *et al.*, 1990; Swallow, 1992; Gibbons *et al.*, 1993). On the other hand, according to the Standard Model picture, the channel  $K_L^0 \rightarrow \pi^0 e^+ e^-$  should be dominated by the direct  $CP$  violation process and thus could provide an alternative way to test the Standard Model prediction. The drawback, of course, is the very low ( $\leq 10^{-11}$ ) predicted branching fraction.

The overall situation is quite complex. Three separate processes, all of roughly equal *a priori* magnitude, can contribute to the  $K_L^0 \rightarrow \pi^0 e^+ e^-$  decay. The first two have been mentioned already; the direct  $CP$  violation in this decay, predictable from the Cabibbo-Kobayashi-Maskawa phase, is one of them. The indirect  $CP$  violation due to the admixture of the  $CP$  even state ( $K_1^0$ ) in  $K_L^0$  is the other. The latter will be proportional to the  $\epsilon$  parameter which gives the relative amplitude of the  $K_1^0$  state in  $K_L^0$ . Finally, there is also the  $CP$ -conserving amplitude, due to an intermediate  $\pi^0 \gamma \gamma$  state, a state of odd  $CP$  parity (in contrast to the even  $CP$  quantum number of the intermediate  $\pi^0 \gamma$  state) that can mediate both the  $K_L^0 \rightarrow \pi^0 e^+ e^-$  and the  $K_L^0 \rightarrow \pi^0 \mu^+ \mu^-$  channels.

The relative contributions of these three mechanisms can be disentangled by studying the time dependence of this decay mode, in a manner analogous to the study of interference effects in the  $K^0 \rightarrow 2\pi$  channels. Close to the point of production, the  $K^0$  beam will yield mainly  $K_S^0$  decays; thus the  $K^0 \rightarrow \pi^0 e^+ e^-$  events detected in that region will have mainly  $K_S^0 \rightarrow \pi^0 e^+ e^-$  as their source. Hence the observed rate and time dependence in that time domain will yield information that will allow us to extract the magnitude of indirect  $CP$  violation. In the long-time regime, when all the  $K_S^0$  have decayed away, we shall see just the contributions from  $K_L^0$  decays, both  $CP$ -conserving and  $CP$ -violating. In general, these modes will interfere and could give an  $e^+/e^-$  asymmetry on the  $\pi^0 e^+ e^-$  Dalitz plot (Donoghue *et al.*, 1987). The region between these two extremes, i.e.,  $\tau \approx 10\tau_S$ , will give interference effects due to the  $K_S^0$  and  $K_L^0$  channels beating

against each other in a manner similar to the  $K^0 \rightarrow 2\pi$  case.

Even though the situation described above is quite straightforward in principle, in practice the task of disentangling these modes is very difficult and probably not possible in the foreseeable future. The difficulties stem from the large numbers of events required, estimated low branching fractions, and potential very serious backgrounds. To quantify some of these statements, we turn next to a discussion of our present theoretical ideas, including relevant data, about the expected magnitude of each one of the three processes discussed above. Discussion of important background considerations will be deferred until later, when we consider prospects for future measurements (see Sec. II.A.6).

2. Direct  $CP$  violation

Most of this contribution is due to the short-distance effects, generally characterized as box diagrams and  $Z^0$  or  $\gamma$  penguin diagrams. They can be calculated in principle, even though in practice the calculation is fraught with numerous theoretical and experimental uncertainties. The diagrams in question are illustrated in Fig. 1. In the following, we give a very brief outline of the general issues involved in calculating the magnitude of these diagrams.

The box and penguin diagrams responsible for direct  $CP$  violation in  $K_L^0 \rightarrow \pi^0 e^+ e^-$  decay also govern the decays  $K_L^0 \rightarrow \mu^+ \mu^-$ ,  $K^+ \rightarrow \pi^+ \nu \bar{\nu}$ , and  $K^+ \rightarrow \pi^0 \nu \bar{\nu}$  discussed elsewhere in this review. Thus the general remarks made here about calculational techniques will also apply to those other decay modes. The original calculations evaluated the QCD contributions to these processes by means of renormalization-group techniques and the operator product expansion (Dib *et al.*, 1989; Flynn and Randall,

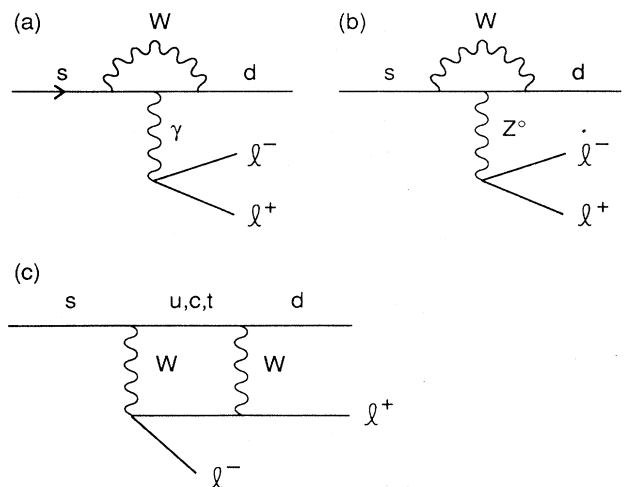


FIG. 1. Three diagrams responsible for short-distance contributions to the process  $K \rightarrow \pi l^+ l^-$ : (a) the “electromagnetic penguin”; (b) the “Z penguin”; (c) the “W box.”

1989a). One drawback of this method is the fact that the very important dependence on the mass of the top quark,  $m_t$ , is somewhat obscured.

An alternative technique has been developed recently by Buchalla, Buras, and Harlander (1991), which allows us to treat flavor-changing neutral-current (FCNC) processes, like the decays in question, in a somewhat different way. It expresses the decay amplitudes as linear combinations of process-independent, but  $m_t$ -dependent, one-loop diagram functions. The coefficients in the expansion depend on the specific processes considered. Both the coefficients and the loop diagram functions can be made separately gauge independent. The authors refer to the technique as the penguin-box expansion (PBE). One of the advantages of this method is that the dependence on  $m_t$  is exhibited more clearly.

The scope of this review does not permit any detailed discussion of these calculational methods. We shall limit ourselves here mainly, somewhat arbitrarily, to a summary of the formulas derived using operator product expansion.

The explicit form for the short-distance contribution to the decay mode  $K_L^0 \rightarrow \pi^0 e^+ e^-$  is free of uncertainties having to do with dependence on the hadronic matrix elements in  $K$  decays, since these can be obtained directly from the well-studied  $K_{e3}$  decays. The rate depends on the  $A$  and  $\eta$  parameters of the Cabibbo-Kobayashi-Maskawa matrix [we adopt throughout this paper] the Wolfenstein (1983) parametrization, which is discussed below, the size of the Weinberg mixing angle  $\sin\theta_w$ , and the mass of the top quark. More explicitly, one can write the expression for the branching fraction as (Gilman and Wise, 1980; Dib *et al.*, 1989)

$$B(K_L^0 \rightarrow \pi^0 e^+ e^-)_{\text{dir}} = 2.6 \times 10^{-14} A^4 (C_V^2 + C_A^2) \eta^2, \quad (2.1)$$

with

$$C_V \simeq F_1(x_t) + \frac{1}{\sin^2\theta_w} [F_2(x_t) + (1 - 4\sin^2\theta_w)F_3(x_t)], \quad (2.2)$$

$$C_A \simeq -\frac{1}{\sin^2\theta_w} [F_2(x_t) + F_3(x_t)],$$

where  $x_t = m_t^2/M_W^2$  and

$$F_1(x_t) = -17 - \frac{2(25 - 19x_t)x_t^2}{9(1-x_t)^3} - \frac{4(3x_t^4 - 30x_t^3 + 54x_t^2 - 32x_t + 8)\ln x_t}{9(1-x_t)^4},$$

$$F_2(x_t) = \frac{2x_t(1-x_t + \ln x_t)}{(1-x_t)^2}, \quad (2.3)$$

$$F_3(x_t) = -\frac{x_t[(x_t - 6)(x_t - 1) + (3x_t + 2)\ln x_t]}{(1-x_t)^2}.$$

In evaluating the expression above, however, one has to confront the serious issue that the parameters of the weak-mixing (CKM) matrix are not determined precisely by the present experimental data. Hence the values of  $A$  and  $\eta$  that will serve as input in the formula for the branching fraction above [Eq. (2.1)] depend strongly on a variety of experimental data and on the assumptions one makes about various hadronic matrix elements. To appreciate this situation, we briefly review the overall technique of evaluating the Cabibbo-Kobayashi-Maskawa matrix elements.

In the Wolfenstein parametrization of the CKM matrix,

$$V \simeq \begin{pmatrix} 1 - \frac{1}{2}\lambda^2 & \lambda & A\lambda^3[\rho - i\eta(1 - \frac{1}{2}\lambda^2)] \\ -\lambda & 1 - \frac{1}{2}\lambda^2 - iA^2\lambda^4\eta & A\lambda^2(1 + i\lambda^2\eta) \\ A\lambda^3(1 - \rho - i\eta) & -A\lambda^2 & 1 \end{pmatrix}, \quad (2.4)$$

there is one well-determined parameter, viz.  $\lambda$ , the Cabibbo angle (Cabibbo, 1963), which equals approximately 0.22, and three parameters  $A, \rho, \eta$ , to be determined by four different experimental measurements, (a) the  $b$  quark lifetime related to the matrix element  $|V_{cb}|$ , (b) the  $b \rightarrow u$  branching fraction providing the value of  $|V_{ub}/V_{cb}|$ , (c) the  $CP$ -violating parameter  $\epsilon$  in  $K^0 \rightarrow 2\pi$  decays, and (d) the  $B_d^0 - \bar{B}_d^0$  mixing parameter  $x_d$ . The relevant expressions (Geng and Turcotte, 1991) for quantities related directly to these four experimental parameters and the latest Particle Data Group (1992) values for their world averages are given below:

$$|V_{cb}| = A\lambda^2 = 0.043 \pm 0.007, \quad (2.5a)$$

$$|V_{ub}/V_{cb}| = \lambda\sqrt{\rho^2 + \eta^2} = 0.10 \pm 0.03, \quad (2.5b)$$

$$|\epsilon| = \frac{1}{\sqrt{2}\Delta M_K} \frac{G_F^2 M_W^2}{12\pi^2} M_K f_K^2 B_K 2A^2 \lambda^6 \eta [-\eta_{cc} B(x_c) + \eta_{ct} B(x_c, x_t) + \eta_{tt} A^2 \lambda^4 (1 - \rho) B(x_t)]$$

$$= (2.268 \pm 0.023) \times 10^{-3}, \quad (2.5c)$$

$$x_d = \frac{G_F^2}{6\pi^2} M_b f_B^2 B_B \tau_B \eta_B M_W^2 A^2 \lambda^6 [(1-\rho)^2 + \eta^2] B(x_t) = 0.71 \pm 0.11, \tag{2.5d}$$

respectively, where

$$B(x_i) = \frac{x_i}{4} \left[ 1 + \frac{3-9x_i}{(x_i-1)^2} + \frac{6x_i^2 \ln x_i}{(x_i-1)^3} \right], \tag{2.6}$$

$$B(x_i, x_j) = \frac{x_i x_j}{4} \left[ \frac{(x_j^2 - 8x_j + 4) \ln x_j}{(x_j-1)^2 (x_j-x_i)} - \frac{3}{2(1-x_i)(1-x_j)} + (x_i \leftrightarrow x_j) \right],$$

with  $x_i = m_i^2/M_W^2$  and  $i = c, t$ . The last term in the last expression signifies that one repeats the first two terms with  $x_i$  and  $x_j$  interchanged.  $\eta_B, \eta_{cc}, \eta_{ct}$ , and  $\eta_{tt}$  are all reasonably well-defined QCD corrections, which can be calculated if the masses of heavy quarks and gauge bosons are known.

There exists an additional potential constraint from measurement of the branching fraction for  $K_L^0 \rightarrow \mu^+ \mu^-$ , which is discussed elsewhere in this review and is ignored here for clarity.

We can focus on the calculational problem by pointing out that there are two categories of parameters that enter into the above expressions:

(a) Non-CKM matrix element parameters like  $m_c$ , the ‘‘bag factors’’  $B_K$  and  $B_B$ , and decay constants  $f_B$  and  $f_K$ , which are known only poorly (except for  $f_K$ , which is well measured by the  $K^+ \rightarrow \mu^+ \nu$  rate).

(b) Unknown parameters, i.e., the three CKM matrix parameters  $A, \rho$ , and  $\eta$  and the mass of the top quark,  $m_t$ .

One possible calculational procedure is to pick values of the parameters in category (a) and the mass of the top quark and to use the remaining four equations to find the optimum values of  $A, \rho$ , and  $\eta$  which minimize the  $\chi^2$  (four constraints for three parameters). Alternatively, one could allow the mass of the top quark to be a variable also and then calculate (rather than fit) the values of the four unknown parameters. Finally, one can search the three-dimensional  $A, \rho, \eta$  space for a self-consistent set of values that satisfy the experimental and theoretical bounds on parameters in category (a) and on the mass of the top quark. There have been several variants on the methods of calculating these parameters, but the limitations of this review do not allow us to elaborate on them (see, for example, Harris and Rosner, 1992).

At the present time, the mass of the top quark is constrained by Collider Detector Facility (CDF) measurements at Fermilab (Abe *et al.*, 1992a, 1992b) to lie above 91 GeV with 95% confidence level and is estimated from the constrained fit to LEP,  $\bar{p}$ - $p$  collider, and neutrino data (The LEP Collaborations, 1992) to be  $132_{-31}^{+27+18}_{-19}$  GeV. Thus it is interesting and customary to explore the  $A, \rho$ , and  $\eta$  space for values of the  $m_t$  satisfying  $91 < m_t < 250$  GeV/ $c^2$ . The hadronic matrix elements have been a sub-

ject of controversy for quite some time. In principle, they can be calculated using the methods of QCD on a lattice, and considerable progress has been made in this area lately. One noteworthy recent development from these calculations is that the value of  $f_B$ , which has been generally taken to lie in the range  $100 < f_B < 200$  MeV, very likely lies somewhat higher (Allton *et al.*, 1991; Alexandrou *et al.*, 1991, 1992; Bernard *et al.*, 1992), i.e., between 200 and 250 MeV.

Older analyses using these calculational techniques (Bélanger and Geng, 1991) tended to use values of  $f_B$  in the 100–200-MeV region and had values for  $B_{\text{dir}}(K_L^0 \rightarrow \pi^0 e^+ e^-)$  in the  $2 \times 10^{-12}$  region (see Fig. 2). A more recent analysis (Geng and Turcotte, 1991), with a higher value of  $f_B$ , shows that the branching fraction for this process increases as one increases the value of  $f_B$ . Specifically, allowing

$$1.2 \leq m_c \leq 1.8 \text{ GeV}, \tag{2.7}$$

$$90 \leq m_t \leq 200 \text{ GeV},$$

and taking  $B_K = 0.8 \pm 0.2$  and  $B_B \approx 1.0$ , the authors obtain the limits

$$1.2 \times 10^{-12} \leq B_{\text{dir}}(K_L^0 \rightarrow \pi^0 e^+ e^-) \leq 8.6 \times 10^{-12} \tag{2.8a}$$

for  $f_B = 250 \pm 50$  MeV. The results of their calculation, for  $m_c = 1.5$  GeV, as a function of mass of the top quark, are shown in Fig. 3.

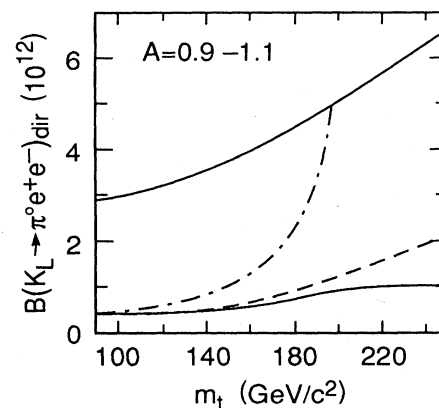


FIG. 2. Lower and upper limits (solid lines) on allowed branching fraction for the direct  $CP$ -violating contribution to  $K_L^0 \rightarrow \pi^0 e^+ e^-$  as a function of mass of the top quark with  $A = 1.0 \pm 0.1$ ,  $f_B = 140 \pm 25$  MeV, and  $B_B = 0.85 \pm 0.10$ . The dashed and dot-dashed curves are boundaries of the allowed region taking into account the constraints from the  $K_L^0 \rightarrow \mu^+ \mu^-$  decay (after Belanger and Geng, 1991).

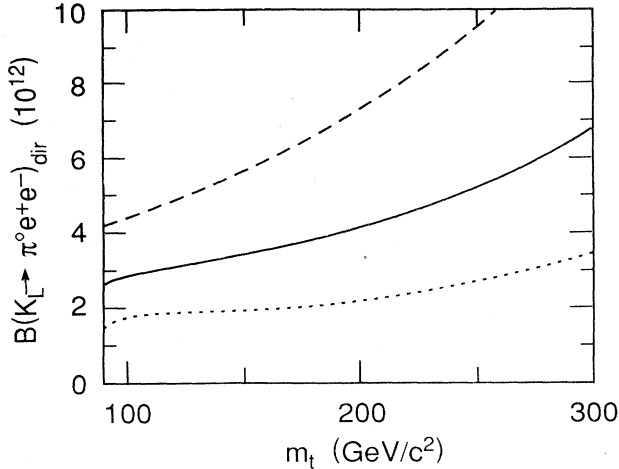


FIG. 3. Estimated range of values for branching fraction of  $K_L^0 \rightarrow \pi^0 e^+ e^-$  as a function of mass of the top quark. The dashed and dotted lines show the contours corresponding to a  $\chi^2$  that equals  $\chi_{\min}^2 + 1$ .  $f_B = 250 \pm 50$  MeV was used (after Geng and Turcotte, 1991).

This result can be compared with the calculations of Buchalla *et al.* (1991) using the penguin-box formalism. The two sets of calculations are in good agreement if the phase  $\delta$ , responsible for  $CP$  violation in the standard form of the CKM matrix (Particle Data Group, 1992), lies in the first quadrant. However, for  $\delta$  in the second quadrant, Buchalla *et al.* obtain a significantly lower range of values, namely,

$$B_{\text{dir}}(K_L^0 \rightarrow \pi^0 e^+ e^-) \leq 3.6 \times 10^{-12}. \quad (2.8b)$$

### 3. Indirect $CP$ violation

The indirect  $CP$ -violating amplitude contributing to the process  $K_L^0 \rightarrow \pi^0 e^+ e^-$  is directly related to the  $CP$ -conserving amplitude for  $K_S^0 \rightarrow \pi^0 e^+ e^-$ . More specifically, the amplitude is essentially given by  $A_L = \epsilon A_S$ , where  $A_S$  is the  $K_S$  amplitude for the  $K^0 \rightarrow \pi^0 e^+ e^-$  decay and  $A_L$  is the  $K_L^0$  amplitude for this decay due to indirect  $CP$  violation. There is a small complication here, having to do with phase conventions, to which we shall return at the end of this subsection.

No measurement of the decay rate  $K_S^0 \rightarrow \pi^0 e^+ e^-$  has been performed as yet, the best upper limit on that branching fraction being (Gibbons *et al.*, 1988)  $4.5 \times 10^{-5}$ . Accordingly, to estimate the  $K_L^0 \rightarrow \pi^0 e^+ e^-$  indirect  $CP$ -violating amplitude we have to go to a related but more distant process,  $K^+ \rightarrow \pi^+ e^+ e^-$ . This channel is of considerable interest in its own right; here, however, we focus mainly on the question of what it can teach us about  $K_L^0$  decay. To see most clearly the measurements that are relevant we write

$$B_{\text{ind}}(K_L^0 \rightarrow \pi^0 e^+ e^-) = B(K^+ \rightarrow \pi^+ e^+ e^-) \frac{\tau_{K_L^0}}{\tau_{K^+}} \times \frac{\Gamma(K_1^0 \rightarrow \pi^0 e^+ e^-)}{\Gamma(K^+ \rightarrow \pi^+ e^+ e^-)} \times \frac{\Gamma_{\text{ind}}(K_L^0 \rightarrow \pi^0 e^+ e^-)}{\Gamma(K_1^0 \rightarrow \pi^0 e^+ e^-)}. \quad (2.9)$$

The last factor, by our definition of what constitutes indirect  $CP$  violation, is just  $|\epsilon|^2$ . The first two factors are known from experimental measurements; the third provides the most uncertainty at the present time because, in the absence of directly relevant data, it has to rely on calculations that are somewhat model dependent.

The  $K^+ \rightarrow \pi^+ e^+ e^-$  branching fraction, the first factor on the right-hand side of the equation, has been measured recently at BNL with good precision and found to be  $(2.75 \pm 0.23 \pm 0.13) \times 10^{-7}$  (Alliegro *et al.*, 1992). The ratio of the lifetimes is 4.2, and in the framework of this discussion the error on that number is negligible. The third factor cannot be calculated reliably from first principles. If it were dominated by a short-distance amplitude involving the  $s \rightarrow d$  transition, we would have a pure  $\Delta I = \frac{1}{2}$  transition and the ratio would be unity. However, there are strong indications (Gilman and Wise, 1980; Dib *et al.*, 1989) that such an assumption is highly unreliable and long-distance effects are important. A pure  $\Delta I = \frac{3}{2}$  transition would give a factor of 4; a mixture of the two amplitudes could give any value.

The problem of calculating the rate and spectrum of both  $K^+$  and  $K_1^0$  into  $\pi^+ e^+ e^-$  and  $\pi^0 e^+ e^-$  final states, respectively, has been addressed by Ecker, Pich, and de Rafael (1987b) using an effective chiral Lagrangian. They evaluate contributions of the one-loop diagrams illustrated in Fig. 4 and derive an expression for the spectrum as a function of  $q^2$  (or alternatively  $M_{ee}$ ), in terms of one unknown renormalization constant which they call  $w_+$ . Measurement of the  $K^+ \rightarrow \pi^+ e^+ e^-$  branching fraction determines  $w_+$ , but only to within a quadratic ambiguity, i.e., two possible solutions. Spectrum measurement in that process, however, allows one to resolve this ambiguity and refine the measurement of  $w_+$ .

Such a determination of  $w_+$  has been performed recently (Alliegro *et al.*, 1992), and the results are illustrated in Fig. 5. The calculated value of  $w_+$  is  $0.89_{-0.14}^{+0.24}$  and the spectrum-constrained fit yields a value for the branching fraction of  $(2.99 \pm 0.22) \times 10^{-7}$ . Using the formalism of Ecker, Pich, and de Rafael, one can then calculate the third factor in the expression above,  $\Gamma(K_1^0 \rightarrow \pi^0 e^+ e^-) / \Gamma(K^+ \rightarrow \pi^+ e^+ e^-)$ . The resulting value lies between  $0.20 \times 10^{-3}$  and 0.21. This large range, spanning three orders of magnitude, corresponds to the set of possible values of  $w_+$  quoted above. The large magnitude of this range is due to an almost total cancellation between  $w_+$  and the rest of the terms that occur in the expression for the branching fraction for some of the allowed values of  $w_+$ . Taking the upper lim-

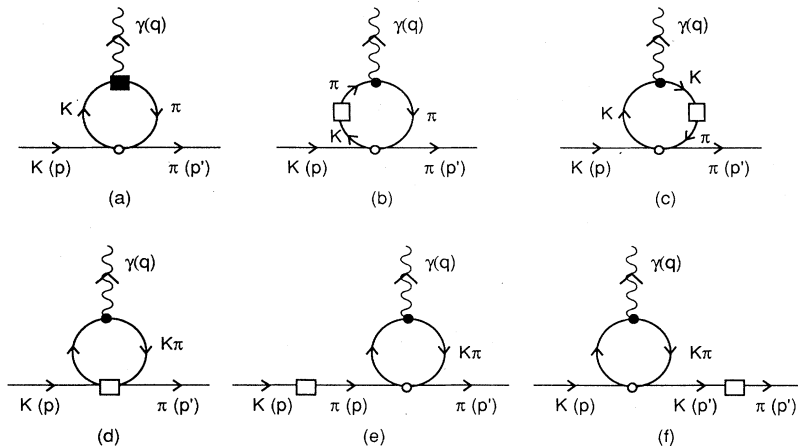


FIG. 4. One-loop diagrams for  $K \rightarrow \pi \gamma \gamma$  which can lead to terms in the amplitude for  $K_L^0 \rightarrow \pi^0 e^+ e^-$  proportional to  $q^2(p+p')_\mu$  (after Ecker, Pich, and de Rafael, 1987b).

it and combining this result with other factors discussed above, we obtain  $B_{\text{ind}}(K_L^0 \rightarrow \pi^0 e^+ e^-) < 1.6 \times 10^{-12}$ ; it could of course be considerably smaller.

As the estimated contributions from the two mechanisms (direct and indirect) to the  $CP$ -violating amplitude could be of comparable magnitude, the interference effects in the total rate could be considerable. In evaluating this effect, one has to be careful about ensuring that a common phase convention is used for both amplitudes (Dib *et al.*, 1989). The standard convention is to assume that the  $K^0 \rightarrow \pi\pi$  amplitude is real when the  $2\pi$  final state is in an  $I=0$  state. However, this is not true when dynamical calculations are made in the quark basis, since there is then a  $CP$ -violating amplitude in the  $2\pi$  transition which is proportional to  $\epsilon'$ . The  $K^0$  state vectors need to be rotated to take that into account, i.e.,

$$|K^0\rangle \rightarrow e^{-i\xi} |K^0\rangle \text{ and } |\bar{K}^0\rangle \rightarrow e^{i\xi} |\bar{K}^0\rangle, \quad (2.10)$$

where the value of  $\xi$  given by  $\xi = \frac{1}{15.6} |\epsilon'/\epsilon|$  is obtained by

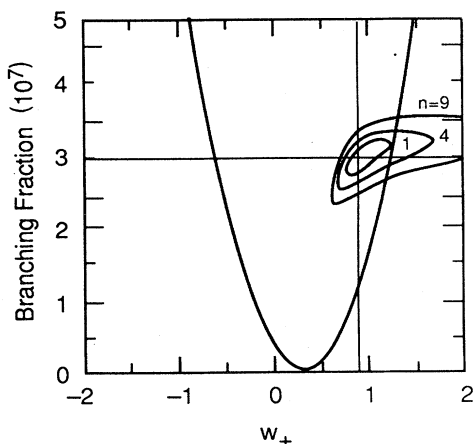


FIG. 5. Contours of  $K_{\pi e e}^+$  branching fraction vs  $w_+$  for constant values of  $\chi^2$  equal to  $\chi_{\text{min}}^2 + n$ , calculated using the formalism of Ecker *et al.* (1987b). The parabolic curve is the predicted relationship.  $\chi^2$  per degree of freedom at minimum equals 1.2 (after Alliegro *et al.*, 1992).

calculating strong-interaction penguin effects. Thus the usual  $\epsilon \approx (2.275 \times 10^{-3}) e^{i\pi/4}$  has to be modified by

$$\epsilon \rightarrow \epsilon - i\xi \quad (2.11)$$

before one uses it to multiply the amplitude for  $K_L^0 \rightarrow \pi^0 e^+ e^-$  to obtain the indirect  $CP$ -violating amplitude in  $K_L^0$  decay.

4.  $CP$ -conserving amplitude:  $K_L^0 \rightarrow \pi^0 \gamma \gamma$

From the point of view of the study of  $CP$  violation, the most relevant question is whether the  $CP$ -conserving contribution to  $K_L^0 \rightarrow \pi^0 e^+ e^-$  is comparable to or larger than contributions due to the two mechanisms discussed above. If so, then this amplitude could swamp the  $CP$ -violating ones and the task of learning more about  $CP$  violation would be correspondingly harder.

The  $CP$ -conserving amplitude is dominated by the  $\pi^0 \gamma \gamma$  intermediate state. Its absorptive part, expected to be dominant, can be represented by the diagram shown in Fig. 6 and thus is quite analogous to the  $K_L^0 \rightarrow \mu\mu$  situation discussed in Sec. IV. The decay  $K_L^0 \rightarrow \pi^0 \gamma \gamma$  has been detected and measured for the first time recently. The long-standing theoretical controversy associated with different calculations of the  $CP$ -conserving amplitude is beginning to be resolved, and future experiments can be expected to shed even more light on this question.

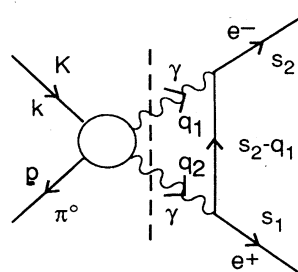


FIG. 6. The unitarity diagram for the decay  $K_L^0 \rightarrow \pi^0 e^+ e^-$  (after Donoghue *et al.*, 1987).

The issue of how to calculate reliably the rate for  $K_L^0 \rightarrow \pi^0 \gamma \gamma$  (and hence  $K_L^0 \rightarrow \pi^0 e^+ e^-$  without  $CP$  violation) is quite complex. We are not able in this review to give a full description of all the complexities. Accordingly, we limit ourselves to a discussion of the key theoretical issues, summary of the experimental situation for  $K_L^0 \rightarrow \pi^0 \gamma \gamma$ , and recapitulation of the current best estimates as to the magnitude of the  $CP$ -conserving contributions to the decay  $K_L^0 \rightarrow \pi^0 e^+ e^-$ .

The general matrix element for the decay  $K_L^0 \rightarrow \pi^0 \gamma \gamma$  can be written as (Sehgal, 1990)

$$M = A (\epsilon \cdot \epsilon' k \cdot k' - \epsilon \cdot k' \epsilon' \cdot k) + B (\epsilon \cdot \epsilon' k \cdot Q k' \cdot Q + k \cdot k' \epsilon \cdot Q \epsilon' \cdot Q - \epsilon \cdot Q \epsilon' \cdot k k' \cdot Q - \epsilon \cdot k' k \cdot Q \epsilon' \cdot q) / k \cdot k', \quad (2.12)$$

where the relevant 4-vectors are defined in Fig. 7 and where the coefficients  $A$  and  $B$  are functions of two independent invariants that can be chosen to be

$$s = (Q - p)^2 = (k + k')^2 \quad \text{and} \quad (2.13)$$

$$\Delta = t - t' = (Q - k)^2 - (Q - k')^2.$$

The total angular momentum of the  $\gamma\gamma$  system in the first term (referred to as the  $A$  amplitude) in the above expression for the matrix element is zero. Accordingly, one might expect *a priori* that this term, when contracted with the  $\gamma\gamma \rightarrow e^+ e^-$  amplitude, would be suppressed by the helicity factor, the amplitude being multiplied by a factor  $m_e$ . No such suppression exists for the second term (called the  $B$  amplitude), but because it involves more powers of momentum, it might be expected to be suppressed by a centrifugal barrier factor. Essentially because of these arguments, it was originally assumed that the rate for  $K_L^0 \rightarrow \pi^0 e^+ e^-$  due to the  $CP$ -conserving amplitude would be  $O(10^{-13})$  or less and thus negligible (Donoghue *et al.*, 1987; Ecker *et al.*, 1987a, 1988).

Sehgal (1988), however, has argued that the  $B$  amplitude can be quite large and can make a significant contribution to  $CP$ -conserving  $K_L^0 \rightarrow \pi^0 e^+ e^-$  decay. He relates this process to the decay  $\eta \rightarrow \pi^0 e^+ e^-$  and to the earlier calculations of this latter decay by Cheng (1967) using the vector-dominance model. Making certain assumptions about  $S=0$  pseudoscalar meson couplings to  $K^0$ , Sehgal obtains a significantly higher branching fraction for  $K_L^0 \rightarrow \pi^0 e^+ e^-$ , namely,  $1.5 \times 10^{-11}$ .

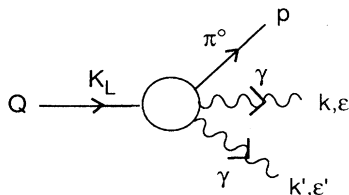


FIG. 7. Definition of momentum 4-vectors in the decay  $K_L^0 \rightarrow \pi^0 \gamma \gamma$  (after Sehgal, 1990).

More recently, there have been significant efforts to evaluate the rate for  $K_L^0 \rightarrow \pi^0 \gamma \gamma$  and its contribution as an intermediate state to  $K_L^0 \rightarrow \pi^0 e^+ e^-$  within the framework of the chiral perturbation theory. This formalism turned out to be a powerful tool for analyzing processes involving photons and pseudoscalar mesons at low energies (Weinberg, 1979c; Gasser and Leutwyler, 1985). The fundamental difficulty in applying the technique to the  $K_L^0 \rightarrow \pi^0 \gamma \gamma$  channel lies in the fact that the first contribution that is not suppressed by the square of the electron mass comes from terms of order  $p^6$  [ $B$  amplitude in Eq. (2.12)]. Evaluation of those terms must take into account both the pole diagrams and the direct weak counterterms and at the present time is highly model dependent.

Thus the most recent calculations of the  $K_L^0 \rightarrow \pi^0 \gamma \gamma$  rate have focused on identifying and calculating the general mechanisms that contribute to this reaction. Figure 8 illustrates the two general categories, the so-called loop or pion-decay mechanism originally calculated by Sehgal (1972), which contributes only to the  $A$  amplitude, and vector-meson dominance (VMD), giving contributions to both amplitudes. It is generally recognized that a realistic calculation would include contributions from both of these mechanisms and from the interference between them, using an effective Lagrangian that takes proper account of all the symmetries relevant in weak decays. Lacking such a general formalism, however, the current calculations tend to be more phenomenological.

There have been a number of extensive calculations of the first general class of diagrams using somewhat different techniques. Specific variants include pseudoscalar-meson pole dominance (Ko and Truong, 1991), a pion-scattering model (Ko and Rosner, 1989), chiral perturbation theory (Ecker *et al.*, 1987a; see also Donoghue *et al.*, 1987 and Ivanov, 1992), and a quark model within the framework of the chiral Lagrangian formalism (Bijnens *et al.*, 1991). Independent of the details of the model, the results are quite similar: a branching fraction for  $K_L^0 \rightarrow \pi^0 \gamma \gamma$  slightly below  $10^{-6}$  (e.g.,  $6.8 \times 10^{-7}$  in Ecker *et al.*, 1987a, 1988; see also Donoghue *et al.*, 1987), strong peaking of the  $\gamma\gamma$  spectrum around  $m_{\gamma\gamma} \approx 325$  MeV, and a relatively small contribution to the  $K^0 \rightarrow \pi^0 e^+ e^-$  rate, i.e.,  $10^{-13}$  or less ( $8 \times 10^{-15}$  in Ecker *et al.*, 1988; see also Donoghue *et al.*, 1987).

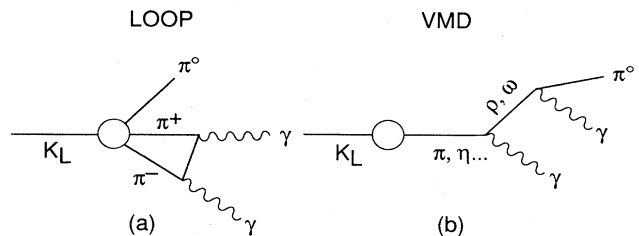


FIG. 8. The decay  $K_L^0 \rightarrow \pi^0 \gamma \gamma$ : (a) Diagram illustrating pion-loop mechanism; (b) diagram illustrating VMD mechanism (after Sehgal, 1990).

The past few years have also seen a number of published efforts to calculate the other set of diagrams, i.e., those for vector-meson dominance, and to include the interference effects between these two classes (Flynn and Randall, 1989b; Morozumi and Iwasaki, 1989; Ko, 1990; Sehgal, 1990). Ecker *et al.* (1990) have examined the contributions of vector mesons in this decay within the context of the chiral perturbation theory. Again, even though details differ, the general features are relatively well defined for the VMD mechanism also: a somewhat larger rate for  $K_L^0 \rightarrow \pi^0 \gamma \gamma$ , a potentially significantly higher contribution to  $K_L^0 \rightarrow \pi^0 e^+ e^-$  due to lack of chirality suppression, and peaking of  $m_{\gamma\gamma}$  below  $m_{\pi^0}$ . To illustrate the differences in the spectrum for the two general hypotheses, we show in Fig. 9 the differential decay rate as a function of  $m_{\gamma\gamma}$  for the pion loop and for the vector-meson-dominance diagrams, as calculated by Sehgal (1990). The importance of interference effects is shown in Fig. 10 from the calculations in the same paper. A somewhat more detailed illustration of sensitivity to various parameters is shown in Fig. 11 and Table I, where the calculations are from Ecker, Pich, and de Rafael (1990).  $a_V$  is the strength of the vector-meson exchange diagram and a value of  $|a_V| = 0.32$  is estimated to be the best guess according to the authors. We note, from Table I, the very rapid rise of  $B(K_L^0 \rightarrow \pi^0 e^+ e^-)$  as the VMD amplitude is introduced and then increased. The corresponding increase in  $B(K_L^0 \rightarrow \pi^0 \gamma \gamma)$  is considerably smaller.

We turn now to the experimental situation on  $B(K_L^0 \rightarrow \pi^0 \gamma \gamma)$ . Two different measurements have been reported in the literature, each a by-product of the  $\epsilon'/\epsilon$  measurements, one at CERN and the other at Fermilab. In both cases, the main experimental background is due

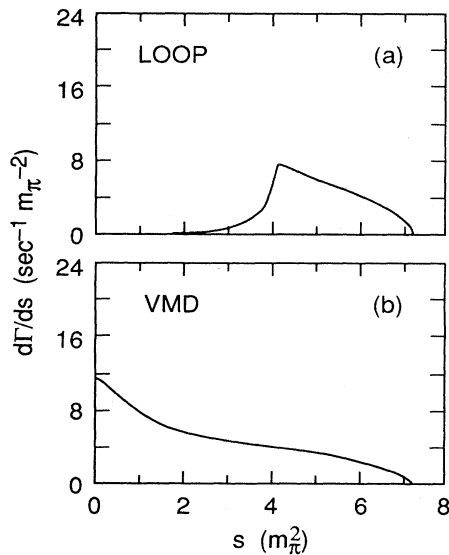


FIG. 9. Differential decay rate for  $K_L^0 \rightarrow \pi^0 \gamma \gamma$  as a function of invariant mass of the photon pair: (a) Loop mechanism alone; (b) VMD mechanism alone (after Sehgal, 1990).

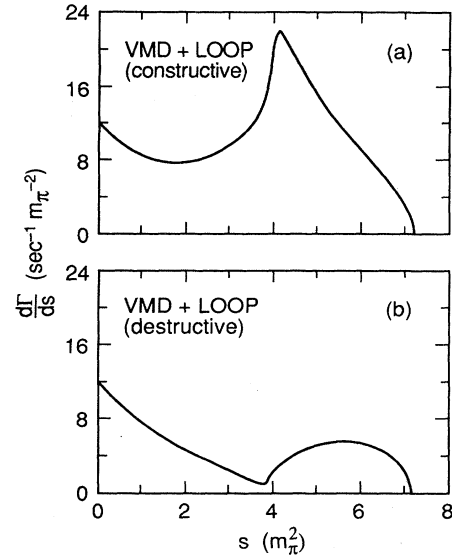


FIG. 10. Differential decay rate for  $K_L^0 \rightarrow \pi^0 \gamma \gamma$  including both loop and VMD contributions: (a) constructive interference; (b) destructive interference (after Sehgal, 1990).

to the decay  $K_L^0 \rightarrow \pi^0 \pi^0 \pi^0$ , either with two of the  $\gamma$ 's being relatively soft and escaping undetected or (especially in the Fermilab experiment) two of the photons overlapping each other in the electromagnetic calorimeter and one photon missing the detectors. Both experiments are relatively insensitive in the region of  $M_{\gamma\gamma} \approx 135$  MeV because of the dominant  $K_L^0 \rightarrow \pi^0 \pi^0$  mode. To be accepted, both analyses require the events to have four and only four visible photons, have a vertex in a restricted fiducial volume, have two photons consistent with a  $\pi^0$  mass, and be completely inconsistent with a  $2\pi^0$  hypothesis. The main difference in the two experimental setups, relevant

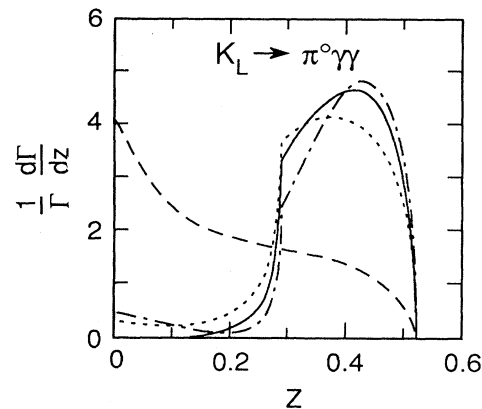


FIG. 11. Normalized spectra for the decay mode  $K_L^0 \rightarrow \pi^0 \gamma \gamma$  as a function of the  $2\gamma$  invariant mass  $z = (q_1 + q_2)^2 / M_K^2$ : solid curve,  $a_V = 0$ ; dot-dashed curve,  $a_V = 0.32$  (dotted curve),  $a_V = -0.32$ . Also shown is the distribution for the pure  $V$  exchange amplitude corresponding to  $|a_V| \rightarrow \infty$  (dashed curve). After Ecker, Pich, and de Rafael, 1990.

TABLE I. Predictions for  $B(K_L^0 \rightarrow \pi^0 \gamma \gamma)$  and  $B(K_L^0 \rightarrow \pi^0 e^+ e^-)$  (absorptive part due to  $\pi^0 \gamma \gamma$  intermediate state only) for various values of the effective vector coupling  $a_V$ . Here  $a_V = 0.32$  corresponds to the weak-deformation model of Ecker, Pich, and de Rafael (1990) and is considered by these authors to be the best guess for that parameter.

$a_V$	$B(K_L^0 \rightarrow \pi^0 \gamma \gamma) \times 10^6$	$B(K_L^0 \rightarrow \pi^0 e^+ e^-) _{\text{abs}} \times 10^{13}$
0	0.67	$8 \times 10^{-2}$
0.32	0.60	4.5
-0.32	0.89	4.5
1.5	1.6	100
-1.5	3.0	100

for this measurement, stems from the different electromagnetic calorimeters. The liquid-argon detector at CERN gives better spatial resolution at the expense of the energy measurement; the Pb-glass detector at Fermilab emphasizes the energy measurement but has coarser position resolution.

The mass spectrum of the two non- $\pi^0$   $\gamma$ 's ( $m_{34}$ ) from the CERN experiment (Barr *et al.*, 1992) is shown in Fig. 12, together with the calculated efficiency. The data show pronounced peaking around 300 MeV/ $c^2$ . One should point out that the theoretical curves shown in earlier figures used an abscissa scale proportional to the square of  $M_{\gamma\gamma}$ . In addition to the spectrum, the experi-

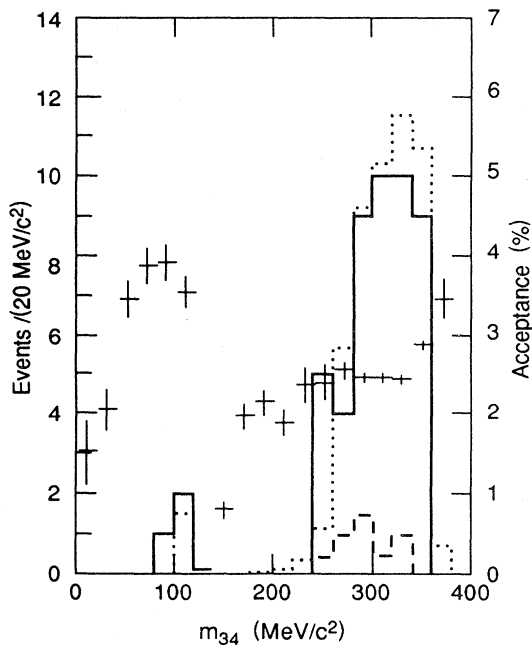


FIG. 12. Invariant  $\gamma\gamma$  mass  $m_{34}$  distribution from the CERN experiment for  $K_L^0 \rightarrow \pi^0 \gamma \gamma$  candidates: solid curve, events passing all cuts in the signal region defined by  $132.5 \text{ MeV} < m_{12} < 137.5 \text{ MeV}$ ; dashed curve, events in the  $m_{12}$  sidebands normalized to the signal interval; dotted curve,  $K_L^0 \rightarrow \pi^0 \gamma \gamma$  events simulated with  $a_V = 0$ . The crosses indicate the calculated acceptance (after Barr *et al.*, 1992).

menters quote two numbers relevant to adjudication of the theoretical issues discussed above. The branching ratio (based on the observed  $57 \pm 8.1$  events) is calculated to be

$$B(K_L^0 \rightarrow \pi^0 \gamma \gamma) = (1.7 \pm 0.2) \times 10^{-6}, \quad (2.14)$$

where the error is statistical only. Furthermore, there is a systematic error of  $0.2 \times 10^{-6}$  due to uncertainties in residual background estimates, the acceptance, energy scale, and value of the  $K_L^0 \rightarrow 2\pi^0$  branching ratio used for normalization. In addition, from the spectrum of events as a function of  $m_{34}$ , Barr *et al.* calculate the limit

$$\frac{\Gamma(m_{34} < 240 \text{ MeV})}{\Gamma(\text{all } m_{34})} < 0.09 \text{ (90\% C.L.)}, \quad (2.15)$$

which gives a 90% C.L. range on  $a_V$  (Ecker *et al.*, 1990) of

$$-0.38 < a_V < 0.41. \quad (2.16)$$

A more precise value of  $a_V$  can be obtained by a maximum likelihood fit using the variables  $m_{34}$  and  $y$ , the latter defined by  $y = |E_3 - E_4|/m_K$ , where  $E_3$  and  $E_4$  are photon energies in the  $K_L^0$  rest frame. The result of the analysis is

$$a_V = -0.05_{-0.17}^{+0.14}, \quad (2.17)$$

which translates into a 90%-confidence-level range of  $-0.32 < a_V < 0.19$ .

A similar  $M_{\gamma\gamma}$  histogram from Fermilab experiment E731 (Papadimitriou *et al.*, 1991) is displayed in Fig. 13,

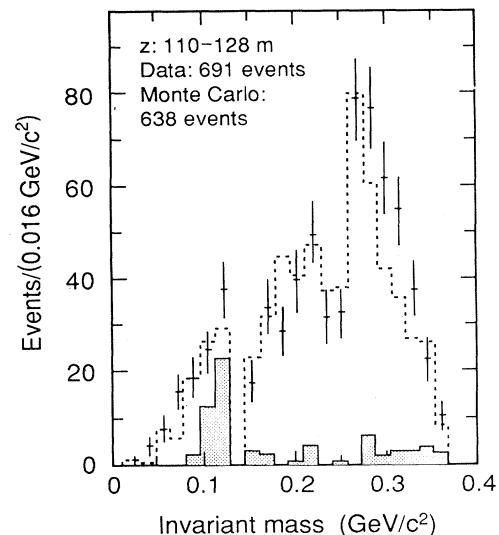


FIG. 13. Data/Monte Carlo comparison of the  $\gamma\gamma$  mass distribution for  $K_L^0 \rightarrow \pi^0 \gamma \gamma$  candidates and for background events from the Fermilab experiment. The normalization is absolute. The error bars correspond to the data, the solid histogram to the  $2\pi^0$ -background Monte Carlo simulation, and the dashed histogram to the sum of the  $3\pi^0$  and  $2\pi^0$  background Monte Carlo simulations (after Papadimitriou *et al.*, 1991).

which shows the data together with the Monte Carlo background calculation normalized to the total flux. Again, peaking of signal events at high  $M_{\gamma\gamma}$  is evident. Normalizing to the  $K_L^0 \rightarrow \pi^0 \pi^0$  branching fraction, Papanimitriou *et al.* obtained

$$B(K_L^0 \rightarrow \pi^0 \gamma \gamma) = (2.2 \pm 0.7 \pm 0.7) \times 10^{-6}, \quad (2.18)$$

where only events with  $M_{\gamma\gamma} > 280$  MeV were used and the contribution from lower values of the  $M_{\gamma\gamma}$  was calculated by assuming the shape of  $M_{\gamma\gamma}$  spectrum as predicted by chiral perturbation theory. In addition, they extracted a limit on contributions with low  $M_{\gamma\gamma}$ ,

$$B(K_L^0 \rightarrow \pi^0 \gamma \gamma, M_{\gamma\gamma} < 264 \text{ MeV}) < 5.1 \times 10^{-6} \text{ (90\% C.L.)}. \quad (2.19)$$

There is consistency between the two sets of data, and one is able to draw some tentative conclusions regarding the main theoretical issues discussed above. The general features of the data, as compared to the theoretical models, can be summarized as follows:

(a) The  $M_{\gamma\gamma}$  spectrum favors dominance of the chiral perturbation-theory model.

(b) The branching fraction is higher than predicted by the simple chiral perturbation theory. Thus some vector-meson contributions are probably required.

(c) The most recent data from the experiment at CERN favor a relatively small amplitude for the  $CP$ -conserving  $K_L^0 \rightarrow \pi^0 e^+ e^-$  process (e.g., see Table I). Their estimate for the branching fraction due to this mechanism is  $4.5 \times 10^{-13}$  (Iconomidou-Fayard, 1992).

### 5. Status of the $K_L^0 \rightarrow \pi^0 e^+ e^-$ experiments

The present experiments in this area are still far from achieving the sensitivities necessary to conduct meaningful studies of  $CP$  violation. Furthermore, it is not clear at this time whether background limitations may not make such studies impossible. On the other hand, the efforts of the last few years have made a significant contribution towards attacking these problems and provided guidelines as to the design of future experiments.

In discussing the  $K_L^0 \rightarrow \pi^0 e^+ e^-$  experimental program, it appears convenient to identify three distinct periods:

(a) An initial phase during which the searches for the  $K_L^0 \rightarrow \pi^0 e^+ e^-$  mode were a spinoff from other experimental programs and thus utilized experimental apparatus and/or trigger logic that were not necessarily optimized for such measurements. These efforts yielded branching-fraction limits in the range  $10^{-7}$ – $10^{-8}$ .

(b) The current phase, representing the first generation of dedicated  $K_L^0 \rightarrow \pi^0 e^+ e^-$  experiments. These experiments are not expected to see a signal unless the decay rate has some large unexpected contribution from a source other than those discussed above. The design goals of these experiments are to achieve sensitivities in the neighborhood of  $10^{-10}$ .

(c) A future phase, in which the next generation of experiments will build on the experience gained during the previous two phases and also rely on improvements in detector and accelerator technology. The obvious goal of that phase would be to begin to probe a sensitivity region that is interesting from the point of view of  $CP$  violation.

In the past five years, four experiments have been completed, each one of them successively improving the branching-fraction limit. The first three have been first-phase experiments in the sense defined above. The last one represented a modified experimental setup, originally constructed for other measurements but subsequently optimized for detection of electrons and photons over a large solid angle. The earliest published result of Jastrzemski *et al.* (1988) used data from an apparatus designed for searches for  $K_L^0 \rightarrow \mu e$  and  $ee$ ; the next two results, Barr *et al.* (1988) and Barker *et al.* (1990; see also Gibbons *et al.*, 1988), are based on the analysis of data taken for an  $e'/\epsilon$  measurement; the  $\pi^0 e^+ e^-$  final state can be studied in these experiments, since topologically the events are similar to those from the  $\pi^0 \pi^0$  final state. The last experiment, Ohl *et al.* (1990a), was a dedicated  $K_L^0 \rightarrow \pi^0 e^+ e^-$  experiment, but used elements from the detector in the experiment of Jastrzemski *et al.* (1988). The results are tabulated in Table II.

In experimental searches for the  $K_L^0 \rightarrow \pi^0 e^+ e^-$  mode it is conventional to display candidate events as points in the two-dimensional,  $\theta_K^2$  (or  $P_T^2$ )– $m_{\pi^0 e^+ e^-}$  space.  $\theta_K$  refers to the angle between the directions of the vector sum of  $\pi^0$ ,  $e^+$ , and  $e^-$  momenta and that of the neutral  $K_L^0$ .  $P_T$  is the transverse momentum of that resultant momentum vector calculated with respect to the direction of the  $K_L^0$ . Both of these quantities should be zero for an ideally measured  $K_L^0 \rightarrow \pi^0 e^+ e^-$  event and an infinitesimally small production target. The final scatter plots from the two most recent and most accurate experiments are displayed in Figs. 14 and 15.

The most important backgrounds in these experiments appear to be due to  $K_L^0 \rightarrow \pi^0 \pi^0 \pi^0$  and  $K_L^0 \rightarrow \pi^0 \pi^0$  with  $\pi^0$  Dalitz decays,  $K_L^0 \rightarrow \pi e \nu$  with a pion misidentified as an electron and an accidental  $\pi^0$ , and the decay  $K_L^0 \rightarrow e^+ e^- \gamma$  with an internal radiation. The last process (Greenlee, 1990) may turn out to provide the ultimate limit on achievable sensitivity, and we shall return to this later in this section.

The first two background processes can be suppressed by high detection efficiency for the photons, and thus it is

TABLE II. Results from the recently published  $K_L^0 \rightarrow \pi^0 e^+ e^-$  experiments.

Experiment	Reference	Laboratory	Result (90% C.L.)
Jastrzemski <i>et al.</i>	(1988)	BNL	$\leq 3.2 \times 10^{-7}$
Barr <i>et al.</i>	(1988)	CERN	$\leq 4 \times 10^{-8}$
Barker <i>et al.</i>	(1990)	Fermilab	$\leq 7.5 \times 10^{-9}$
Ohl <i>et al.</i>	(1990a)	BNL	$\leq 5.5 \times 10^{-9}$

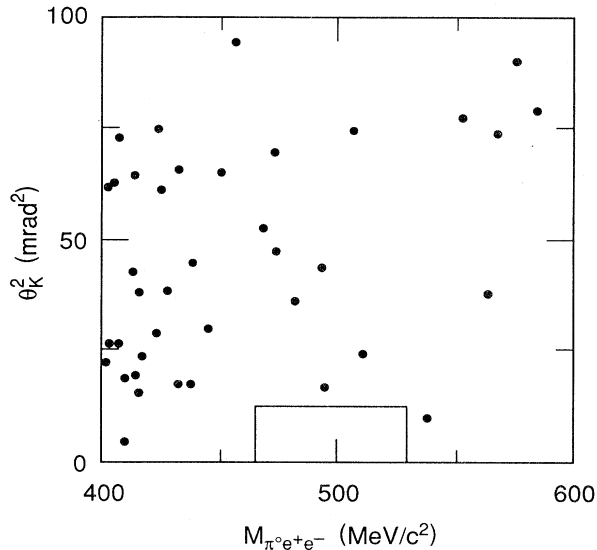


FIG. 14. Event scatter plot of the square of the  $\theta_K$  (defined in the text) vs the  $\pi^0 e^+ e^-$  effective mass for BNL experiment 845. The box represents the signal region (after Ohl *et al.*, 1990a).

helpful to surround the decay region and the active detector volume with veto counters. Clearly, good  $\pi$ - $e$  rejection and good timing help to reject the  $K \rightarrow \pi e \nu$  background. Finally, since the ultimate signal is defined by kinematical variables, there is a premium on good position and energy measurement of the  $\gamma$ 's and on the accurate reconstruction of the electron tracks. One might also mention that an analyzing magnet in the spectrometer helps to remove one additional background, i.e.,  $K_L^0 \rightarrow \pi^0 \pi^0$ , where both photons from one  $\pi^0$  convert into

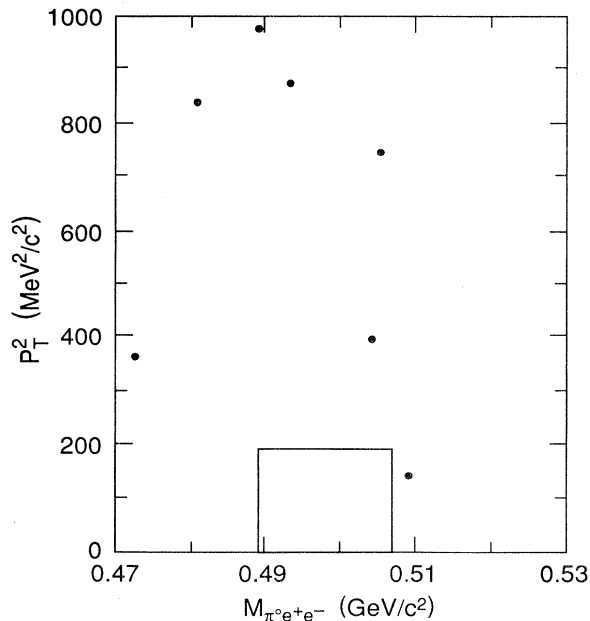


FIG. 15. The square of the transverse momentum vs reconstructed kaon mass for  $K_L^0 \rightarrow \pi^0 e^+ e^-$  from Fermilab experiment 731. The box represents the signal region (after Barker *et al.*, 1990).

TABLE III. Parameters of experiment E162 at KEK.

Institutions	KEK and Kyoto Univ.
Solid angle	320 $\mu$ sr
Accepted $K_L^0$ spectrum	2–10 GeV
Number of protons/spill	$2 \times 10^{12}$
Length of decay volume	4 m
Decay prob. $\times$ acceptance	$3.2\% \times 1.75\% = 5.6 \times 10^{-4}$

$e^+ e^-$  pairs early in the detector. In the absence of the magnet, such pairs would appear as single electrons in the tracking chambers, and the event would satisfy all relevant kinematical constraints. It appears that such a background provided the ultimate limit to the sensitivity of the CERN experiment (Barr *et al.*, 1988).

Figures 16 and 17 show the experimental setups for the Fermilab experiment E731 and the most recent BNL experiment (E845). The fundamental features are quite similar in both detectors: a decay volume followed by a one-magnet spectrometer, a direction-measuring tracking chamber system on both sides of the magnet, a lead glass electromagnetic calorimeter, and a system of photon vetoes. The Fermilab experiment relies entirely on Pb glass for electron identification and thus they find that the shape cuts on shower profiles help to obtain a cleaner electron sample. The BNL experiment used a hydrogen-filled threshold Čerenkov counter in the magnet to give an independent signature for electrons. There is a significant difference in scale for the two experiments, reflecting the quite different energy spectra of  $K_L^0$ 's produced at BNL and at FNAL.

Two other dedicated experiments, experiment E162 at KEK in Japan and experiment E799 at Fermilab, are currently running or in the setting up stage. The KEK experiment will work in an energy domain that is even lower than that of BNL, and its general schematic layout resembles the BNL experiment, as can be seen from Fig. 18. Its stated goal is a sensitivity of  $2 \times 10^{-10}$ , and that goal identifies several areas where technology needs to be pushed forward. The electromagnetic calorimeter is made of pure CsI to achieve excellent energy resolution with short integrating times. To cope with high rates in the tracking chambers, fast gas will be used together with time-to-digital converters with a least count in the one-nanosecond range developed especially for this experiment. An engineering run is planned for the fall of 1993. The general features of E162 at KEK are summarized (Miyake *et al.*, 1988) in Table III.

The other new experiment (Barker *et al.*, 1988), E799 at Fermilab, took its initial data at the end of 1991 and will have an additional period of data taking during the next fixed-target running cycle at Fermilab, probably in 1995. The experiment planned to achieve a  $10^{-10}$  sensitivity for the  $\pi^0 e^+ e^-$  mode in its 1991 run. The detector for that run was essentially the E731 apparatus with improved electron identification obtained by the addition of a set of three transition radiation detectors.<sup>1</sup>

<sup>1</sup>See Addendum at end of this article.

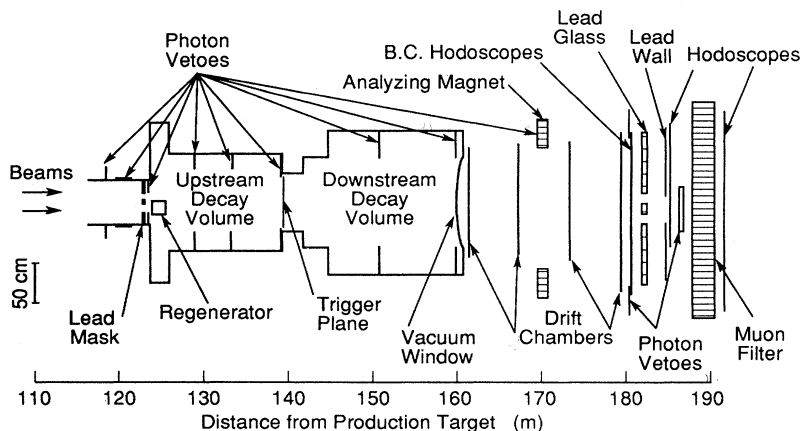


FIG. 16. Detector schematic elevation view for the Fermilab  $\epsilon'/\epsilon$  experiment.

The second phase of this experiment is expected to provide another improvement in sensitivity by a factor of 5–10. The major detector upgrade would consist of replacement of Pb glass with CsI, which should improve the resolution by about a factor of 6. Other modifications are also planned to allow the apparatus to handle higher proton fluxes on target. Monte Carlo simulation studies have indicated that in the proposed configuration one might expect one  $K_L^0 \rightarrow e^+e^-\gamma\gamma$  background event if one reaches a single-event sensitivity level of  $3 \times 10^{-11}$ .

6. Future prospects

Our earlier discussion of phenomenology indicated that the total branching fraction for the process  $K_L^0 \rightarrow \pi^0 e^+ e^-$  is probably no higher than  $10^{-11}$ . Furthermore, to disentangle the  $CP$ -violating direct amplitude, at least 100 events will probably be required, more if nature conspires to make the other two amplitudes

comparable or dominant. Thus single-event sensitivity better than  $10^{-13}$  is probably necessary to make a meaningful attempt to study  $CP$  violation. To put it in perspective, that is about an order of magnitude better than the proposed next generation of lepton-flavor-violating search experiments, looking for  $K_L^0 \rightarrow \mu e$  and  $K^+ \rightarrow \pi^+ \mu^+ e^-$ . It is hard to believe that the detection efficiency for  $K_L^0 \rightarrow \pi^0 e^+ e^-$  could be better than for those two processes, since the latter is essentially a four-body decay. Thus considerably higher  $K_L^0$  fluxes will be required to reach the physics objectives, with a corresponding increase in the demands that will be placed on the performance of the detector.

Besides the question of being able to achieve the required flux, one also has to address the question of backgrounds. Greenlee (1990) has recently looked in some detail at the channel  $K_L^0 \rightarrow e^+ e^- \gamma\gamma$  from the point of view of possible background to the  $K_L^0 \rightarrow \pi^0 e^+ e^-$  study. That process is predicted by QED to occur with a branching fraction of  $5.8 \times 10^{-7}$ , and the prediction has been recently verified (Morse *et al.*, 1992) by an experiment that gave a value for the branching fraction of  $(6.6 \pm 3.2) \times 10^{-7}$ . Clearly, from the purely kinematical

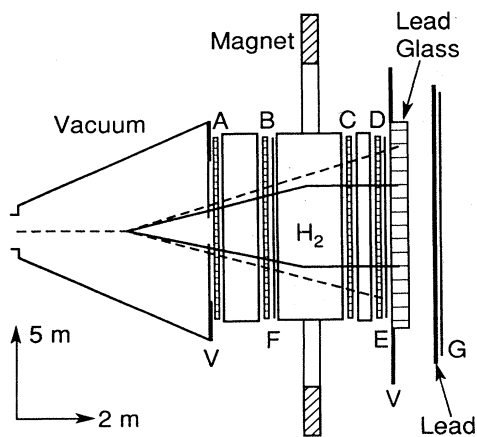


FIG. 17. Schematic of the BNL E845 detector. The neutral beam enters from the left. Note the different horizontal and vertical scales.

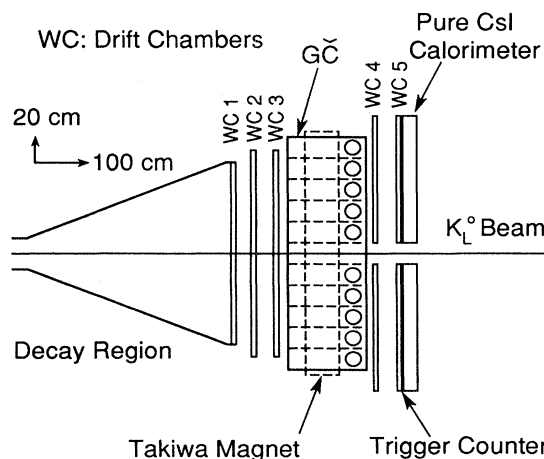


FIG. 18. Schematic of apparatus for experiment E162 at KEK.

point of view, the only handle one has for rejection of this background is the requirement that  $m_{\gamma\gamma} = m_{\pi^0}$ . In addition, however, one might try making various cuts on the data so as to suppress that part of phase space which favors the  $e^+e^-\gamma\gamma$  configurations, but does not decrease significantly the acceptance for  $\pi^0e^+e^-$ .

The Feynman diagrams for this potential background process are indicated in Fig. 19. Because of interference effects between the two  $\gamma$ 's, the obvious cuts on angles between electrons and  $\gamma$ 's do not eliminate as much background as one might naively expect. Greenlee (1990) explored the kinematical space available to see how the background rate would vary as a function of cuts, and how those cuts would decrease the acceptance for  $\pi^0e^+e^-$ . His results are displayed in Fig. 20 and show that, even at the singular point of optimum background rejection, one would have a background at the level of about  $2 \times 10^{-11}$ . Probably a more realistic number would be around  $10^{-10}$ , corresponding to a  $\pi^0e^+e^-$  efficiency of about 50%. This calculation assumes a mass cut on the  $\pi^0$  mass at  $\pm 5$  MeV. Thus, on the basis of these calculations, one can draw two conclusions:

- There is a large premium on good photon resolution and hence precise determination of the  $\gamma\gamma$  effective mass.
- Future experiments with design sensitivities of  $O(10^{-13})$  or better will have to rely on subtracting the  $ee\gamma\gamma$  background on a statistical basis. This should be possible, because one will be able to measure experimentally this background level with very high precision by looking at  $m_{\gamma\gamma}$  sidebands on both sides of the  $\pi^0$  mass. It will, however, make the experiment more difficult and require somewhat more statistics, especially if the

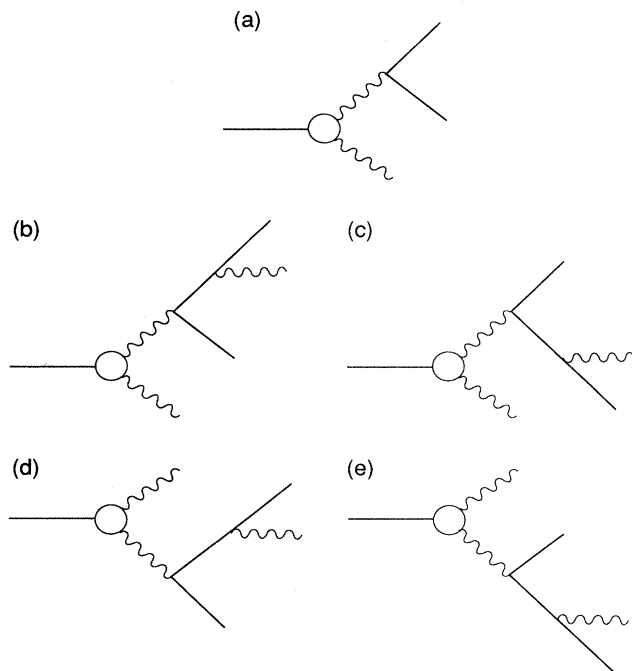


FIG. 19. Feynman diagrams for (a)  $K_L^0 \rightarrow ee\gamma$  and (b)–(e)  $K_L^0 \rightarrow ee\gamma\gamma$  (after Greenlee, 1990).

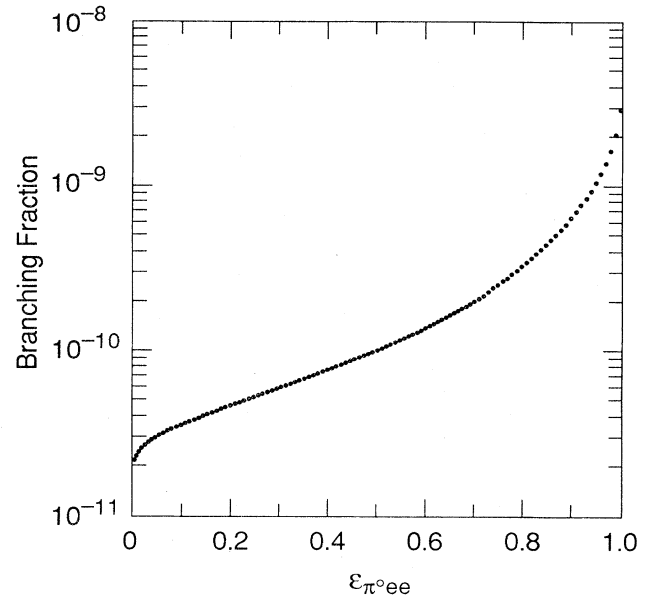


FIG. 20. Contribution to branching fraction due to  $ee\gamma\gamma$  background as a function of the efficiency for  $K_L^0 \rightarrow \pi^0 ee$  when different cuts are applied (after Greenlee, 1990).

differentiation between the three contributing  $K_L^0 \rightarrow \pi^0 e^+ e^-$  mechanisms turns out to be important because of the comparable amplitudes.

One might consider the optimum beam energy for these experiments. Most  $K_L^0$ -decay experiments are relatively insensitive to the energy of the primary proton (or secondary  $K_L^0$ ) beam because most relevant experimental parameters scale in such a way as to keep the cost of the apparatus independent of energy for the same performance. However, one parameter that does not scale is the photon energy measurement via calorimetric technique, where the fractional error tends to decrease as  $E_\gamma^{-1/2}$ . In light of the high premium on precise  $\pi^0$  mass determination, this feature is probably quite important and argues for reasonably high energies in future high-sensitivity experiments.

At the present time there are no firm proposals for a  $K_L^0 \rightarrow \pi^0 e^+ e^-$  experiment at the  $CP$  violation sensitivity level. There have been some preliminary studies (KTeV Design Report, 1992) in connection with the possibility of using medium-energy beams from Fermilab's Main Injector, currently under construction. The high intensity that would be potentially available would offer high enough fluxes to allow one to achieve the sensitivities required from the statistical point of view. Clearly, detailed studies will be necessary to see if the backgrounds can be kept at sufficiently low levels to make a meaningful experiment possible.

## B. $K \rightarrow \pi\mu^+\mu^-$ decays

The  $\pi\mu^+\mu^-$  final-state channel offers a complementary way of studying some of the questions discussed in the

preceding section. From both the experimental and theoretical points of view it presents some advantages and disadvantages with respect to the  $\pi e^+e^-$  mode. We discuss briefly the present status of these decay modes.

1. Phenomenology

The ratio of phase space for  $K^+ \rightarrow \pi^+\mu^+\mu^-$  vs  $K^+ \rightarrow \pi^+e^+e^-$  and for  $K^0 \rightarrow \pi^0\mu^+\mu^-$  vs  $K^0 \rightarrow \pi^0e^+e^-$  is 0.196 and 0.212, respectively. Thus naively one might expect a suppression factor of about 5 in the obtainable statistical precision for the  $\pi\mu\mu$  modes. However, the questions of experimental cuts and acceptance are quite different for the two modes. For example, it is quite likely that at least a fraction of the lower  $m_{ee}$  spectrum must be eliminated from the analysis because of possible backgrounds from the  $2\pi$  decay followed by a Dalitz decay of a  $\pi^0$ . If a cut of 140 MeV is used, the numbers quoted above increase to 0.317 and 0.337 (Ecker *et al.*, 1987b).

The areas in which the  $\pi\mu\mu$  mode provides additional or better information than the  $\pi ee$  mode are (a) alternative measurement of the contribution due to a single-photon intermediate state; (b) better sensitivity to the  $A$  amplitude in the  $\pi^0\gamma\gamma$  intermediate state, since it is not made negligible by the  $m_l$  suppression factor (Sehgal, 1988); and (c) smaller sensitivity to the  $ll\gamma\gamma$  background (Greenlee, 1990) because of the relatively lower frequency of internal radiation from the  $\mu$ 's.

Ecker, Pich, and de Rafael (1987b) have considered the  $K \rightarrow \pi\mu^+\mu^-$  processes in conjunction with the study of the  $K \rightarrow \pi ee$  decay using chiral perturbation theory and the one-photon intermediate state. They show that  $\pi\mu\mu$  shows approximately the same rate dependence on the  $w_+$  parameter (discussed previously in Sec. II.A.3) as the  $\pi ee$  mode. Thus it offers a complementary technique for obtaining the value of that parameter.

Sehgal (1988) and Ecker, Pich, and de Rafael (1988) have looked at the effect of the  $\pi\gamma\gamma$  intermediate state on the  $\pi\mu\mu/\pi ee$  ratio. Because of the  $m_l$  factor in the  $A$  amplitude, the  $\pi\mu\mu$  rate will be considerably enhanced. The important consequence of that fact for  $K_L^0$  decays is that, for a certain range of parameters, the contribution of the  $\pi\mu\mu$   $CP$ -conserving amplitude can actually dominate the  $CP$ -violating one, and the  $\pi\mu\mu$  rate can be comparable to the  $\pi ee$  rate. As an example, we quote some relevant results from the calculation of Ecker, Pich, and de Rafael (1988). For two values of the renormalization parameter  $w_s$  (linearly related to the previously discussed  $w_+$ ), deduced from an earlier measurement of the  $K^+ \rightarrow \pi^+e^+e^-$  branching fraction, they obtain the results in Table IV.

The parameter  $\text{Im}w_s$  measures the direct  $CP$  violation in  $K_L^0 \rightarrow \pi^0e^+e^-$  decay, and the three different values used in the table cover the expected range of that parameter. The parameter  $w_s$  is related to the previously used one,  $w_+$ , by

$$w_s = w_+ + \frac{1}{6} \ln \frac{m_{\pi^2}}{m_K^2} \quad (2.20)$$

TABLE IV. Calculated branching fractions for  $K_L^0 \rightarrow \pi^0\mu^+\mu^-$  and  $K_L^0 \rightarrow \pi^0e^+e^-$ .

$\text{Re}w_s$	$\text{Im}w_s$	$B(K_L^0 \rightarrow \pi^0e^+e^-)$	$B(K_L^0 \rightarrow \pi^0\mu^+\mu^-)$
0.73	$-10^{-3}$		$5.4 \times 10^{-12}$
0.73	0	$1.5 \times 10^{-12}$	$5.5 \times 10^{-12}$
0.73	$10^{-3}$		$6.3 \times 10^{-12}$
-1.00	$-10^{-3}$		$10.2 \times 10^{-12}$
-1.00	0	$15 \times 10^{-12}$	$8.4 \times 10^{-12}$
-1.00	$10^{-3}$		$7.2 \times 10^{-12}$

This relation is a consequence of the assumption of octet dominance for the decays  $K^+ \rightarrow \pi^+\gamma^*$  and  $K^0 \rightarrow \pi^0\gamma^*$  and does not follow directly from chiral perturbation theory (Ecker, Pich, and de Rafael, 1987b). We recall that the recent high-statistics experiment on  $K^+ \rightarrow \pi^+e^+e^-$  favors the positive value of  $w_s(w_+)$  and thus the smaller value of single-photon contribution. However, one must remember that the question of magnitude of the contribution of the  $\pi^0\gamma\gamma$  intermediate state to  $K_L^0 \rightarrow \pi^0e^+e^-$  is still not completely resolved; Table IV uses the Ecker, Pich, and de Rafael (1988; see also Donoghue *et al.*, 1987) calculation, which gives the result that this particular contribution is negligible. This

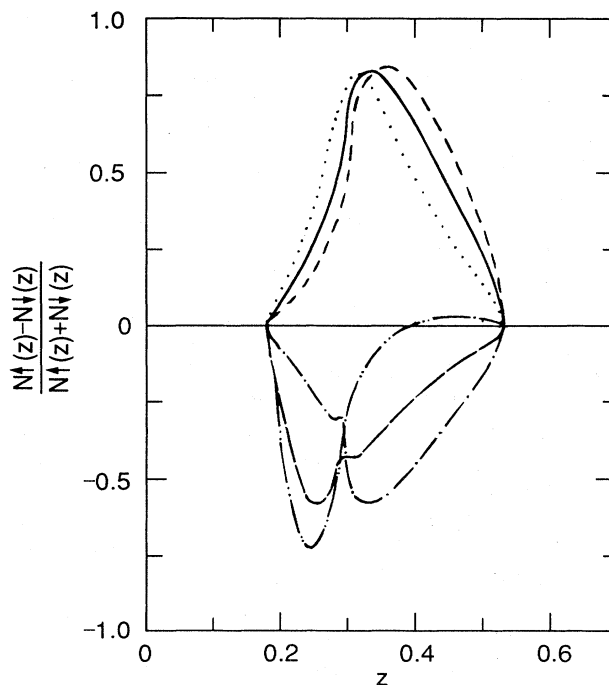


FIG. 21. Up-down asymmetry as a function of  $z$  (defined as  $z = m_{\mu\mu}^2/m_K^2$ ) for the two possible values of  $\text{Re}w_s$  and for three different values of  $\text{Im}w_s$  covering the expected range for this parameter. The different curves correspond to the following values of  $(\text{Re}w_s, \text{Im}w_s)$ : double-dot-dashed curve, (0.73,  $-10^{-3}$ ); long-dashed curve, (0.73, 0); dot-dashed curve, (0.73,  $+10^{-3}$ ); dashed curve, ( $-1.00, -10^{-3}$ ); solid curve ( $-1.00, 0$ ); dotted curve, ( $-1.00, +10^{-3}$ ) (after Ecker, Pich, and de Rafael, 1988).

should be contrasted, for example, with Sehgal's (1988) result of

$$B(K_L^0 \rightarrow \pi^0 e^+ e^-)|_{2\gamma} = 1.5 \times 10^{-11}. \quad (2.21)$$

As has been discussed previously, however, the latter model predicts a spectrum in  $K_L^0 \rightarrow \pi^0 \gamma \gamma$  that is in strong disagreement with the recent data.

From the results displayed in Table IV, we see that we can have comparable  $CP$ -violating and  $CP$ -conserving amplitudes, and thus one would expect large interference effects and hence possible large polarization effects. Specifically, in the  $K_L^0$  rest frame, one would expect up-down asymmetries with respect to the decay plane. The results of asymmetry calculations by Ecker, Pich, and de Rafael (1988) are shown in Fig. 21.

## 2. Experimental status

At present, only upper limits exist for both  $K^+ \rightarrow \pi^+ \mu^+ \mu^-$  and  $K_L^0 \rightarrow \pi^0 \mu^+ \mu^-$ . The best number for the first decay mode comes from experiment E787 (Atiya *et al.*, 1990a), optimized for the search for  $K^+ \rightarrow \pi^+ \nu \bar{\nu}$ . The main source of background in that experiment is believed to be the decay mode  $K^+ \rightarrow \pi^+ \pi^+ e^- \nu$  with a  $\pi \rightarrow \mu \nu$  decay and misidentification of an electron as a muon. Monte Carlo calculations predict  $0.3 \pm 0.3$  events from that source in the data sample that has been analyzed so far. Three events consistent with  $K^+ \rightarrow \pi^+ \mu^+ \mu^-$  have been found, a number insufficient, according to the authors, to establish the presence of this decay mode with sufficient statistical significance. Accordingly, they quote a 90%-confidence-level upper limit of  $B(K^+ \rightarrow \pi^+ \mu^+ \mu^-) \leq 2.3 \times 10^{-7}$ . This should be compared with the theoretical calculation (Ecker *et al.*, 1987b) of  $(4.5-6.1) \times 10^{-8}$ .

The best limit (Carroll *et al.*, 1980) at present for the decay mode  $K_L^0 \rightarrow \pi^0 \mu^+ \mu^-$  is  $1.2 \times 10^{-6}$ , still some five orders of magnitude higher than the current theoretical estimates. The biggest potential background channel here is the decay  $K_L^0 \rightarrow \pi^+ \pi^- \pi^0$  followed by two  $\pi \rightarrow \mu \nu$  decays. Experiment E799 at Fermilab (Barker *et al.*, 1988) will trigger on this mode, and the proponents hope to make a significant improvement in our knowledge of the possible magnitude of this particular branching fraction. In addition, this experiment should provide a first measurement of the decay rate  $K_L^0 \rightarrow \mu^+ \mu^- \gamma \gamma$ , which will allow one to estimate more precisely the potential background from that channel.<sup>2</sup>

Clearly this mode, if it can be studied with good statistics, is very interesting. It is probably less sensitive to the radiative background and, as discussed above, can provide an additional handle via polarization of the decay muons. Whether sufficient statistics can be obtained in the near future and whether the events can be background free is unclear.

<sup>2</sup>See Addendum at end of this article.

## C. $K_L^0 \rightarrow \pi^0 \nu \bar{\nu}$

This  $CP$  violation decay mode avoids some of the theoretical complexities associated with interpretation of the decay  $K_L^0 \rightarrow \pi^0 e^+ e^-$ , i.e., possibly significant contributions from indirect  $CP$  violation and from the  $CP$ -conserving  $2\gamma$  diagrams. This theoretical gain, however, is probably more than offset by the additional experimental difficulties associated with the detection of this process. In this section we discuss briefly the phenomenology of this decay mode, its experimental status today, and future prospects.

### 1. Phenomenology

Since there is no  $\gamma \gamma \rightarrow \nu \bar{\nu}$  coupling and since other long-distance contributions will be suppressed by the GIM mechanism and/or  $CP$  violation, the amplitude for  $K_L^0 \rightarrow \pi^0 \nu \bar{\nu}$  can be written as

$$A(K_L^0 \rightarrow \pi^0 \nu \bar{\nu}) = \epsilon A(K_1^0 \rightarrow \pi^0 \nu \bar{\nu}) + A(K_2^0 \rightarrow \pi^0 \nu \bar{\nu}), \quad (2.22)$$

and the appropriate  $K^0$  and  $\bar{K}^0$  amplitudes can be expected to be dominated by short-distance effects [ $Z$ -penguin and  $W$ -box diagrams; see Figs. 1(b) and 1(c)] and related to the  $K^+ \rightarrow \pi^+ \nu \bar{\nu}$  amplitude by isospin. Thus to estimate the  $K^0 \rightarrow \pi^0 \nu \bar{\nu}$  rate we can use the results of the calculations for the charged process (Inami and Lim, 1981). The range of values that are possible for the  $K^0$  decay rate into this channel were estimated initially by Littenberg (1989) and more recently by Bélanger and Geng (1991), Buchalla, Buras, and Harlander (1991), Dib, Dunietz, and Gilman (1991), and Geng and Turcotte (1991). The general conclusion is that the indirect contri-

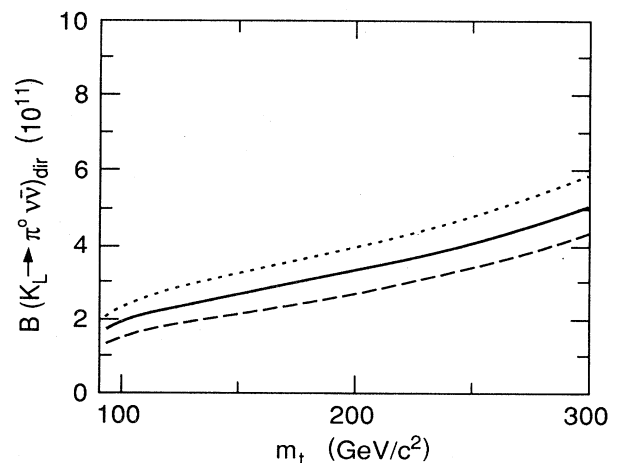


FIG. 22. Estimated value of the branching fraction for  $K_L^0 \rightarrow \pi^0 \nu \bar{\nu}$  (for three neutrino flavors) as a function of the mass of the top quark for  $f_B = 250 \pm 50$  MeV: dotted curve,  $m_c = 1.2$  GeV/ $c^2$ ; solid curve,  $m_c = 1.5$  GeV/ $c^2$ ; dashed curve,  $m_c = 1.8$  GeV/ $c^2$  (after Geng and Turcotte, 1991).

bution is about three orders of magnitude smaller than the direct one and that a branching fraction for three neutrino flavors should be in the neighborhood of  $10^{-11}$ .

The theoretical estimate for the  $K_L^0 \rightarrow \pi^0 \nu \bar{\nu}$  is uncertain by about an order of magnitude. Thus, for example, Geng and Turcotte (1991) obtain the range

$$0.8 \times 10^{-11} \leq B(K_L^0 \rightarrow \pi^0 \nu \bar{\nu})_{\text{dir}} \leq 7.0 \times 10^{-11} \quad (2.23)$$

for  $f_B = 250 \pm 50$  MeV. As with the direct contribution to  $K_L^0 \rightarrow \pi^0 e^+ e^-$ , the theoretical uncertainty here stems from our imperfect knowledge of such quantities as  $f_B$ ,  $B_B$ ,  $B_K$ , the CKM matrix elements,  $m_c$ , and  $m_t$ . The explicit functional dependence of that calculation on the masses of charm and top quark is shown in Fig. 22. The rather strong dependence on the mass of the charm quark exhibited there is, however, at variance with the Buchalla *et al.* (1991) result that the charm contribution is less than 0.5% for  $m_t > 90$  GeV.

## 2. Experimental situation

Until now there have been no planned and/or dedicated experiments to search for the decay mode  $K_L^0 \rightarrow \pi^0 \nu \bar{\nu}$ . Limits on its branching fraction, however, have been extracted from experiments designed to study other  $K_L^0$  decays.

An experiment optimized to search for the decay in question must be able to handle a high flux of  $K_L^0$ 's, have good hermiticity so that photons can be vetoed at a very high level, possess good ability to distinguish electrons from pions, have good photon energy resolution, and preferably also be able to measure photon direction. In addition, the quality of vacuum in the decay volume must be quite high to suppress possible neutron and  $K_L^0$  interactions.

The signature of  $K_L^0 \rightarrow \pi^0 \nu \bar{\nu}$  decay is a  $\pi^0$  emerging from the decay volume unaccompanied by any other particle. Thus, to suppress the much more abundant  $2\pi^0$  and  $3\pi^0$  modes, extremely high rejection of additional  $\gamma$ 's is needed. To achieve sensitivities low enough to confront theoretical predictions, it will probably be necessary to accept a statistical loss of about an order of magnitude and accept only those events with  $P_T^{\pi^0} > 209$  MeV/c. This value corresponds to the kinematical limit for the  $\pi^0$  from  $K_L^0 \rightarrow 2\pi^0$  decay and is well above the limit from  $3\pi^0$  decay. About 9.5% of all  $K_L^0 \rightarrow \pi^0 \nu \bar{\nu}$  will pass that cut (Littenberg, 1989).

To obtain sufficient rejection of backgrounds, some  $\gamma$  directional information is needed. This can be obtained either by converting  $\gamma$ 's in a thin radiator before the energy-measuring calorimeter or by relying on Dalitz decay of the  $\pi^0$ . Clearly, both would reduce the statistics and the latter would result in a loss by a factor of about  $\frac{1}{80}$ .

The first attempt to look for a possible  $K_L^0 \rightarrow \pi^0 \nu \bar{\nu}$  signal was made by Littenberg (1989), who analyzed the data originally taken for measurement of the  $K_L^0 \rightarrow \pi^0 \pi^0$

branching fraction (Cronin *et al.*, 1967; Wheeler, 1968). In that experiment, the  $2\pi^0$  mode was identified by the presence of photons with energy in the  $K_L^0$  rest frame greater than the kinematical limit for photons from the  $3\pi^0$  final state ( $E_{\text{max}} = 165$  MeV), but incompatible with  $K_L^0 \rightarrow 2\gamma$  decay ( $E_\gamma = 249$  MeV). To allow for experimental measurement errors, the  $2\pi^0$  search accepted only events with  $\gamma$ 's in the range  $180 < E_\gamma < 225$  MeV. Those photons could also have come from the  $\pi^0 \nu \bar{\nu}$  final state, and the fractional acceptance that results by using that cut is indicated graphically in Fig. 23. In the original Princeton experiment, 156 events were observed with a photon in the accepted energy range. If one subtracts the expected contribution from  $2\pi^0$  decay as well as the calculated backgrounds (Cronin *et al.*, 1967; Wheeler, 1968) and normalizes to the  $K_L^0 \rightarrow 3\pi^0$  decays, then one obtains a 90% confidence-level upper limit of  $B(K_L^0 \rightarrow \pi^0 \nu \bar{\nu}) < 7.6 \times 10^{-3}$ .

A more recent search, relying on  $\pi^0$  Dalitz decay, was performed by the E731 collaboration at Fermilab using a dedicated trigger requiring a charged track on each side of the beam (Graham *et al.*, 1992). For the event to be accepted, the charged tracks had to be of opposite charge and pass the electron criteria, the mass of the  $e^+e^-$  pair had to satisfy  $12 < m_{ee} < 48$  MeV and  $P_T^{ee} > 17$  MeV/c, the energy of the photon had to exceed 5 GeV, and the invariant mass of the detected system had to satisfy  $M_{\pi e \gamma} < 500$  MeV/c<sup>2</sup> (where one of the electrons was assigned pion mass). In addition, events from two background channels  $K_L^0 \rightarrow \pi e \gamma \nu$  and  $\Lambda \rightarrow n \pi^0$  ( $\pi^0 \rightarrow e^+ e^- \gamma$ ) were further suppressed by cuts on the angle between the  $e$  and  $\gamma$  and energy deposited in the beam hole calorimeter. The signal events were defined as those satisfying the requirements

$$140 \leq P_T^{\pi^0} < 240 \text{ MeV}/c \quad (2.24)$$

and

$$115 \leq m_{ee\gamma} \leq 155 \text{ MeV}/c \quad (2.25)$$

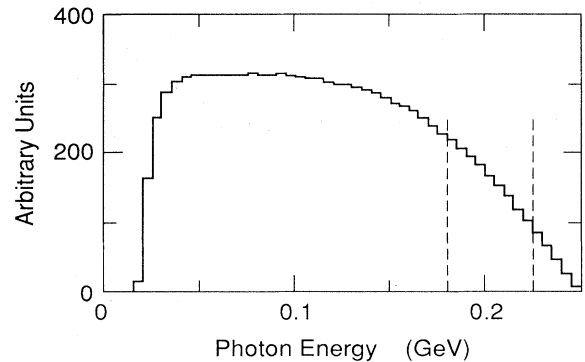


FIG. 23. Expected distribution of gamma energy in the  $K_L^0$  center of mass for the decay  $K_L^0 \rightarrow \pi^0 \nu \bar{\nu}$ . Vertical lines indicate region used by Littenberg to obtain the upper limit for that mode, as discussed in the text.

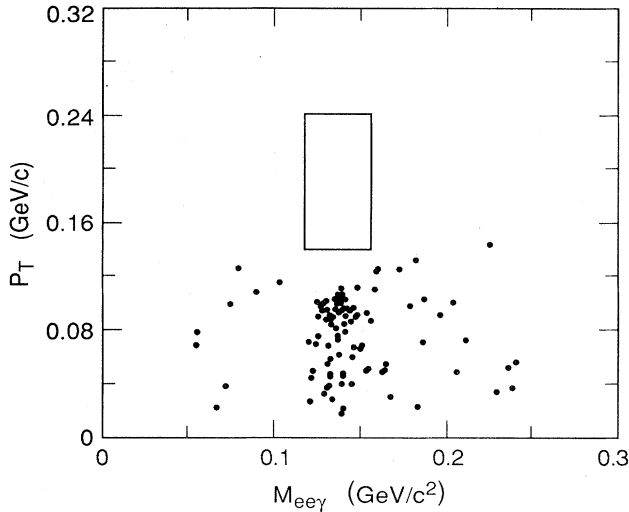


FIG. 24. Scatter plot of the transverse momentum of the  $ee\gamma$  system vs mass of that system for events surviving all cuts from Fermilab E731. The box represents the signal region for the  $K_L^0 \rightarrow \pi^0\nu\bar{\nu}$  events (after Graham *et al.*, 1992).

No events were seen in the signal box (Fig. 24), giving a 90%-confidence-level upper limit of  $B(K_L^0 \rightarrow \pi^0\nu\bar{\nu}) \leq 2.2 \times 10^{-4}$ . The radiative decay  $K_L^0 \rightarrow e^+e^-\gamma$  was used as a normalization.

Regarding future prospects, the second phase of the E799 experiment at Fermilab (Barker *et al.*, 1988), scheduled to run in a couple of years, anticipates being able to achieve a sensitivity for this mode of about  $3 \times 10^{-9}$ . Again, they will rely on using only events with the  $\pi^0$  Dalitz decay to give the  $P_T$  of the  $\pi^0$ . A CsI calorimeter, resulting in better electromagnetic energy measurement, will replace the lead glass in the experiment.

Clearly, the experimental state of the art is still quite far from achieving sensitivities of the order of  $10^{-11}$  that would enable one actually to see the signal. Even with a perfect  $P_T^{\pi^0}$  measurement, which would allow one to reject the  $2\pi^0$  background completely, one must still suppress two possible backgrounds that can give  $P_T^{\pi^0}$  greater than the maximum allowed for the  $2\pi^0$  mode. One of these is the  $\pi^0\gamma\gamma$  decay mode occurring at a level of about  $10^{-6}$ ; the other is the dominant  $K_L^0 \rightarrow \pi e\nu$  channel, which could simulate the Dalitz decay of a  $\pi^0$  via  $\pi \rightarrow e$  misidentification and could give a false  $K_L^0 \rightarrow \pi^0\nu\bar{\nu}$  decay signature by an additional chance coincidence with an accidental photon.

#### D. $K_L^0 \rightarrow \mu^+\mu^-$ polarization

The study of polarization in  $K_L^0 \rightarrow \mu^+\mu^-$  decay provides, in principle at least, another way of studying  $CP$  violation. In the Standard Model one predicts a very small effect due to the nonzero value of  $\epsilon$  ( $\sim 10^{-3}$  polar-

ization), and thus it is unlikely that such polarization could be detected in the foreseeable future. Thus observation of polarization in that channel with a magnitude significantly higher than 0.1% would indicate contributions from mechanisms outside of the Standard Model. In this section, we discuss the phenomenology of this process and experimental prospects.

#### 1. Phenomenology

The lepton pair in the final state can be either in the  $^1S_0$  or the  $^3P_0$  state; both of them have  $C = +$  quantum number, but different parities. Thus they are states with different  $CP$  quantum numbers. Since muon polarization, a parity-violating effect, requires the presence and interference of both of these states, finite  $\mu$  polarization will also signify  $CP$  violation in that decay. This process was considered in general terms some time ago by Pais and Treiman (1968) and more recently by Herczeg (1983). To introduce the subject we treat first the case of  $K_2^0$  decay, i.e., decay of a state with pure  $CP = -1$ . The most general invariant amplitude for this process can be written as

$$A = \bar{u}(l)[a + ib\gamma_5]v(\bar{l}), \quad (2.26)$$

where  $a$  is the  $CP$ -violating part and  $b$  the  $CP$ -conserving part. The longitudinal polarization, defined by

$$P = \frac{N_R - N_L}{N_R + N_L}, \quad (2.27)$$

where  $N_R$  ( $N_L$ ) is the number of  $\mu^+$ 's with positive (negative) helicity, is given by

$$P = \frac{2r \operatorname{Im}(ba^*)}{r^2|a|^2 + |b|^2}, \quad (2.28)$$

with

$$r \equiv \left[ 1 - \frac{4m_\mu^2}{m_K^2} \right]^{1/2} = 0.905. \quad (2.29)$$

Thus  $b$  and  $a$  must have a relative phase for polarization to exist. They have to be relatively real by  $CPT$  invariance, except for two effects. One is the final-state interactions, which here would be of electromagnetic origin and hence small; the second is "unitarity phases" originating from the existence of real intermediate states (Sehgal, 1969a). Since the intermediate  $2\gamma$  states have different  $CP$  quantum numbers for the two amplitudes, the relative phases of  $a$  and  $b$  can be different without violating  $CPT$ .

Still in the approximation that  $K_L^0 = K_2^0$ , Herczeg showed that to a very good approximation the expression for polarization can be written as

$$P = \frac{m_K r^2}{4\pi\Gamma} a^{(n)} \operatorname{Im}(b^{(e)})_{\gamma\gamma}, \quad (2.30)$$

where  $\Gamma$  is the decay rate of  $K_L^0$  and the superscripts  $(e)$  and  $(n)$  refer to electroweak and nonelectroweak (i.e., beyond the Standard Model) contributions to the ampli-

tudes. The  $\gamma\gamma$  subscript is written to emphasize that  $\text{Im}(b^{(e)})$  is due to the intermediate  $2\gamma$  state only.

Using the values of  $\Gamma(K_L^0 \rightarrow \text{all})$  and  $\Gamma(K_L^0 \rightarrow 2\gamma)$ , from the latest (at that time) edition of the Particle Data Group compilation (Kelly *et al.*, 1980), Herczeg then obtained

$$|P| \approx (5.7 \times 10^{11}) |a^{(n)}|. \quad (2.31)$$

Since the total  $K_L^0 \rightarrow \mu^+ \mu^-$  decay rate can be written as

$$\Gamma = \frac{m_K r}{8\pi} (|a|^2 + |b|^2), \quad (2.32)$$

knowledge of the  $K_L^0 \rightarrow \mu^+ \mu^-$  branching fraction would allow us to calculate an upper limit on the maximum value of polarization allowed. That limit is obtained by taking  $\text{Re}(b) = 0$ . Again, with the then current value of  $B(K_L^0 \rightarrow \mu^+ \mu^-) = (9.1 \pm 1.9) \times 10^{-9}$ , Herczeg obtained 96% as a maximum value of polarization. If we use the more current value of  $B(K_L^0 \rightarrow \gamma\gamma) = 5.7 \times 10^{-4}$  and take  $7.2 \times 10^{-9}$  for the  $K_L^0 \rightarrow \mu^+ \mu^-$  branching fraction, the maximum allowed polarization value reduces to 46%.

There are a number of mechanisms which could contribute towards generating a significant value of  $a$  (Herczeg, 1983; Botella and Lim, 1986; Geng and Ng, 1989) and thus yield a polarization value close to the allowed maximum. Flavor-changing Higgs boson exchange or leptoquark exchange are two of the possibilities explicitly considered by Herczeg. He showed that if appropriate values were chosen for some of the presently unrestricted parameters, high values of polarization could be obtained. The former possibility (Higgs boson) has been considered in more detail by Botella and Lim (1986) and Geng and Ng (1989), who showed that very large polarizations can be expected from light Higgs bosons, especially if their mass is comparable to that of  $K_L^0$ . The polarization decreases to a level of about 0.1% for Higgs masses around 10 GeV. Thus the recent LEP results, which rule out a light Higgs boson (Decamps *et al.*, 1990), exclude the possibility of significant polarization in the  $K_L^0 \rightarrow \mu^+ \mu^-$  decay channel due to this mechanism.

If we finally consider an actual case, i.e., a  $K_L^0$  state that is a non- $CP$  eigenstate but has a small admixture of  $CP$ -even  $K_1^0$ , then we can rewrite our  $a$  and  $b$  amplitudes as

$$\begin{aligned} a &= a_2 + i\epsilon a_1, \\ b &= b_2 + i\epsilon b_1, \end{aligned} \quad (2.33)$$

where the subscripts refer to the appropriate amplitudes for  $K_2^0$  and  $K_1^0$  decays into  $\mu^+ \mu^-$ .

The expression for polarization will then be given by

$$P \approx \frac{m_K r^2}{4\pi\Gamma} \text{Im}(a_2 b_2^* - i\epsilon^* a_2 b_1^* + i\epsilon a_1 b_2^*), \quad (2.34)$$

where the first term corresponds to the expression we have discussed above. The second term is negligible because it requires  $CP$  violation in the  $K_1^0 \rightarrow \mu^+ \mu^-$  decay;

the part of the third term that involves only the absorptive amplitudes can be calculated readily. Using the value obtained by Smith and Uy (1973) as the best estimate of  $\text{Im}(a)$ , Herczeg obtained the Standard Model prediction for  $K_L^0 \rightarrow \mu^+ \mu^-$  polarization (with inclusion of only absorptive amplitudes in the third term):

$$P^{\text{SM}} \approx 7.1 \times 10^{-4}. \quad (2.35)$$

The remaining parts of the third term are expected to give a comparable contribution.

## 2. Experimental prospects

There are at present no firm experimental plans to explore this area of physics. Measurement of polarization is difficult and requires large statistics; since the  $K_L^0 \rightarrow \mu^+ \mu^-$  decays are observed in flight, the  $\mu$ 's from that decay give generally a broad energy-band spectrum, and thus a very large apparatus is needed to stop a significant number of muons. In addition, the granularity of that part of the detector where  $\mu$ 's are stopped (referred to as the polarimeter) must be quite fine to be sensitive to the decay positron. The experiment is made even more complicated by the need to impose a weak magnetic field in the polarimeter to precess the muons and thus to decrease sensitivity to systematic errors.

There have been some experimental and calculational studies done as part of experiment E791 at BNL to try to understand potential sensitivity (Cousins *et al.*, 1984) for this measurement. The conclusion was that a measurement of polarization with an accuracy of 14% could be obtained if 10 000  $K_L^0 \rightarrow \mu^+ \mu^-$  events were detected.

## III. FORBIDDEN DECAYS

The kaon system is one of the best laboratories for the study of conservation laws in particle physics and in particular for the search for processes forbidden in the Standard Model. No process that violates separate lepton number (i.e., electron, muon, or tau-lepton number), also called lepton flavor or lepton family number, has ever been observed. This has led to separate lepton number conservations being formalized in the Standard Model. Examples of forbidden decays in the  $K$  system include  $K_L^0 \rightarrow \mu e$  and  $K^+ \rightarrow \pi^+ \mu e$ . Recent experiments have searched for these decays. The motivation for these searches, the theoretical context in which they are viewed, the experimental results, and prospects for future improvements will be discussed in this section. Other possible forbidden decays include  $K^+ \rightarrow \pi^- l^+ l'^+$  and  $K_L^0 \rightarrow \pi^- \pi^- l^+ l'^+$ , where  $l$  and  $l'$  denote  $e$  or  $\mu$ . These decays would violate the conservation of total lepton number, as well as potentially separate lepton number. These modes will be discussed only briefly.

The experimental absence of muon-electron transitions without neutrinos led to the hypothesis that muon number was a conserved quantity (Nishijima, 1957; Feinberg

and Weinberg, 1961). This was subsequently generalized to include transitions between all lepton generations after the discovery of the tau lepton. However, the underlying basis for this conservation law remains mysterious. An additive conservation law, such as charge conservation, baryon number conservation, and each type of separate lepton number conservation, implies the existence of global  $U(1)$  invariance (see, for example, Sakurai, 1964). In the case of charge conservation, the global invariance is understood as the result of the stronger local  $U(1)$  gauge invariance, from which the form of the electromagnetic interaction is derived (Weyl, 1950). Such an unbroken gauge symmetry requires the existence of a massless boson (Kibble, 1967), namely, the photon. No known massless boson is associated with baryon number or separate lepton number conservation (Lee and Yang, 1955), indicating that the global invariance associated with these additive conservation rules is not a consequence of a gauge principle. Therefore baryon number and separate lepton number conservation appear not to be fundamental (Weinberg, 1979a; De Rújula *et al.*, 1975) and may be expected to be inexact. Indeed, early attempts at grand unification (Georgi and Glashow, 1974) predicted the violation of baryon and lepton number, and it is frequently the case that theoretical extensions to the Standard Model provide mechanisms for separate lepton number violation.

In view of the above considerations, it seems likely that lepton flavor transitions are not strictly forbidden, but are highly suppressed in some dynamical process which lies outside the Standard Model. This is the general motivation for searches for separate lepton number-violating processes, such as  $\mu \rightarrow e\gamma$ ,  $\mu \rightarrow eee$ ,  $\mu^- A \rightarrow e^- A$  (muon-electron conversion in the field of a nucleus),  $\tau \rightarrow \mu\gamma$ , and in the kaon system the decays  $K_L^0 \rightarrow \mu e$  and  $K^+ \rightarrow \pi^+ \mu e$ . In recent years, experimental programs have been underway at several laboratories around the world to search for each of these and others. It is beyond the scope of this review to discuss topics outside the kaon system, such as rare muon decays or searches for separate lepton number violation in tau-lepton decays, heavy-meson decays, etc. Nevertheless, it should be kept in mind that a battery of experimental

tests, complementary to the rare kaon decay searches described here, are in progress and may provide important information on separate lepton number violation if and when it is observed. (See, for example, the review of Melese, 1989.) For completeness, Table V gives the current experimental limits on a number of possible lepton flavor-violating decays and the associated references. The kaon decays listed in the table are discussed below.

## A. $K_L^0 \rightarrow \mu e$

### 1. General phenomenology

The decay  $K_L^0 \rightarrow \mu e$ , or other separate lepton number-violating processes, can occur in the Standard Model if the neutrino masses are not zero or degenerate. In a gauge theory such as the Weinberg-Salam electroweak model, the eigenstates of the weak interaction need not be mass eigenstates. The quark weak eigenstates differ from the mass eigenstates and are connected through the unitary Cabibbo-Kobayashi-Maskawa mixing matrix (Kobayashi and Maskawa, 1973). The same sort of mixing among the leptons would be expected (Cheng and Li, 1977; Lee and Shrock, 1977) were it not for the fact that the neutrinos are massless, or very nearly so. However, existing limits on neutrino masses and mixing angles imply (Langacker *et al.*, 1988)  $B(K_L^0 \rightarrow \mu e) \lesssim 10^{-25}$ , which is unobservable. Consequently, observation of  $K_L^0 \rightarrow \mu e$  would be clear evidence of new physics outside the Standard Model.

The state of the experimental art in these searches, as described in the next subsection, has progressed considerably in recent years, so that the current upper limit on the  $K_L^0 \rightarrow \mu e$  branching ratio is  $3.3 \times 10^{-11}$ . To put this in context, it is useful to establish a sense of scale. To do this, we shall begin with a simple phenomenological approach.

A new interaction may induce the  $K_L^0 \rightarrow \mu e$  decay via a tree-level exchange of a heavy boson  $X$ , as illustrated in Fig. 25(a). The  $X$  has coupling  $f$  to the quarks  $s$  and  $d$  and coupling  $f'$  to the leptons  $\mu$  and  $e$ . This interaction will also couple  $K^0$  to  $\bar{K}^0$ , as shown in Fig. 25(b), unless some additional mechanism or symmetry suppresses it. Therefore the interaction will also contribute to the  $K_L^0$ - $K_S^0$  mass difference ( $\Delta m_K = 3.5 \times 10^{-15}$  GeV), and as a result the measured value of  $\Delta m_K$  provides a constraint on the mass of the  $X$  boson and the strength of its coupling  $f$ . In contrast,  $K_L^0 \rightarrow \mu e$  could occur through the exchange of a heavy  $Y$  boson, as illustrated in Fig. 25(c). Here,  $Y$  couples to quark-lepton vertices, rather than to quark-quark or lepton-lepton vertices. Such an object is sometimes referred to as a leptoquark. Since the  $Y$  does not induce transitions between  $K^0$  and  $\bar{K}^0$ , such an interaction is not constrained by  $\Delta m_K$ .

The  $K_L^0 \rightarrow \mu e$  decay through  $X$  exchange can be compared to the familiar  $K^+ \rightarrow \mu^+ \nu$  decay shown in Fig. 25(d). Assuming the same  $V - A$  form of the interaction,

TABLE V. Current limits on several lepton flavor-violating decays.

Decay	Branching fraction (90% C.L.)	Reference
$\mu \rightarrow e\gamma$	$< 4.9 \times 10^{-11}$	Bolton <i>et al.</i> , 1988
$\mu \rightarrow eee$	$< 1.0 \times 10^{-12}$	Bellgardt <i>et al.</i> , 1988
$\tau \rightarrow \mu\gamma$	$< 4.2 \times 10^{-6}$	Bean <i>et al.</i> , 1993
$\pi^0 \rightarrow \mu e$	$< 1.6 \times 10^{-8}$	Lee <i>et al.</i> , 1990
$K_L^0 \rightarrow \mu e$	$< 3.3 \times 10^{-11}$	Arisaka <i>et al.</i> , 1993
$K^+ \rightarrow \pi^+ \mu^+ e^-$	$< 2.1 \times 10^{-10}$	Lee <i>et al.</i> , 1990
$K^+ \rightarrow \pi^+ \mu^- e^+$	$< 6.9 \times 10^{-9}$	Diamant-Berger <i>et al.</i> , 1976
$D^0 \rightarrow \mu e$	$< 1.0 \times 10^{-4}$	Albrecht <i>et al.</i> , 1988
$B^0 \rightarrow \mu e$	$< 4 \times 10^{-5}$	Avery <i>et al.</i> , 1989

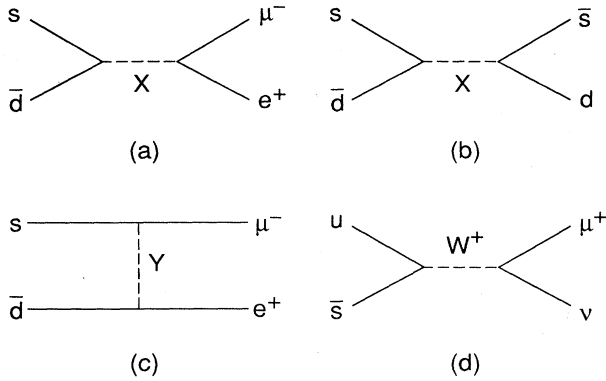


FIG. 25. Diagrams relevant to  $K_L^0 \rightarrow \mu e$ : (a)  $K_L^0 \rightarrow \mu e$  through the exchange of a heavy  $X$  boson; (b)  $K^0 \leftrightarrow \bar{K}^0$  via  $X$  exchange; (c)  $K_L^0 \rightarrow \mu e$  through the exchange of a  $Y$  leptoquark; and (d) the decay  $K^+ \rightarrow \mu^+ \nu$ .

$$\frac{\Gamma(K_L^0 \rightarrow \mu e)}{\Gamma(K^+ \rightarrow \mu^+ \nu)} \simeq \left[ \frac{ff'/M_X^2}{g^2 \sin^2 \theta_c / M_W^2} \right]^2, \quad (3.1)$$

where  $g$  is the electroweak coupling,  $\theta_c$  the Cabibbo angle, and  $M_W$  the mass of the  $W$  boson. The branching fraction is given by

$$B(K_L^0 \rightarrow \mu e) = \frac{\Gamma(K_L^0 \rightarrow \mu e)}{\Gamma(K_L^0 \rightarrow \text{all})} \simeq \frac{\Gamma(K^+ \rightarrow \mu^+ \nu)}{\Gamma(K_L^0 \rightarrow \text{all})} \left[ \frac{ff'/M_X^2}{g^2 \sin^2 \theta_c / M_W^2} \right]^2. \quad (3.2)$$

Plugging in all the known numbers leads to

$$B(K_L^0 \rightarrow \mu e) \simeq (1.2 \times 10^{-2} \text{ TeV}^4) \left[ \frac{f^2}{M_X^2} \right]^2 \left[ \frac{f'}{f} \right]^2. \quad (3.3)$$

Inverting this equation under the assumption that  $f = f' = g$  gives

$$M_X \simeq 220 \text{ TeV} \left[ \frac{10^{-12}}{B(K_L^0 \rightarrow \mu e)} \right]^{1/4}. \quad (3.4)$$

In this scenario, the current upper limit of  $3.3 \times 10^{-11}$  implies a lower bound of 90 TeV on  $M_X$ . This illustrates the conventional wisdom that high-sensitivity searches for rare processes probe mass scales that are inaccessible to any existing or planned accelerator.

Next, we wish to address the question of how this process is constrained by  $\Delta m_K$ . The contribution to  $\Delta m_K$  from the diagram in Fig. 25(b) is approximated (Kane and Thun, 1980) by

$$\Delta m_K \simeq f_K^2 m_K \left[ \frac{f^2}{M_X^2} \right], \quad (3.5)$$

where  $f_K$  is the usual kaon-decay constant taken to be 160 MeV and  $m_K$  the  $K_L^0$  mass. This formula is only an order-of-magnitude estimate, but will suffice for our purpose. Plugging in known numbers leads to

$$\frac{f^2}{M_X^2} \simeq (2.8 \times 10^{-7} \text{ TeV}^{-2}). \quad (3.6)$$

In addition to being only a rough estimate, this should be viewed as an upper limit, since  $\Delta m_K$  is reasonably well accounted for by conventional physics, and here the new interaction has been assumed to be the only contribution. Using the limit on  $f^2/M_X^2$  to bound the branching fraction, we have

$$B(K_L^0 \rightarrow \mu e) \lesssim 1 \times 10^{-15} \left[ \frac{f'}{f} \right]^2. \quad (3.7)$$

Since our definitions of  $f$  and  $f'$  have absorbed any mixing factors that might exist, it is plausible that one or even two orders of magnitude might come from  $(f'/f)^2$ . For example, pursuing the analogy to the  $K^+ \rightarrow \mu^+ \nu$  decay, one might expect  $f'/f \simeq 1/\sin \theta_c$ . Nonetheless, the resulting branching fraction is likely to be well below what is observable in the foreseeable future. While we have come to this result by considering tree-level contributions to  $K_L^0 \rightarrow \mu e$  and  $\Delta m_K$ , the same basic conclusion applies in cases where the  $s\bar{d} \leftrightarrow \bar{s}d$  and  $s\bar{d} \leftrightarrow \mu e$  transitions involve loops. Therefore we conclude that  $K_L^0 \rightarrow \mu e$  at observable levels very likely depends on new interactions either involving leptoquarks or respecting a symmetry that somehow strongly suppresses  $K^0 \leftrightarrow \bar{K}^0$  transitions. These conditions are met in a number of theoretical models, including some with horizontal symmetries, technicolor, and compositeness. At the same time, other models in which  $K_L^0 \rightarrow \mu e$  may occur are so seriously restricted that the allowed level is unobservable; right-left symmetry and supersymmetry appear to be in this category.

Next, we shall briefly comment on how  $K_L^0 \rightarrow \mu e$  can occur in some specific models. A modest extension of the Standard Model would be the existence of a fourth family within the standard  $SU(2)_L \otimes U(1)$  model. The charged members of the new family would have to be heavy to explain their non-observation, and the new neutrino would have to be heavy ( $\gtrsim M_Z/2$ ) to escape experimental constraints on its mass (e.g., LEP results).  $K_L^0 \rightarrow \mu e$  and related processes could occur through mass mixing between the light neutrinos and the new heavy neutrino. Acker and Pakvasa (1992) have used the experimental upper bound on  $\mu \rightarrow e \gamma$  to determine a constraint on the allowed mixing of a heavy neutrino with the electron and muon neutrinos, and from that derived an upper limit of  $2 \times 10^{-15}$  on the branching fraction for  $K_L^0 \rightarrow \mu e$ . A much lower estimate was reached by Langacker, Sankar, and Schilcher (1988), who argue that the mixing between the standard light neutrinos and the heavy neutrino will most likely be governed by a seesaw mechanism (Gell-Mann *et al.*, 1979). Such an assumption gives a much lower estimate of the allowed light-heavy neutrino mixing, namely, of the order of the ratio of the light to heavy masses, and results in a maximum  $B(K_L^0 \rightarrow \mu e)$  as low as  $10^{-24}$ .

An appealing idea is to extend the electroweak theory by introducing right-handed weak interactions based on  $SU(2)_L \otimes SU(2)_R \otimes U(1)$ , leading to a right-left symmetric electroweak model. This would imply the existence of new weak gauge bosons  $W_R^\pm$  and  $Z_R$ , which must be very heavy ( $\gtrsim 300$  GeV, or considerably heavier in some scenarios) in order to avoid previously observable effects. Lepton flavor violation need not occur in such models, but if massive right-handed neutrinos also appear in the model, then the branching fraction for  $K_L^0 \rightarrow \mu e$  could be as large as  $10^{-13}$  (Barroso *et al.*, 1984; Langacker *et al.*, 1988). This level, however, occurs only in an extreme corner of the allowed parameter space, leading Langacker, Sankar, and Schilcher (1988) to conclude that a more realistic bound is probably much lower (about  $10^{-15}$ ). Related approaches, which impose additional restrictions on the right-handed sector [such as a horizontal symmetry (Hou and Soni, 1985, 1987) of the sort discussed below] to avoid a constraint from the  $K_L^0 - K_S^0$  mass difference, can achieve significantly higher decay rates.

Another natural extension of the minimal Standard Model is to extend the Higgs sector by introducing multiple Higgs doublets (McWilliams and Li, 1981). In right-left symmetric models, such additional Higgs doublets are needed to provide the required spontaneous  $SU(2)_R$  symmetry breaking that gives the right-handed bosons their mass. Once additional Higgs are admitted, the physical Higgs particles can in general mediate flavor-changing processes, of which  $K_L^0 \rightarrow \mu e$  is one example. However, nothing in such models automatically suppresses  $K^0 \leftrightarrow \bar{K}^0$  transitions (Mainland and Tanaka, 1979), so that  $\Delta m_K$  provides a strong constraint, rendering  $K_L^0 \rightarrow \mu e$  very small, as discussed above.

Horizontal gauge models hypothesize the existence of a gauge symmetry connecting different generations. Interactions between fermions of different generations can occur via their coupling to horizontal gauge bosons. A process such as  $K_L^0 \rightarrow \mu e$  can occur via a tree-level exchange, as illustrated in Fig. 25(a), where the  $X$  would be a horizontal gauge boson. The constraint from  $\Delta m_K$  can be avoided (Shanker, 1981) in these models. This can be illustrated with a simple model (following Cahn and Harari, 1980), in which the quarks and leptons are assigned a generation number  $G$ , which follows their apparent family grouping in nature. That is, the first generation consists of the up and down quark, the electron, and its neutrino ( $u, d, e, \nu_e$ ), and the second generation consists of the charm and strange quarks, the muon, and its neutrino ( $c, s, \mu, \nu_\mu$ ). (The third generation need not be considered for kaon decay.) If  $G=1$  for the first generation and  $G=2$  for the second, then a  $\Delta G$  value can be identified for a given interaction. In the decay  $K_L^0 \rightarrow \mu e$ ,  $\Delta G=0$  for the  $\bar{s}d \rightarrow \mu^+ e^-$  case and for its charge conjugate. However, for  $K^0 \leftrightarrow \bar{K}^0$  (i.e.,  $\bar{s}d \leftrightarrow \bar{s}d$ ),  $|\Delta G|=2$ . Thus, if there is no generation mixing ( $G$  is exactly conserved), the horizontal gauge bosons do not contribute to  $\Delta m_K$ . In addition, other lepton flavor-violating processes,

such as  $\mu \rightarrow e \gamma$ ,  $\mu \rightarrow eee$ , and  $\mu^- A \rightarrow e^- A$ , for which  $|\Delta G|=1$ , may be suppressed if generation mixing is small or eliminated if  $G$  is exactly conserved. Equation (3.3) gives the  $K_L^0 \rightarrow \mu e$  branching ratio for a  $V-A$  interaction in this scenario. If we assume, for the sake of concreteness, that  $ff'=g^2$ , then the previously derived lower mass bound from the current experimental  $K_L^0 \rightarrow \mu e$  limit of 90 TeV applies to such a horizontal gauge boson.

Pati and Salam (1974) proposed an  $SU(4)$ -based unification scheme in which leptons are treated on the same basis as quarks. Leptons then carry a fourth color, which is lepton number. This model predicts the existence of gauge mesons which couple to quarks and leptons (i.e., leptoquarks). The decay  $K_L^0 \rightarrow \mu e$  can occur as shown in Fig. 25(c). Pati-Salam leptoquark mass bounds based on the  $K_L^0 \rightarrow \mu e$  branching-ratio limit have been calculated by several authors (Dimopoulos, Raby, and Kane, 1981; Deshpande and Johnson, 1983; Pirogov, 1983). Scaling the result of Deshpande and Johnson to the current limit on  $K_L^0 \rightarrow \mu e$  indicates that the mass of a Pati-Salam leptoquark must be above 970 TeV.

Technicolor models (Weinberg, 1976, 1979b; Susskind, 1979; Farhi and Susskind, 1981) have been proposed to avoid a fundamental scalar Higgs, which requires an unnatural fine tuning of parameters to avoid divergences in the radiative corrections to the Higgs mass. In technicolor models, the Higgs is composed of new massless fermions, which are bound together by a technicolor gauge interaction. The picture is complicated by the need to provide a mechanism by which quarks and leptons acquire mass. This is solved in extended technicolor (ETC) models (Dimopoulos and Susskind, 1979; Eichten and Lane, 1980) by introducing additional ETC bosons which couple ordinary fermions to technifermions. ETC models predict a rich phenomenology and a variety of signatures (Eichten *et al.*, 1986). Several possibilities for lepton flavor violation appear in ETC models. In particular,  $K_L^0 \rightarrow \mu e$  could occur as illustrated in Fig. 25(a) by the exchange of either an ETC boson or a technipion (a bound state of techniquarks) or, as illustrated in Fig. 25(c), by the exchange of pseudoscalar leptoquarks or vector leptoquarks of the Pati-Salam type. Generally, ETC models predict significant rates for  $K_L^0 \rightarrow \mu e$  and other neutral flavor-changing processes. Several authors (Dimopoulos and Ellis, 1981; Dimopoulos *et al.*, 1981; Holdom, 1984; King, 1987) have predicted that the  $K_L^0 \rightarrow \mu e$  branching fraction should be above  $10^{-10}$ . If technicolor is to solve the problem for which it was designed, the technicolor scale  $\Lambda_{TC}$  must be about 300 GeV. The ordinary fermion masses are related to the ETC boson masses by  $m_f \approx g_{ETC}^2 \Lambda_{TC}^3 / m_{ETC}^2$ . Therefore predictions for neutral flavor-changing interactions in ETC models cannot easily be adjusted downward simply by invoking higher masses. A scheme in which the ETC coupling constant slowly varies, or slowly runs, has been advanced to address the flavor-changing neutral interaction problem. Referred to as walking technicolor (Appel-

quist *et al.*, 1986, 1987; King, 1989; King and Ross, 1989), the scheme allows the ETC mass scale to be considerably increased while still generating appropriate masses for the ordinary fermions. This mechanism may provide a means of escape from the problems with neutral flavor-changing interactions. Nonetheless, the current limit of  $3.3 \times 10^{-11}$  on  $K_L^0 \rightarrow \mu e$  presents a serious challenge to ETC models.

With the proliferation of quarks and leptons, it is natural to consider the possibility that these fermions are still not fundamental and may be composite. Preon models hypothesize that quarks and leptons are composite. In these models, rare processes such as  $K_L^0 \rightarrow \mu e$  could occur through rearrangement of preon constituents. Some such models (Pati, 1984; Pati and Stremnitzer, 1986) predict  $K_L^0 \rightarrow \mu e$  at levels above the current limit. Others (Greenberg *et al.*, 1984) have argued that lepton flavor-violating processes can be suppressed in composite models by invoking a conserved generation number at the constituent level.

Supersymmetry (Wess and Zumino, 1974; Salam and Strathdee, 1974) is a popular idea, which introduces a superpartner for every particle. The spin of each superpartner differs by  $\frac{1}{2}$  unit from its partner, so for every fermion there is a new boson, and vice versa. Tree-level couplings conserve flavor. Flavor changes may arise in loops through mixing among the quark and lepton superpartners (i.e., squarks and sleptons), since the quark (lepton) and squark (slepton) mass matrices are not simultaneously diagonal. The amount of mixing will depend on the magnitude of the squark (slepton) mass splitting. The mass splitting between squarks is constrained by the  $K_L^0 - K_S^0$  mass difference. The slepton mass splitting is constrained by the limit on  $\mu \rightarrow e \gamma$ . Subject to these bounds, the  $K_L^0 \rightarrow \mu e$  branching fraction is expected (Mukhopadhyaya and Raychaudhuri, 1990) to be below  $10^{-14}$ .

The preceding discussion is not by any means complete. The intent has been to provide an overview of the types of models which permit  $K_L^0 \rightarrow \mu e$  and to provide some indication of the level at which  $K_L^0 \rightarrow \mu e$  is allowed, or, looking at it from a different perspective, which types of models are challenged by current searches for  $K_L^0 \rightarrow \mu e$ . (See also Langacker, 1992.) Models that invoke horizontal symmetries or introduce leptoquarks (such as extended technicolor, Pati-Salam unification, and compositeness) are the most likely to induce  $K_L^0 \rightarrow \mu e$  at observable levels. Indeed, non-observation of  $K_L^0 \rightarrow \mu e$  at current levels of experimental sensitivity is a problem for extended technicolor theories.

## 2. Status of $K_L^0 \rightarrow \mu e$ experiments

In the past few years, three experiments, two at BNL and one at KEK in Japan, have carried out searches for  $K_L^0 \rightarrow \mu e$ . In these experiments, it is necessary to sample large numbers of  $K_L^0$  decays, implying high detector

rates, and also to suppress possible backgrounds. Since the  $K_L^0 \rightarrow \pi e \nu$  ( $K_{e3}$ ) decay occurs with a 39% branching fraction, and typically about 10% of the daughter pions decay to muons inside the spectrometer, legitimate  $K_L^0$  decays will result in observed  $\mu e$  pairs in roughly 4% of all decays. This presents significant challenges for triggers and background suppression.

One of the most important sources of potential background is the decay  $K_L^0 \rightarrow \pi e \nu$ , followed by  $\pi \rightarrow \mu \nu$  in flight or, alternatively, misidentification of the pion as a muon. If the center-of-mass energy of the neutrino in the  $K_{e3}$  decay is close to zero, the event can be confused with a real  $K_L^0 \rightarrow \mu e$  decay. Fortunately, the  $E_\nu \simeq 0$  case is suppressed by the  $V - A$  matrix element. Rejection of this background depends on the fact that the invariant mass distribution of the two charged tracks from the background process has an end point 8.4 MeV below the mass of the  $K_L^0$ . To see this, consider a  $K_{e3}$  decay with  $E_\nu = 0$ . Then  $m_K^2 = (P_\pi + P_e)^2$ , where  $P_\pi$  and  $P_e$  are the pion and electron 4-momenta. To evaluate the reconstructed mass when the event is misinterpreted as  $K_L^0 \rightarrow \mu e$  we must consider two cases: the pion decays ( $\pi \rightarrow \mu \nu$ ) or the pion is misidentified (i.e., the muon mass  $m_\mu$  is assigned to the pion). In both cases, the reconstructed mass  $M$  will be given by  $M^2 = (P_\mu + P_e)^2$ . Combining these two expressions for mass squared leads to

$$M^2 = m_K^2 + m_\mu^2 - m_\pi^2 - 2P_e \cdot (P_\pi - P_\mu) . \quad (3.8)$$

For the case in which the pion decays, it is easily shown that  $P_e \cdot (P_\pi - P_\mu) > 0$ , so the maximum reconstructed mass is

$$M_{\max}^2 = m_K^2 + m_\mu^2 - m_\pi^2 . \quad (3.9)$$

For the case in which the pion is misidentified, the only difference in  $P_\pi$  and  $P_\mu$  is the assignment of the particle mass, so

$$P_\pi - P_\mu = (\sqrt{p_\pi^2 + m_\pi^2} - \sqrt{p_\pi^2 + m_\mu^2}, 0, 0, 0) , \quad (3.10)$$

and again it follows that  $P_e \cdot (P_\mu - P_\pi) > 0$ , leading once more to Eq. (3.9). Then

$$M_{\max} = 489.24 \text{ MeV} = m_K - 8.43 \text{ MeV} . \quad (3.11)$$

This bound applies experimentally only so far as the resolution smearing of the spectrometer is insignificant. Therefore very precise tracking and momentum measurement is a critical detector feature. At the rather low (BNL and KEK) energies at which the recent experiments have been performed, the major contribution to resolution errors is multiple scattering in vacuum windows and the tracking chambers themselves. Mistakes in pattern recognition which result in incorrectly measured track quantities can also create background events, so redundancy in the tracking system is also a critical requirement. Further rejection of pion decay in flight in the spectrometer can be achieved by having two consecu-

tive spectrometer magnets and making two independent momentum measurements. The decay can occur downstream of the two magnets, however, and it is therefore also useful to measure the muon momentum a third time via its depth of penetration into a massive degrader.

The 489-MeV bound on reconstructed mass is circumvented in the second important source of possible background events, i.e., misidentification of both charged particles in the  $K_{e3}$  decay. Specifically, if the pion is classified as an electron and the electron as a muon, then the reconstructed mass  $M$  is approximated by

$$M \simeq M_{\pi e}^2 + \left[1 + \frac{p_{\pi}}{p_e}\right] m_{\mu}^2 - \left[1 + \frac{p_e}{p_{\pi}}\right] m_{\pi}^2, \quad (3.12)$$

where  $M_{\pi e}$  is the actual  $\pi e$  invariant mass. Therefore, if  $p_{\pi} > p_e$ , the apparent  $\mu e$  invariant mass can equal or exceed the  $K_L^0$  mass. Good particle identification is required to reject this background.

An additional potential background, but small (at the current beam intensities) compared to those previously discussed, is the overlap of two  $K_L^0$  decays ( $K_L^0 \rightarrow \pi e \nu$  and  $K_L^0 \rightarrow \pi \mu \nu$ ), with the pions being missed. Precise kinematic reconstruction and good timing are important to suppress this background.

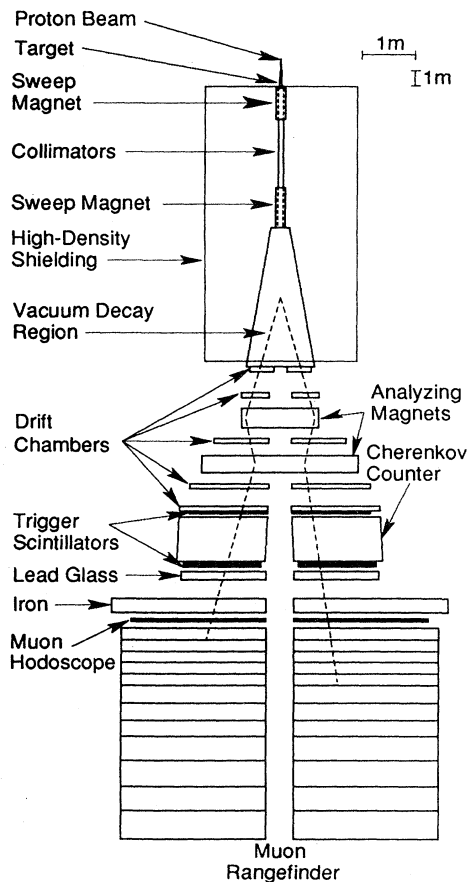


FIG. 26. Plan view of the BNL E791 spectrometer.

BNL E780 completed data taking at the Alternating Gradient Synchrotron (AGS) in 1988 and established a 90%-confidence-level upper limit of  $1.9 \times 10^{-9}$  on the  $K_L^0 \rightarrow \mu e$  branching ratio (Schaffner *et al.*, 1989). Since then, an improvement by almost two orders of magnitude has been made by another experiment, E791, at the AGS.

The BNL E791 spectrometer is shown in Fig. 26. The experiment was performed in the B5 neutral beam at the AGS. Protons with 24 GeV in energy were incident on a one-interaction-length copper target. A neutral beam was defined by a series of collimators centered at a  $2.75^\circ$  angle from the incident proton beam direction. Two dipole sweeping magnets removed charged particles from the beam. The decay volume was a region extending from roughly 10 m from the target to the most upstream drift chamber at 18 m from the target. Most of the collimation channel and the entire decay volume were under vacuum. The beam volume within the spectrometer was filled with helium. Tracking was performed by five drift-chamber modules (each module made two  $x$  and two  $y$  measurements). The regions between drift chambers were filled with helium to reduce multiple scattering and particle interactions. Each of the two dipole magnets provided  $\Delta p_T \simeq 300$  MeV/ $c$ , but with opposite sign. Downstream of the final drift chamber, a finely segmented scintillator hodoscope, a gas threshold Čerenkov counter, another hodoscope and a large lead-glass array followed in sequence. The scintillation counter hodoscopes provided the signals used in the lowest-level (fast-logic) trigger. The Čerenkov counter provided a fast signal, corresponding to the presence of an electron, which was also used in the low-level trigger. The lead glass provided a calorimetric energy measurement, which was used for offline  $\pi:e$  discrimination. A meter of steel followed the lead glass to stop all particles except muons. Behind the steel, a segmented scintillation hodoscope provided a fast-muon signal for the low-level trigger. Finally, muons were stopped in a segmented absorber stack with large proportional wire chambers spaced throughout the stack. This "rangefinder" provided a muon range measurement which corresponds to a 10% measurement of momentum.

E791 recorded data during 1988, 1989, and 1990. The combined data set yielded a single-event sensitivity for the  $K_L^0 \rightarrow \mu e$  decay of  $1.5 \times 10^{-11}$ . The sensitivity was measured by counting observed  $K_L^0 \rightarrow \pi \pi$  events, which have the same topology as  $K_L^0 \rightarrow \mu e$ . The detector acceptance for these two decay modes is similar, and many systematic effects (such as pattern-recognition efficiency) are common to both modes. Figure 27 shows a scatter plot of the square of the transverse momentum imbalance versus reconstructed mass for  $K_L^0 \rightarrow \mu e$  candidates. No events appear in the signal region, allowing a 90%-confidence upper limit of  $3.3 \times 10^{-11}$  to be set (Arisaka *et al.*, 1993). This is the lowest sensitivity ever achieved in a kaon experiment. E791 has also searched for and set limits on  $K_L^0 \rightarrow ee$  and observed a large sample of  $K_L^0 \rightarrow \mu \mu$  decays. These modes are discussed elsewhere in

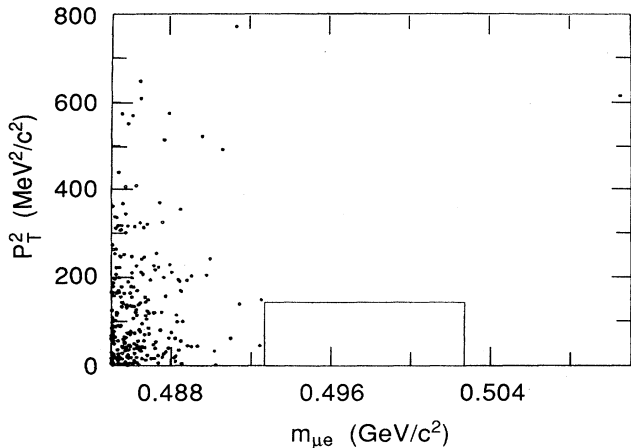


FIG. 27. A scatter plot of  $p_T^2$  vs  $M_{\mu e}$  for  $K_L^0 \rightarrow \mu e$  candidates from BNL E791 (after Arisaka *et al.*, 1993).

this article.

The KEK E137 spectrometer is shown in Fig. 28. It differs in many details from the E791 spectrometer, but is conceptually very similar. A critical feature of both detectors is that the consecutive dipole magnets allow independent momentum measurements, so that  $\pi \rightarrow \mu \nu$  decay in flight in the spectrometer can be rejected. However, magnetic deflection in the two magnets is in the same direction in E137 and in opposite directions in E791. The total field integral in E137 was tuned to cause particles from two-body  $K_L^0$  decays to have trajectories downstream of the magnets approximately parallel to the initial beam direction. This parallelism was exploited in the trigger. The KEK experiment (Akagi *et al.*, 1991a) set a 90%-confidence-level upper limit on  $K_L^0 \rightarrow \mu e$  of  $9.4 \times 10^{-11}$ . The values of the most important parameters of experiments E791 at BNL and E137 at KEK are summarized in Table VI.

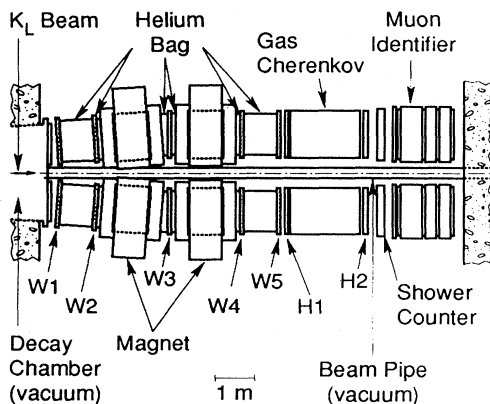


FIG. 28. Plan view of the KEK E137 spectrometer. W1-5 are the tracking chambers; H1 and H2 are the trigger scintillators.

TABLE VI. Parameters of recent  $K_L^0 \rightarrow \mu e$  experiments.

Parameter	BNL E791	KEK E137
Proton energy (GeV)	24	12
Protons on target/spill	$4.5 \times 10^{12}$	$1.5 \times 10^{12}$
Target angle	$2.75^\circ$	$0^\circ$
Beam solid angle ( $\mu\text{sr}$ )	60	154
Length of decay region (m)	8	10
Useful $K_L^0$ momentum range (GeV/c)	4-16	2-8
Acceptance (%)	4	0.9
$\int B dl$ of spectrometer magnets (Tm)	2	0.79
Mass resolution for $K_L^0 \rightarrow \pi\pi$ ( $\text{MeV}/c^2$ )	1.4	1.3
$\theta^2$ resolution ( $\text{mrad}^2$ )	0.3	1.0
90% C.L. limit on $K_L^0 \rightarrow \mu e$	$3.3 \times 10^{-11}$	$9.4 \times 10^{-11}$

### 3. Future prospects

A new experiment, E871, is planned at BNL to exploit the increase in proton flux which will become available with the new AGS Booster. E871 is an upgrade of E791 and is being mounted by a collaboration that substantially overlaps with the E791 group. The experiment is expected to begin physics running in 1994 and ultimately to reach a single-event sensitivity to  $K_L^0 \rightarrow \mu e$  below  $10^{-12}$ . The beam and target will be hardened for higher-intensity running. Gains over E791 will be made by running with about a factor of 4 more beam, by lengthening the decay volume and increasing magnet apertures to more than double the acceptance, and by eliminating known inefficiencies and deadtimes. Small (5-mm)-diameter straw chambers with a fast drift gas will be used in a majority of the tracking stations. The spectrometer magnets will be run in a mode in which the deflections are in opposite directions, but the net  $\Delta p_T$  cancels the transverse momentum in two-body decays, leading to parallel tracks downstream of the magnets. This provides the strong trigger constraint of parallelism, while maintaining good resolution on the comparison of momenta measured with the two magnets. The full field integral will be about 2.4 Tm. A novel feature of the new detector is a beam stop, or plug, which will be inserted in the upstream dipole magnet to stop the neutral beam. The beam plug will dramatically reduce the rates in the detector elements downstream of the second dipole magnet at the cost of increased rates in the tracking chambers near the plug. Extensive beam tests have been conducted to optimize the plug design and to verify that the chamber rates near the plug are acceptable. Background rejection must also be improved over E791. This will be accomplished through a number of changes in the detector, which will increase tracking system redundancy, improve the resolution for some kinematic quantities, and decrease the particle misidentification probability. The layout of E871 is shown in Fig. 29.

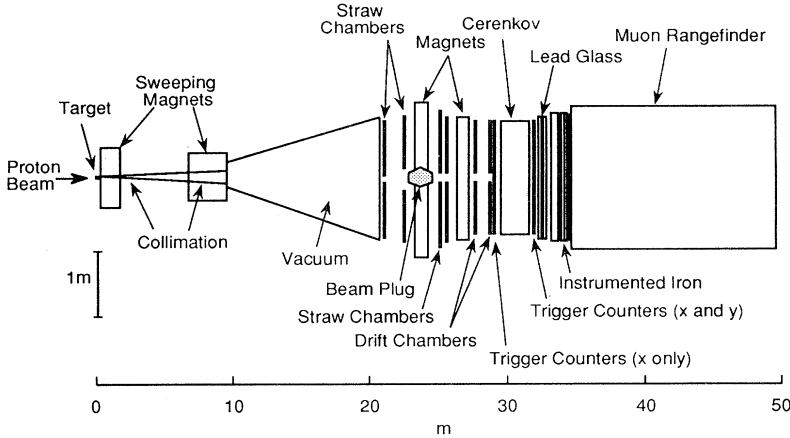


FIG. 29. Plan view of the planned BNL E871 spectrometer.

## B. $K^+ \rightarrow \pi^+ \mu e$

### 1. Phenomenology

Another promising probe of lepton flavor violation in the kaon system is the decay  $K^+ \rightarrow \pi^+ \mu e$ . Most of the theoretical considerations discussed earlier in the  $K_L^0 \rightarrow \mu e$  context apply here as well and there is no need to repeat the discussion of specific models. However, we wish to emphasize the complementary nature of a search for  $K^+ \rightarrow \pi^+ \mu e$ . In particular, owing to the pseudoscalar nature of the hadronic current in the  $K_L \rightarrow \mu e$  case, that mode essentially probes pseudoscalar or axial-vector interactions. The  $K^+ \rightarrow \pi^+ \mu e$  mode is sensitive to scalar or vector interactions. It would be imprudent to rely on only a search for  $K_L^0 \rightarrow \mu e$  for this reason.

It is necessary to distinguish between the  $K^+ \rightarrow \pi^+ \mu^+ e^-$  and  $K^+ \rightarrow \pi^+ \mu^- e^+$  channels, for both a theoretical and an experimental reason. The theoretical reason is that  $K^+ \rightarrow \pi^+ \mu^+ e^-$  is a  $\Delta G=0$  process, in which  $G$  is the generation number discussed earlier in the context of horizontal gauge symmetry. In contrast,  $K^+ \rightarrow \pi^+ \mu^- e^+$  is a  $|\Delta G|=2$  process. Therefore the rates for the two channels could be significantly different if a horizontal symmetry is respected. Experimentally, the  $K^+ \rightarrow \pi^+ \mu^+ e^-$  channel has received the most attention because it is easier to trigger on (an  $e^-$  occurs much less frequently than an  $e^+$  in  $K^+$  decays, as discussed below). If the  $K^+ \rightarrow \pi^+ \mu e$  decay occurs through the same sort of  $X$  boson exchange as we considered for  $K_L^0 \rightarrow \mu e$ , then the rate can be estimated by a comparison to the  $K_L^0 \rightarrow \pi \mu \nu$  decay. Here, we assume the  $X$  couples to  $us$  quarks with strength  $f$  and to  $\mu e$  with strength  $f'$ . Then,

$$\frac{\Gamma(K^+ \rightarrow \pi^+ \mu e)}{\Gamma(K_L^0 \rightarrow \pi^+ \mu \nu)} \simeq \left[ \frac{ff'/M_X^2}{g^2 \sin^2 \theta_c / M_W^2} \right]^2. \quad (3.13)$$

The branching fraction is

$$\begin{aligned} B(K^+ \rightarrow \pi^+ \mu e) &= \frac{\Gamma(K^+ \rightarrow \pi^+ \mu e)}{\Gamma(K^+ \rightarrow \text{all})} \\ &\simeq \frac{\Gamma(K_L^0 \rightarrow \pi^+ \mu \nu)}{\Gamma(K^+ \rightarrow \text{all})} \left[ \frac{ff'/M_X^2}{g^2 \sin^2 \theta_c / M_W^2} \right]^2. \end{aligned} \quad (3.14)$$

Plugging in all the known numbers leads to

$$B(K^+ \rightarrow \pi^+ \mu e) \simeq (3.0 \times 10^{-4} \text{ TeV}^4) \left[ \frac{f^2}{M_X^2} \right]^2 \left[ \frac{f'}{f} \right]^2. \quad (3.15)$$

Then if  $f = f' = g$ ,

$$M_X \simeq 86 \text{ TeV} \left[ \frac{10^{-12}}{B(K^+ \rightarrow \pi^+ \mu e)} \right]^{1/4}. \quad (3.16)$$

As can be seen from a comparison of this expression for  $M_X$  to Eq. (3.4), under our implicit assumption of a  $V-A$  interaction, the  $K_L^0$  decay has a greater mass reach for the  $X$  boson. The  $K_L^0 \rightarrow \mu e$  mode is favored mainly because of the additional phase space and the longer  $K_L^0$  lifetime. With the assumption  $f = f' = g$ , the current best upper limit on  $K^+ \rightarrow \pi^+ \mu e$  of  $2.1 \times 10^{-10}$  implies a lower bound of 23 TeV on  $M_X$ . However, we emphasize that a new lepton flavor-violating interaction need not be  $V-A$  and that this particular choice is simply a convenient illustration. Indeed, in the sort of horizontal gauge symmetry model discussed earlier, a pure vector interaction may be more likely (Cahn and Harari, 1980).

### 2. Experimental status

The recently completed Experiment 777 at BNL has set a 90%-confidence-level upper limit (A. M. Lee *et al.*, 1900) on  $K^+ \rightarrow \pi^+ \mu^+ e^-$  of  $2.1 \times 10^{-10}$ . Also, using tagged  $\pi^0$ 's from the  $K^+ \rightarrow \pi^+ \pi^0$  decay, an upper limit on  $\pi^0 \rightarrow \mu^+ e^-$  of  $1.6 \times 10^{-8}$  was established. The experiment is by design sensitive only to modes with an  $e^-$  in the final state. This choice was made because the natural

occurrence of an  $e^-$  in  $K^+$  decays enters only at the  $2 \times 10^{-3}$  level (from  $K^+ \rightarrow \pi^+ \pi^0$ , followed by  $\pi^0 \rightarrow e^+ e^- \gamma$ ), while an  $e^+$  appears at the 5% level (from  $K^+ \rightarrow \pi^0 e^+ \nu$ ). Requiring an  $e^-$  in the trigger considerably suppresses the trigger rate. Nonetheless, the current limit on the  $K^+ \rightarrow \pi^+ \mu^- e^+$  decay is quite good, especially in view of the fact it is from an experiment performed over 15 years ago at the CERN PS (Diamant-Berger *et al.*, 1976). It is  $6.9 \times 10^{-9}$ .

The most troublesome background to  $K^+ \rightarrow \pi^+ \mu^+ e^-$  comes from  $K^+ \rightarrow \pi^+ \pi^0$  followed by  $\pi^0 \rightarrow e^+ e^- \gamma$ , where the  $e^+$  is misidentified as a  $\pi^+$  and the  $\pi^+$  either decays ( $\pi^+ \rightarrow \mu^+ \nu$ ) or is misidentified as a  $\mu^+$ . Particle misidentification does not lead to background if a particle is classified as a lighter particle, since that only lowers the reconstructed mass. But in this scenario, because the positron is classified as a pion, the reconstructed mass can equal or exceed the kaon mass. Another potentially serious background can come from  $K^+ \rightarrow \pi^0 \mu^+ \nu$  followed by  $\pi^0 \rightarrow e^+ e^- \gamma$ , where the  $e^+$  is misidentified as a  $\pi^+$ . Finally, the decay  $K^+ \rightarrow \pi^+ \pi^+ \pi^-$  can mimic  $K^+ \rightarrow \pi^+ \mu^+ e^-$  if the  $\pi^-$  is misidentified as an  $e^-$  and one of the  $\pi^+$ 's either is misidentified as a  $\mu^+$  or decays in flight in the spectrometer ( $\pi \rightarrow \mu \nu$ ); here the mass misassignments push the total effective mass so far down that tracking errors must also be present for these events to appear as background. From these considerations, it is clear that particle identification is critical in this experiment.

The E777 spectrometer is shown in Fig. 30. The experiment ran with a 6-GeV positively charged beam, which contained approximately  $2 \times 10^8$  particles per spill, of which about 5% were  $K^+$ 's. About 10% of the  $K^+$ 's decayed in a 5-m decay volume. A dipole magnet deflected positively charged daughters to the right side of the spectrometer, which was instrumented to detect  $\pi^+$ 's and  $\mu^+$ 's. Negatively charged particles were deflected to the left side, which was instrumented for electrons. The spectrometer used multiwire proportional chambers for tracking and a second dipole magnet for momentum analysis. The experiment relied on two consecutive threshold Čerenkov counters for particle identification. Both right-side Čerenkov counters were filled with  $\text{CO}_2$

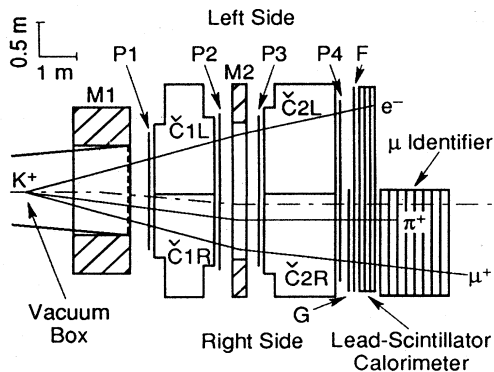


FIG. 30. Plan view of the BNL E777 spectrometer.

at one atmosphere. These counters were unlikely to fire for real  $K^+ \rightarrow \pi^+ \mu^+ e^-$  events, but were efficient at vetoing positrons. Both left-side Čerenkov counters were filled with hydrogen gas at one atmosphere for electron identification. A lead-scintillator shower counter followed. Finally, an instrumented iron muon detector was located on the right side at the rear of the spectrometer.

The  $K^+ \rightarrow \pi^+ \pi^+ \pi^-$  decay was used to calculate the sensitivity of this search. Figure 31(a) shows a scatter plot of a quantity  $S$  versus reconstructed invariant mass for  $K^+ \rightarrow \pi^+ \pi^+ \pi^-$  events. The variable  $S$  is the root-mean-square distance of closest approach for the three tracks to a common vertex. The final results of the  $K^+ \rightarrow \pi^+ \mu^+ e^-$  search are shown in a similar scatter plot in Fig. 31(b). The signal region is enlarged for the  $K^+ \rightarrow \pi^+ \mu^+ e^-$  over that for  $K^+ \rightarrow \pi^+ \pi^+ \pi^-$  because the larger kinetic-energy release in the decay results in a poorer mass resolution. No events appear in the signal box.

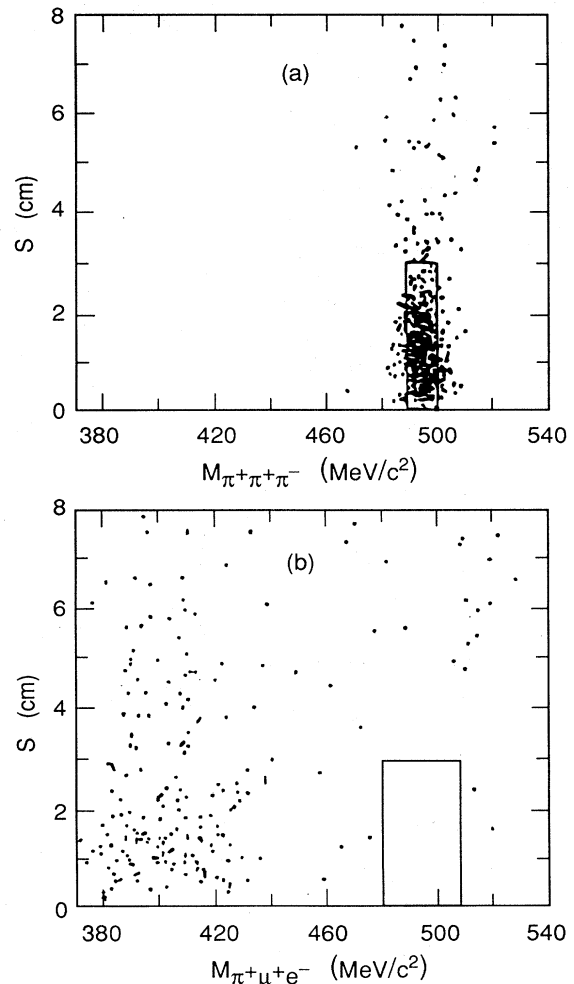


FIG. 31. The variable  $S$  (defined in the text) vs invariant mass for (a)  $K^+ \rightarrow \pi^+ \pi^+ \pi^-$  decays; (b)  $K^+ \rightarrow \pi^+ \mu^+ e^-$  candidates (after Lee *et al.*, 1990).

### 3. Future prospects

A new experiment, E865, is planned at BNL to begin running in 1994. The E865 goal is to reach a sensitivity of  $10^{-12}$ . This corresponds to an improvement over E777 of about a factor of 70 and will be achieved through a number of improvements to the beam and apparatus. The basic approach of the new experiment is the same as E777. The new beam will again run at 6 GeV, but will provide higher flux with reduced halo. A much-larger-aperture spectrometer magnet will increase the spectrometer acceptance by about a factor of 3. A more redundant tracking system will provide better reconstruction efficiency and reduce the potential for backgrounds resulting from tracking mistakes. The number of candidate events close to the signal box in Fig. 31(b) emphasizes the importance of improved background rejection in this experiment over E777 in order actually to realize the factor-of-70 improvement. A study of the events in E777 that were closest to the signal region indicates that the E851 detector would have been able to reject them. An additional gain results from the improved E851 tracking resolution, which will allow the size of the signal box to be reduced by more than a factor of 2.

#### C. $K^+ \rightarrow \pi^- l^+ l'^+$ and $K_L^0 \rightarrow \pi^- \pi^- l^+ l'^+$

The decays  $K^+ \rightarrow \pi^- l^+ l'^+$  and  $K_L^0 \rightarrow \pi^- \pi^- l^+ l'^+$ , where  $l$  and  $l'$  denote  $e$  or  $\mu$ , would violate total lepton number. These modes have recently been discussed by Littenberg and Shrock (1992), who consider them in a model involving a heavy Majorana neutrino. The model predicts branching fractions that are unobservable (below  $10^{-25}$ ). No searches for these modes have been reported, leading Littenberg and Shrock to derive an upper limit of  $1.5 \times 10^{-4}$  on the branching fraction for  $K^+ \rightarrow \pi^- \mu^+ \mu^+$  from bubble-chamber results published in 1968. BNL E787 has an existing data sample that can probably improve this limit to the  $10^{-8}$  level. No dedicated experiments are planned, although the E787 detector is well suited for detecting these modes in stopping  $K^+$  decays. No limit exists at the present time for the decay  $K_L^0 \rightarrow \pi^- \pi^- l^+ l'^+$ . Conventional  $K_L^0$  experiments are not well suited for detecting such decays, since the probability is high that at least one daughter particle will go undetected, for example by remaining in the beam.

## IV. SUPPRESSED DECAY MODES

### A. $K^+ \rightarrow \pi^+ \nu \bar{\nu}$ decay

This decay is forbidden to first order because it involves a flavor-changing neutral-current interaction. It is, however, allowed via higher-order weak interactions, but with a considerably lower rate than is typical of ordinary weak-interaction processes. It is this special nature

of this process that makes it an interesting laboratory for the study of a variety of physics issues, normally not readily accessible to experimental investigations. In this section we first describe the phenomenology of this decay and then discuss the experimental situation.

### 1. Phenomenology

We can look at the decay process  $K^+ \rightarrow \pi^+ \nu \bar{\nu}$  from two different points of view. On the one hand, it can be viewed as an interesting channel through which to look for physics beyond the Standard Model, since the conventional wisdom predicts a very low branching fraction. The new physics can exhibit itself in one of two different ways. It can introduce new particles, which will produce additional diagrams that will have to be included when calculating the rate for this process. Or it can introduce new particles, which can generate additional decay channels that experimentally will be indistinguishable from the  $\pi^+ \nu \bar{\nu}$  final state. In this section we shall consider the first set of possibilities; the second will be discussed in Sec. V.

Alternatively, if we accept the Standard Model as the ultimate truth, the process in question can be used as a means to determine values of some of the Standard Model's parameters that are unknown or poorly measured today. The obvious examples are the mass of the top quark and the  $V_{td}$  element of the CKM matrix (e.g., Dib, 1992).

In reality, the present experimental situation is such that there are still too many unknown Standard Model parameters to make a precise prediction of the decay rate, and the immediate experimental prospects do not anticipate an accurate measurement of the branching fraction in the near future. Thus the main interest in the process at this time stems from the large window for new physics that can be explored here. Our goal in this section is to describe the theoretical formalism developed for this decay, enumerate the results of the relevant calculations together with their limitations, and outline the estimates that have been made as to how the Standard Model predictions could be modified by new physics.

The theoretical prediction of the  $K^+ \rightarrow \pi^+ \nu \bar{\nu}$  branching fraction is based on the assumption that the rate can be calculated by evaluating the diagrams illustrated in Fig. 32, i.e., the box diagram and the  $Z$ -penguin diagrams. The general problem is very similar to that encountered in evaluating the direct  $CP$ -violating amplitude in the decay  $K_L^0 \rightarrow \pi^0 e^+ e^-$  and has been elaborated on in some detail in the earlier discussion of that channel. Accordingly, we limit ourselves here to a review of some of the most salient points. The accuracy of the calculation is limited by our imperfect knowledge of several parameters that should, in our estimation, be determined in the future with a much higher precision. The relevant parameters fall naturally into three categories: (a) mass of the top quark,  $m_t$ , and, less importantly, mass of the charm quark,  $m_c$ , (b) values of certain hadronic matrix

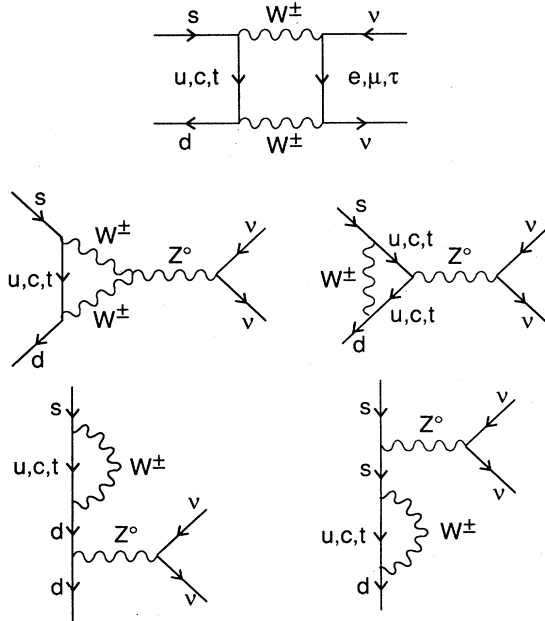


FIG. 32. Diagrams contributing to  $K^+ \rightarrow \pi^+ \nu \bar{\nu}$  in the Standard Model (after Bigi and Gabbiani, 1991).

elements, e.g.,  $B_B, B_K, f_B$ , and (c) values of elements of the Cabibbo-Kobayashi-Maskawa matrix.

We discuss next the present limitations on our knowledge of these parameters and prospects for future improvement. The impact of these uncertainties on the estimates of the branching fraction will be discussed as part of our subsequent discussion about the results of theoretical calculations of this rate.

The present mass range for the mass of the top quark is about  $91 < m_t < 200$  GeV, the lower limit coming from the CDF search for dileptons in  $\bar{p}p$  collisions (Abe *et al.*, 1992a, 1992b) and the upper from the analysis of all electroweak data, dominated by the recent LEP results (LEP Collaborations, 1992). If the mass of the top quark is in the lower part of the indicated range, it should be discovered in the near future at the Fermilab collider and its mass should then be known to better than  $\pm 10$  GeV. The present range on the charm quark mass is generally taken to be  $1.2 < m_c < 1.8$  GeV. The best information comes from studies of charm photoproduction and hadroproduction (Kernan and VanDalen, 1984) and of charmonium spectroscopy (Appelquist *et al.*, 1978). It is dependent somewhat on adequate understanding of all the QCD effects. Recently, there has been quite a bit of progress in accumulating a great deal of accurate photoproduction data, and thus one might expect that the uncertainty on this parameter should shrink by a factor of 2 or 3 in the near future.

The estimates of the bag factors  $B_K$  and  $B_B$  are based on theoretical arguments and vary quite widely. The theoretical origin of the bag factor, e.g.,  $B_K$ , is in efforts to calculate hadronic matrix elements between states that

involve hadrons in both initial and final state, for example, the  $\Delta S = 2$  transition responsible for the  $K^0-\bar{K}^0$  mixing. The value of  $B_K$  is then defined as the ratio of the matrix element

$$M = \langle \bar{K}^0 | \bar{s} \gamma_\mu (1 - \gamma_5) d \bar{s} \gamma^\mu (1 - \gamma_5) d | K^0 \rangle \quad (4.1)$$

calculated in a specific model to the value calculated using the vacuum insertion method (Gaillard and Lee, 1974). This effectively puts all the nonperturbative QCD effects into  $B_K$ .

The techniques used to calculate the bag factors have been quite diverse and include, among others, bag models (Shrock and Treiman, 1979), constituent quark models (Colic *et al.*, 1983; Godfrey, 1986), and chiral perturbation theory (Donoghue *et al.*, 1982). More recently, lattice QCD calculations have been used in the quenched approximation (Kilcup *et al.*, 1990). Because of the large dispersion of results, the range for  $B_K$  is generally taken to be  $0.3 < B_K < 1.0$ .  $B_B$  is assumed to be  $O(1)$  and, since it occurs in the relevant expressions multiplied by  $f_B$ , its imprecise knowledge can be effectively absorbed by the uncertainty in  $f_B$ .

The values of  $f_B$  calculated in the literature span a wide range (Altarelli, 1987); numbers ranging from 100 to 340 MeV have been used. The value of  $f_B$  has been estimated using a variety of theoretical models, e.g., potential and bag models (Godfrey and Isgur, 1985), QCD sum rules (Reinders, 1988), and lattice QCD calculations (Alexandrou *et al.*, 1991, 1992; Allton *et al.*, 1991; Bernard *et al.*, 1992). The ever increasing sophistication of lattice QCD calculations should result in a more reliable estimate of these parameters in the future. Experimentally,  $f_B$  could be extracted from the measurement of the rates of  $B^+ \rightarrow \tau^+ \nu$  and  $B^+ \rightarrow \mu^+ \nu$  decays. These are difficult processes to measure because of anticipated low branching fractions (Harris and Rosner, 1992) and serious background limitations, and it is unlikely that they will be measured before the end of this decade. One might comment that in most theoretical models  $f_B/f_D$  is quite similar; thus an experimental measurement of  $f_D$  via  $D^+ \rightarrow \mu^+ \nu$  or  $D^+ \rightarrow \tau^+ \nu$  might provide a better estimate of  $f_B$  (Kim, 1989).

Of the four CKM matrix parameters, one of them ( $\lambda$  in the Wolfenstein parametrization) is constrained quite well by the  $\Delta S = \pm 1$  transitions. The other three,  $A$ ,  $\rho$ , and  $\eta$  in the same parametrization, are constrained by experimental measurements of bottom meson lifetimes ( $V_{cb}$ ), the magnitude of CP violation in the  $K^0-\bar{K}^0$  matrix ( $\epsilon$ ), the charmless decay rate of the B mesons ( $|V_{ub}/V_{cb}|$ ), and the  $B_d^0-\bar{B}_d^0$  mixing (parameter  $x_d \equiv \Delta M/\Gamma$ ). The  $K^0-\bar{K}^0$  mass difference has a relatively weak dependence on the mass of the top quark (Vysotskii, 1980; Ellis *et al.*, 1988) and the associated top quark CKM matrix elements and does not contribute very much to determination of  $A$ ,  $\rho$ , and  $\eta$ . The experimental input is becoming quite good, and considerable improvement in our knowledge of the last two param-

ters is expected during the next few years. Thus one might expect that very shortly experimental uncertainties in this sector will not contribute significantly to the determination of the CKM parameters, but rather that our knowledge of these parameters will be limited by the uncertainties on the quantities in the first two categories discussed above.

The expression for the  $K^+ \rightarrow \pi^+ \nu \bar{\nu}$  branching fraction with three quark families was originally obtained by Inami and Lim (1981). QCD effects in processes involving second-order box diagrams were included in the calculations for the first time by Novikov *et al.* (1977). More recently the numerical values for the  $K^+ \rightarrow \pi^+ \nu \bar{\nu}$  decay have been recalculated by a number of authors by

inclusion of new and/or better experimental input. The most recent calculations have been done by Kim, Rosner, and Yuan (1990), Bélanger and Geng (1991), Dib, Dunietz, and Gilman (1991), Geng and Turcotte (1991), and Harris and Rosner (1992). A new calculational technique for box and penguin diagrams, the so-called penguin-box expansion, has been developed recently by Buchalla, Buras, and Harlander (1991) and applied to several FCNC processes, including the decay  $K^+ \rightarrow \pi^+ \nu \bar{\nu}$ . All the calculations include only the short-distance effects, i.e.,  $Z$ -penguin and  $W$ -box diagrams, since the long-distance effects have been shown to be several orders of magnitude smaller (Rein and Sehgal, 1989). The expression for the branching fraction is

$$B(K^+ \rightarrow \pi^+ \nu \bar{\nu}) = 7.01 \times 10^{-7} \sum_{l=e,\mu,\tau} \left[ \left[ -\frac{2x_c}{x_l - x_c} (\eta_{B,l} x_l \ln x_l - \eta_B x_c \ln x_c) + \frac{1}{2} \eta_Z x_c \ln x_c - \frac{1}{2} x_c + A^2 \lambda^4 (1 - \rho) C_v(x_l, x_c) \right]^2 + A^4 \lambda^8 \eta^2 |C_v(x_l, x_c)|^2 \right], \quad (4.2)$$

where  $B(K^+ \rightarrow \pi^0 e^+ \nu) = 0.048$  has been used to obtain the numerical coefficient in front.  $A$ ,  $\lambda$ ,  $\rho$ , and  $\eta$  are CKM parameters in the Wolfenstein representation,  $x_i \equiv m_i^2/m_W^2$ , with  $m_i$  being the mass of  $i$ th lepton or quark,  $\eta_Z$  and  $\eta_B$  are the QCD correction factors in the  $Z$ -penguin and  $W$ -box diagrams, respectively, that are functions of masses and  $K_{ij}$ 's, where  $K_{ij} \equiv \alpha_s(m_i^2)/\alpha_s(m_j^2)$ .  $C_v(x_l, x_c)$  is an algebraic expression depending on  $x_l$  and  $x_c$ , and  $\eta_{B,l}$  is another QCD correction factor that is a function of  $K_{ij}$ 's.

As can be seen from the above, the branching-fraction expression depends explicitly on all four parameters of the CKM matrix and on the lepton, quark, and  $W$ -boson masses. Its dependence on the hadronic matrix elements discussed above, even though not explicit, is strong because they (as well as quark masses) enter into the determination of  $A$ ,  $\eta$ , and  $\rho$ .

The dependence on  $m_c$  and  $m_t$  is indicated in Fig. 33, taken from Geng and Turcotte (1991). As for dependence on  $f_B$ , again from the same reference, it is illustrated by the calculated allowed range

$$\begin{aligned} 0.5 < B(K^+ \rightarrow \pi^+ \nu \bar{\nu}) < 1.2 \times 10^{-10} & \text{ for } f_B = 250 \pm 50 \text{ MeV}, \\ 0.5 < B(K^+ \rightarrow \pi^+ \nu \bar{\nu}) < 3.9 \times 10^{-10} & \text{ for } f_B = 130 \pm 40 \text{ MeV}, \end{aligned} \quad (4.3)$$

where they have used  $m_c = 1.5$  GeV and allowed a  $90 < m_t < 200$  GeV range for the top-quark mass. Thus higher  $f_B$  values tend to decrease the estimated branching fraction and to narrow the dependence on the top-quark mass. Alternatively, we can display the minimum and maximum values of the branching fraction as a function of the mass of the top quark, where the whole range of CKM matrix parameter space was explored to obtain the minimum and maximum. The results of this exploration are shown in Fig. 34 (from Dib *et al.*, 1991), where the authors used  $[B_B f_B^2]^{1/2} = 150 \pm 50$  MeV.

A deeper insight into the dependence of this branching fraction on the mass of the top quark can be obtained from the work of Buchalla *et al.* (1991). Their results are in qualitative agreement with those quoted above and they show separately the dependence of the rate on the mass of the top quark for two allowable regions of  $\delta$ . They obtain rough analytic bounds:

$$\begin{aligned} \delta \text{ in first quadrant: } 0.36 \times 10^{-10} x_t^{0.37} & \leq B(K^+ \rightarrow \pi^+ \nu \bar{\nu}) \leq 0.64 \times 10^{-10} x_t^{0.52}, \\ \delta \text{ in second quadrant: } 0.44 \times 10^{-10} x_t^{0.70} & \leq B(K^+ \rightarrow \pi^+ \nu \bar{\nu}) \leq 0.87 \times 10^{-10} x_t^{0.97}. \end{aligned} \quad (4.4)$$

Furthermore, they argue that when the most recent results from  $B^0$ - $\bar{B}^0$  mixing are taken into account, the most likely value for this branching fraction lies in the range  $(1-2.5) \times 10^{-10}$ .

We turn now to the question of possible influence on this rate of other diagrams, involving particles outside

the Standard Model. A most economical extension of the Standard Model would be a fourth generation of quarks (and/or leptons). Even though the LEP experiments exclude the possibility of a fourth light neutrino (LEP Collaborations, 1992), they do not forbid a less esthetically pleasing fourth generation of quarks without an accom-

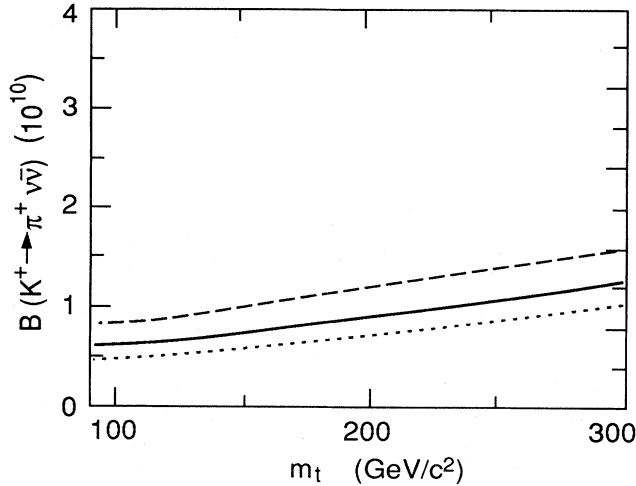


FIG. 33. The calculated branching-fraction ratio (at  $\chi^2_{\min}$ ) for  $K^+ \rightarrow \pi^+ \nu \bar{\nu}$  as a function of  $m_t$ , for  $f_B = 250 \pm 50$  MeV: dotted curve,  $m_c = 1.2$  GeV/ $c^2$ ; solid curve,  $m_c = 1.5$  GeV/ $c^2$ ; dashed curve,  $m_c = 1.8$  GeV/ $c^2$  (after Greg and Turcotte, 1991).

panying lepton family, or with a fourth lepton generation with a massive neutrino. The eight-quark situation was analyzed almost a decade ago by Ellis and Hagelin (1983), using experimental input data that is now somewhat obsolete. Nevertheless, their general arguments and conclusions remain unchanged.

Three salient points are relevant:

(a) Three separate and relevant pieces of experimental input could be affected by the fourth quark generation: the  $K_L^0 - K_S^0$  mass difference, the  $K^+ \rightarrow \pi^+ \nu \bar{\nu}$  branching fraction, and the short-distance contribution to  $K_L^0 \rightarrow \mu^+ \mu^-$ . Thus, if we construct an amplitude that contains contributions from both the third and fourth generations, we must satisfy constraints from all three measurements.

(b) These two contributions are either constructive in

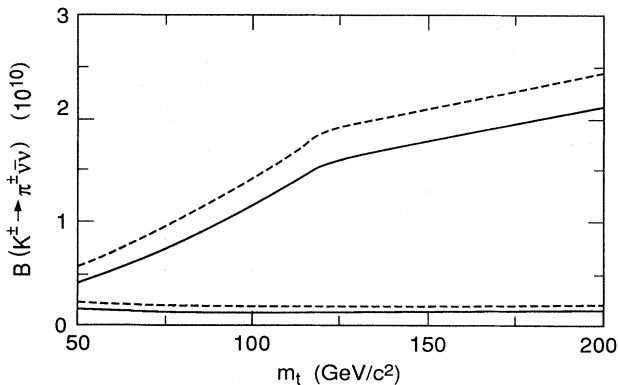


FIG. 34. The maximum and minimum of the branching fraction (per neutrino flavor) for  $K^+ \rightarrow \pi^+ \nu \bar{\nu}$ : dashed curve, without QCD corrections; solid curve, with QCD corrections (after Dib *et al.*, 1991).

both  $K_L^0 \rightarrow \mu^+ \mu^-$  and  $K^+ \rightarrow \pi^+ \nu \bar{\nu}$  or destructive in both.

(c) The lighter of the two quarks is more efficient in contributing to the  $K^+ \rightarrow \pi^+ \nu \bar{\nu}$  rate than the heavier quark. The opposite is true for  $K_L^0 \rightarrow \mu^+ \mu^-$ .

From these points, it then follows:

(a) An additional quark generation cannot increase the upper bound per neutrino generation for  $K^+ \rightarrow \pi^+ \nu \bar{\nu}$ , since that limit is effectively determined by the short-distance contribution to  $K_L^0 \rightarrow \mu^+ \mu^-$ .

(b) If the interference is destructive, it is in principle possible to choose couplings and masses such that the lower bound on the  $K^+ \rightarrow \pi^+ \nu \bar{\nu}$  rate would be decreased. It is even possible, though highly unlikely, to make the rate totally vanish in that case. It is the need to satisfy the constraint of  $K_L^0 - K_S^0$  mass difference that makes a large modification of the lower bound rather difficult.

The arguments given above can be generalized to any number of generations, and thus one can conclude that such an extension of the Standard Model will not modify the  $K^+ \rightarrow \pi^+ \nu \bar{\nu}$  rate significantly.

There have been published calculations (Marciano and Parsa, 1986; Türke, 1986) which reach a somewhat different conclusion, namely, that a fourth-generation quark family can generate a significant enhancement for the  $K^+ \rightarrow \pi^+ \nu \bar{\nu}$  rate. All of the constraints that have been put in by Ellis and Hagelin (1983), however, have not been included in those calculations. The work of Eilam *et al.* (1987), who claim to include in their calculations all of the appropriate constraints, does indicate some possible enhancement for the  $K^+ \rightarrow \pi^+ \nu \bar{\nu}$  due to the existence of a fourth quark family if very large mixing effects are postulated between the third and fourth quark generations.

The effects on  $K^+ \rightarrow \pi^+ \nu \bar{\nu}$  of other extensions of the Standard Model have been recently considered by Bigi and Gabbiani (1991) and were previously studied by Hagelin and Littenberg (1989). In brief, the general conclusion is that the simplest extensions of the Standard Model do not alter significantly the expected rate for that decay mode. Some more exotic theories, however, are able to change the expected rate significantly. The basic reason for this somewhat surprising result is that the  $B^0 - \bar{B}^0$  mixing and  $K^+ \rightarrow \pi^+ \nu \bar{\nu}$  are governed by many of the same parameters, for example,  $m_t$  and  $V_{td}$ , and by similar second-order diagrams. Thus the recent measurements of the  $B^0 - \bar{B}^0$  mixing parameter strongly constrain the latitude that one has in independently varying the parameters of the Standard Model and the contributions of new diagrams. We discuss below the possible effects due to some of the more popular recent models.

The simplest extension of the nonminimal Higgs sector is a model with two Higgs doublets and five physical scalars. The implications of that model for the decay rate have been studied recently by a number of authors (Barger *et al.*, 1990; Buras *et al.*, 1990; Bigi and Gabbiani, 1991). The diagrams that contribute to the decay mode discussed are illustrated in Fig. 35. The authors generally adopt the procedure of searching the parameter

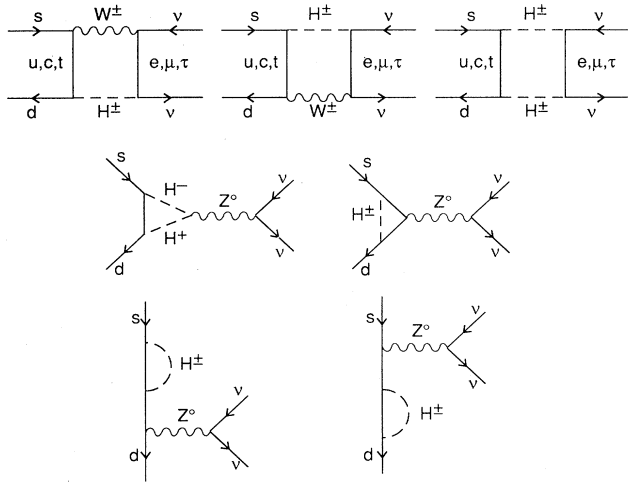


FIG. 35. Diagrams with charged Higgs exchanges contributing to  $K^+ \rightarrow \pi^+ \nu \bar{\nu}$  (after Buras *et al.*, 1990).

space for those values of top-quark mass and CKM matrix parameters which will satisfy the constraints imposed by measurements of other processes governed by box diagrams, especially the  $CP$  violation parameter  $\epsilon$  and  $B^0-\bar{B}^0$  mixing,  $x_d$ . The general conclusions are that it is difficult to generate a significant enhancement of the  $K^+ \rightarrow \pi^+ \nu \bar{\nu}$  rate via this mechanism, and for some range of parameters a small suppression can be obtained.

Another attractive extension of the Standard Model is provided by models based on left-right symmetric gauge theories (Pati and Salam, 1974; Mohapatra and Pati, 1975; Senjanovic and Mohapatra, 1975). They introduce additional flavor-changing possibilities via couplings of right-handed bosons and additional Higgs scalars (Ecker and Grimus, 1985). Lower limits on the masses of these new particles can be derived from the observed structure of the weak charged and neutral currents (Beall *et al.*, 1982; Ecker and Grimus, 1985). Using those limits, Bigi and Gabbiani (1991) derived an estimate for contributions from additional parts in the effective Hamiltonian due to these new couplings; their estimate is several orders of magnitude below the contributions from the Standard Model.

The minimal supersymmetric (SUSY) extensions of the Standard Model (Barbieri *et al.*, 1982) provide additional mechanisms to the  $K^+ \rightarrow \pi^+ \nu \bar{\nu}$  decay via box diagrams, with winos  $\tilde{W}$  and zinos  $\tilde{Z}$  replacing the  $W^\pm$ , and via penguin graphs, with gluinos or charged higgsinos (Giudice, 1987). Evaluation of those contributions (Bigi and Gabbiani, 1991) shows that even the largest of them contributes at a level somewhat smaller than  $10^{-11}$ .

The supersymmetric models with broken  $R$  parity (Barger *et al.*, 1989) offer the possibility of significant departures from the predictions of more standard SUSY models.  $K^+ \rightarrow \pi^+ \nu \bar{\nu}$  can be generated in tree-level diagrams (Bigi and Gabbiani, 1991) in these models and, because of very few bounds from experimental data on the

key parameters of the model, a very large branching ratio for  $K^+ \rightarrow \pi^+ \nu \bar{\nu}$  is in principle possible.

## 2. Experimental status

The decay  $K^+ \rightarrow \pi^+ \nu \bar{\nu}$  attracted initial interest some time ago because of the realization that it offered a fruitful ground for studying flavor-changing neutral-current interactions. The early experiments (Klems *et al.*, 1971; Cable *et al.*, 1973) at the LBL Bevatron and by Asano *et al.* (1981) at KEK gave the initial upper limits at 90% C.L. of  $5.6 \times 10^{-7}$  and  $1.4 \times 10^{-7}$ , respectively. More recently, an ambitious experimental program was started at BNL (experiment E787) to search for this decay mode, with an eventual goal of reaching a level of sensitivity that would probe the Standard Model predictions. In the remainder of this section we shall describe the technique of this experiment, results to date, and future prospects.

Unlike most other rare decay processes discussed in this review, the  $K^+ \rightarrow \pi^+ \nu \bar{\nu}$  decay events cannot be defined by specific constraints. The signatures of this decay mode in the E787 experiment are (a) a stopping  $K^+$ , (b) a decay  $\pi^+$  that is associated in space, but somewhat delayed in time, and (c) absence of any other interacting particle anywhere in the detector.

In practice, to suppress the most dominant backgrounds, it turns out to be necessary to impose an additional constraint, (d) a pion energy inconsistent with coming from  $K^+ \rightarrow \pi^+ \pi^0$  or  $K^+ \rightarrow \mu^+ \nu$  if the  $\mu^+$  is misidentified as a  $\pi^+$ .

In the initial phases of the experiment, this last requirement was made even more stringent, i.e., the pion energy had to be higher than  $E_\pi$  corresponding to the  $2\pi$  decay mode.

Figure 36 illustrates the relevance of the last point. The  $\pi^+ \pi^0$  decay is the second most dominant mode, with a branching fraction of about 21%. Thus to achieve the goal of  $2 \times 10^{-10}$  sensitivity, individual  $\gamma$  rejection of  $10^{-4}$ – $10^{-5}$  would be necessary if one accepted events in that region. That is considered to be well below the present experimental capability. The only potential decay mode with a pion in the momentum domain currently accepted ( $213 < P_\pi < 237$  MeV/c) is  $\pi^+ \gamma \gamma$ . That decay mode has not been observed as yet (Atiya *et al.*, 1989b) but is expected to be  $O(10^{-7})$  (Cheng, 1990; Ecker *et al.*, 1990).

We should also consider other decay modes as potential sources of background in light of the fact that initial attempts are being made to extend the analysis range in  $P_\pi$  space. The next most copious decay mode with a  $\pi^+$  is the  $\pi^+ \pi^0 \pi^0$ , which has  $P_\pi^{\max} = 133$  MeV/c, a branching fraction of only 1.7%, and four  $\gamma$ 's. Thus it should not present an insurmountable problem. Other decay modes, like  $\mu \nu$ ,  $\mu^+ \pi^0 \nu$ , and  $\mu^+ \nu \gamma$ , can be rejected via  $\pi$ - $\mu$  discrimination in addition to rejection by observation of extra photon(s) or by eliminating events with a certain charged track energy. The four-body decays  $\pi \pi e \nu$  and

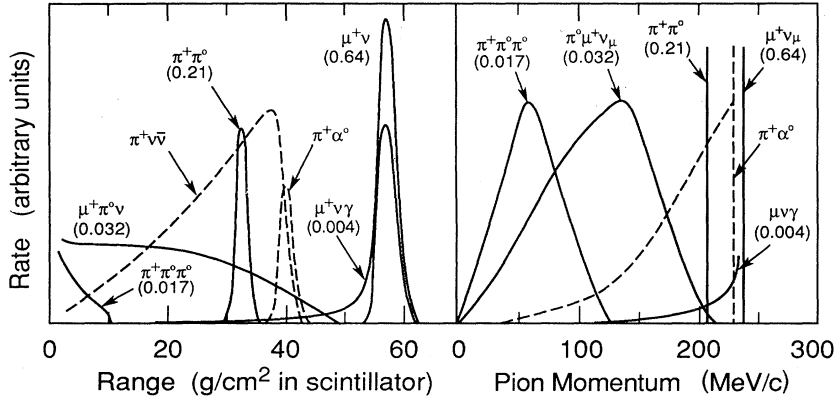


FIG. 36. Range and momentum spectra of  $\pi^+$  from  $K^+ \rightarrow \pi^+ \nu \bar{\nu}$  and from  $K^+ \rightarrow \pi^+ \alpha^0$ , where  $\alpha^0$  is some massless particle, and of  $\pi^+$  and  $\mu^+$  from the background decays.

$\pi\pi\mu\nu$  have relatively low branching ratios (few  $\times 10^{-5}$ ) and involve three charged tracks.  $\pi^+\pi^0\gamma$  and  $\pi^+\pi^0\pi^0\gamma$  are also strongly suppressed  $\sim O(10^{-4})$  and  $O(10^{-6})$  and in addition have more photons in the final state. Thus it is possible that one will be able to accept for analysis the region with  $P_{\pi^+} < 200$  MeV/c and thus improve experimental sensitivity.

The Brookhaven experiment achieves the goals identified above in the following general manner (Atiya *et al.*, 1989a):

(a) A beam of 775-MeV/c charged particles ( $\pi$ -to- $K$  ratio of about 2.5 to 1) enters a live stopping target located in the middle of a hermetic detector. A Čerenkov counter before the target gives a pulse in different sets of phototubes depending on whether the particle is a  $K^+$  or a  $\pi^+$ .

(b) A  $\pi^+$  is identified in two ways. First, independent measurements of range, momentum, and kinetic energy are made and are required to be consistent with a pion mass assignment. Second, the highly characteristic  $\pi^+ \rightarrow \mu^+ \rightarrow e^+$  decay chain has to be detected.

(c) The detector is completely hermetic and presents a

sufficient number of radiation lengths in all directions to ensure that practically all the produced photons are detected and thus can be vetoed.

(d) Both on-line and off-line cuts are made on pion energy to accept only pions in the preselected energy range.

The E787 detector is illustrated in Fig. 37. It is a  $4\pi$  detector, similar in many of its features to a colliding-beam apparatus. Starting from the center, and going out in radius, its main elements are (Atiya *et al.*, 1992) (a) a stopping target, composed of scintillating fibers, (b) a cylindrical drift chamber, (c) a range stack composed of plastic scintillators with photomultipliers at each end and of two layers of imbedded multiwire proportional chambers to improve tracking, and (d) a lead-scintillator electromagnetic calorimeter.

All of these detectors are contained in a solenoidal field of 1 T, and the end-cap regions are covered by additional photon vetoes.

The scintillators in the range stack give approximately 15 photoelectrons in each photomultiplier per 1 MeV of deposited energy. Thus photons of energy as low as 1 MeV are vetoed with very high efficiency. As far as  $\pi\mu$

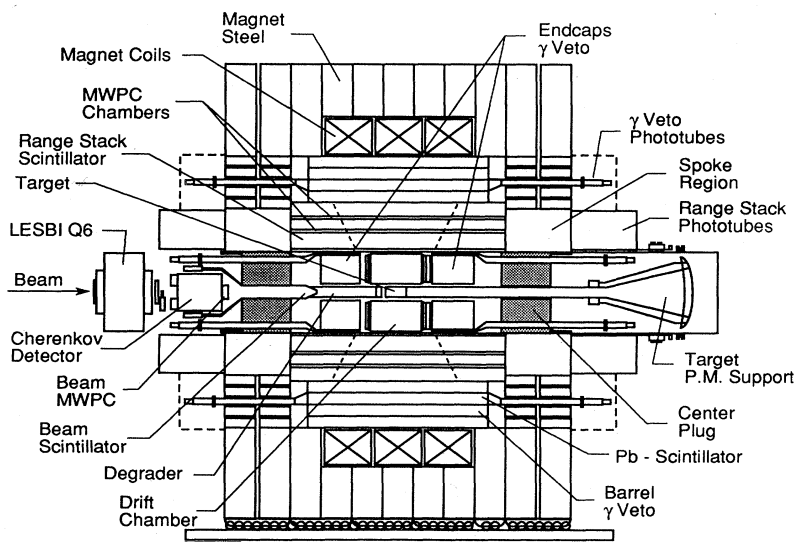


FIG. 37. Schematic side view of the detector for Brookhaven experiment E787.

rejection is concerned, one method of pion identification is the required consistency of energy (from total  $dE/dx$  deposition), momentum (from curvature), and range (from penetration). A second very powerful handle is the  $\pi$ - $\mu$ - $e$  decay sequence. The occurrence of such a sequence is determined by means of transient digitizers associated with all the counters in the range stack. An accepted event must have the correct spatial and time pattern as well as pulse heights within the acceptable range. Such an electronics signature of one good  $\pi \rightarrow \mu \rightarrow e$  decay is shown in Fig. 38.

A whole series of cuts are applied to the data to ensure compliance with the criteria established for good  $\pi^+ \nu \bar{\nu}$  candidates. The overall acceptance is 0.55%, which includes the fact that only 17% of the total  $K^+ \rightarrow \pi^+ \nu \bar{\nu}$  spectrum is accepted.

The initial data from this experiment were taken in the winter of 1988 and the results are displayed in Fig. 39. No events were seen in the signal box, allowing one to set a 90%-confidence-level limit on the decay of  $3.4 \times 10^{-8}$  (Atiya *et al.*, 1990a). Approximately an order of magnitude more data were obtained in the winter of 1989. Analysis of these data (Atiya *et al.*, 1993a) yielded no candidates, giving a 90%-confidence-level upper limit of  $7.5 \times 10^{-9}$ . In addition, an analysis was performed for the kinematical region with  $P_\pi < 192$  MeV/c. That analysis (Atiya *et al.*, 1993b) also yielded no candidate events and provides by itself a 90%-confidence-level limit of  $1.7 \times 10^{-8}$ . Combining these two independent results provides an overall limit of  $5.2 \times 10^{-9}$ .

Additional data were taken in early 1990 which will increase the statistics by close to a factor of 3. Subsequent

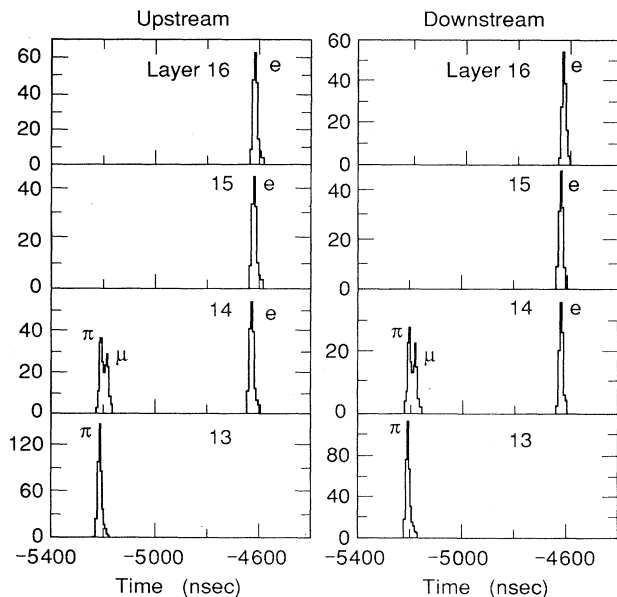


FIG. 38. Transient digitizer data of different layers for one typical event. The pion came from the target, passed through layer 13 and stopped in layer 14. The  $\pi \rightarrow \mu$  decay was observed in layer 14. The decay positron from  $\mu \rightarrow e$  decay went outwards through the layers 14, 15, and 16.

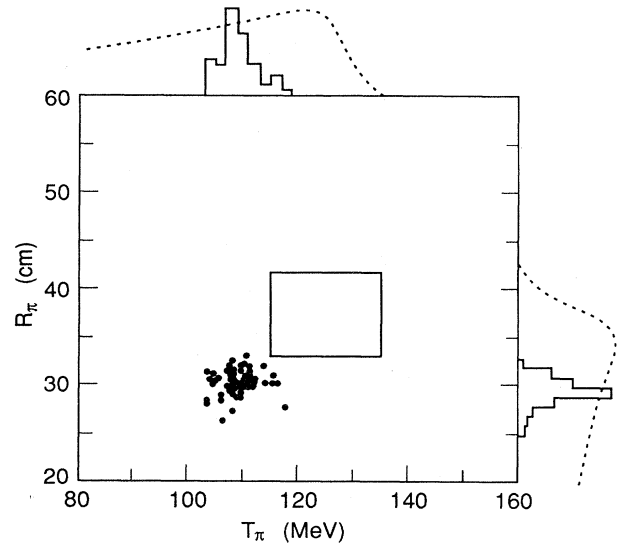


FIG. 39. Range vs kinetic energy for events satisfying all the selection criteria for  $K^+ \rightarrow \pi^+ \nu \bar{\nu}$  candidates and having measured momentum  $205 < P_\pi < 243$  MeV/c. The rectangular box indicates the search region for  $K^+ \rightarrow \pi^+ \nu \bar{\nu}$ . The dotted curves on the projection axes show the shape of the Standard Model spectrum for  $K^+ \rightarrow \pi^+ \nu \bar{\nu}$ , folded with the experimental resolution (after Atiya *et al.*, 1990a).

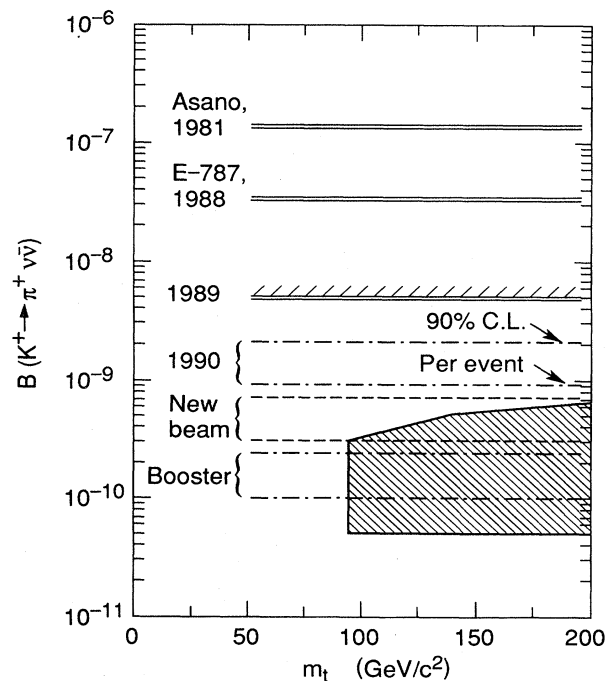


FIG. 40. Present upper limit and expected future improvement for  $K^+ \rightarrow \pi^+ \nu \bar{\nu}$  decay for BNL experiment E787. The shaded region indicates the maximum range, as calculated by Dib *et al.* (1991), of allowable branching fraction values for the Standard Model.

to that data-taking period, significant modifications were being made to the AGS accelerator, the beam line, and the detector to improve the expected sensitivity by more than an order of magnitude. The AGS intensity will be increased by about a factor of 4 by addition of the Booster; the beam line was rebuilt to increase the flux and to improve the  $K/\pi$  ratio and thus to decrease the dead time due to incoming  $\pi^+$  and possible background due to  $\pi^+$  scatterers. Several major modifications were made to the detector. The most important ones are probably a new drift chamber operating with a low- $Z$  gas to improve momentum resolution and a new electromagnetic calorimeter consisting of CsI to improve soft-photon rejection. Data taking with most of the upgrades in place should commence in 1994. The expected improved sensitivity as a function of time is shown in Fig. 40.

**B.  $K_L^0 \rightarrow \mu\mu$**

**1. Phenomenology**

The  $K_L^0 \rightarrow \mu\mu$  decay is the classic example of a flavor-changing neutral-current process. Its suppression relative to  $K^+ \rightarrow \mu\nu$  posed a serious problem to a gauge theory of the weak interaction based on  $SU(2)$ . The solution in 1974 by Glashow, Illiopoulos, and Maiani (1970) invoking the existence of a fourth (charm) quark was a major theoretical advance. The mode continues to be interesting because of its potential to probe second-order weak processes in the Standard Model (Gaillard *et al.*, 1976; Shrock and Voloshin, 1979; Buras, 1981; Gilman and Hagelin, 1983; Bergström *et al.*, 1984; Geng and Ng, 1990; Buchalla *et al.*, 1991). In fact, it is sensitive to much of the same short-distance physics as  $K^+ \rightarrow \pi^+ \nu\bar{\nu}$  (i.e., the  $V_{td}$  element of the CKM mixing matrix and the top-quark mass). While the theoretical situation with respect to interpreting a measurement of the  $K_L^0 \rightarrow \mu\mu$  branching ratio is far more complex and uncertain than in the  $K^+ \rightarrow \pi^+ \nu\bar{\nu}$  case, experimentally the situation is completely reversed. A precise, high-statistics measurement of  $K_L^0 \rightarrow \mu\mu$  is now possible, while it remains a major struggle to observe the first instance of  $K^+ \rightarrow \pi^+ \nu\bar{\nu}$ . As a result, the two modes can provide complementary information, leading to a situation that can be summarized as good systematics but poor statistics for  $K^+ \rightarrow \pi^+ \nu\bar{\nu}$ , and poor systematics but good statistics for  $K_L^0 \rightarrow \mu\mu$ .

The amplitude for the  $K_L^0 \rightarrow \mu\mu$  has a real (dispersive) and an imaginary (absorptive) part. The absorptive part is known to dominate the observed  $K_L^0 \rightarrow \mu\mu$  decay rate. The largest contribution to the absorptive part comes from the real two-photon intermediate state (i.e.,  $K_L^0 \rightarrow \gamma\gamma \rightarrow \mu\mu$ ), shown in Fig. 41(a). The decay rate for this process is given by (Sehgal, 1969b)

$$\frac{\Gamma(K_L^0 \rightarrow \mu\mu)_{2\gamma}}{\Gamma(K_L^0 \rightarrow \gamma\gamma)} = \alpha^2 \left[ \frac{m_\mu}{m_K} \right]^2 \frac{1}{2\beta} \left[ \ln \frac{1+\beta}{1-\beta} \right]^2, \quad (4.5)$$

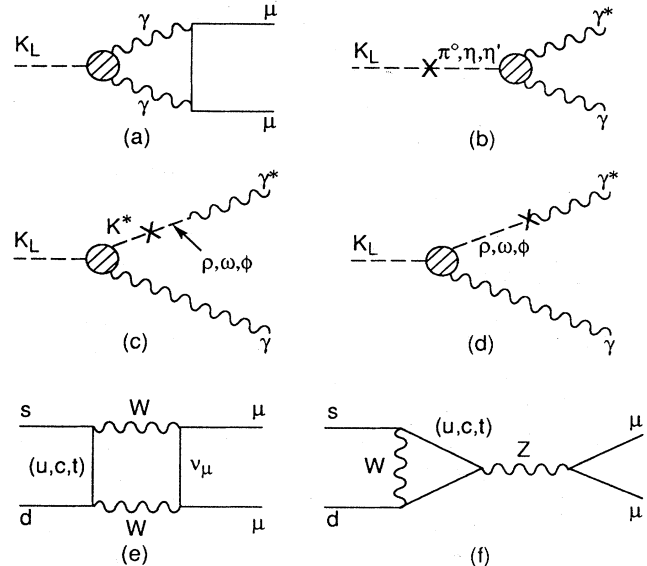


FIG. 41. Diagrams relevant to  $K_L^0 \rightarrow \mu^+ \mu^-$ : (a) the two-photon absorptive contribution to  $K_L^0 \rightarrow \mu\mu$ ; (b)  $\pi, \eta, \eta'$  pole-dominance graph for  $K_L^0 \rightarrow \mu\mu$ ; (c) vector-meson dominance graph for  $K_L^0 \rightarrow \mu\mu$ ; (d) vector-meson dominance graph included by Ko; (e) and (f) short-distance graphs contributing to  $K_L^0 \rightarrow \mu\mu$ .

where  $\beta = \sqrt{1 - 4m_\mu^2/m_K^2}$ . This leads to

$$B(K_L^0 \rightarrow \mu\mu)_{2\gamma} = (1.2 \times 10^{-5}) B(K_L^0 \rightarrow \gamma\gamma). \quad (4.6)$$

Using the Particle Data Group value for  $B(K_L^0 \rightarrow \gamma\gamma)$ , this corresponds to a  $K_L^0 \rightarrow \mu\mu$  branching fraction of  $(6.8 \pm 0.3) \times 10^{-9}$ , where the quoted error is entirely from the  $K_L^0 \rightarrow \gamma\gamma$  uncertainty. This value of the branching fraction is usually referred to as the “unitarity bound.” Contributions from other intermediate states (e.g.,  $\pi\pi\gamma$ ,  $\pi\pi\pi$ ) to the absorptive amplitude are believed to be small (Martin *et al.*, 1970).

The dispersive amplitude is the sum of both long-distance and short-distance contributions. The extent to which the long-distance part of the amplitude can be understood separately will ultimately determine the power of  $K_L^0 \rightarrow \mu\mu$  to probe short-distance effects in the Standard Model. That is, the difference between the measured  $K_L^0 \rightarrow \mu\mu$  branching fraction and the unitarity bound provides a measure of the total dispersive contribution. Knowledge of the magnitude and sign of the long-distance part may permit determination of the short-distance part, from which information on CKM parameters and the top-quark mass may be inferred.

The long-distance part is due mainly to the virtual two-photon intermediate state ( $K_L^0 \rightarrow \gamma^* \gamma^* \rightarrow \mu\mu$ ). The  $K_L^0 \rightarrow \gamma^* \gamma^*$  vertex is not well understood. It is conventional to treat the decay  $K_L^0 \rightarrow \gamma\gamma$  in terms of pseudoscalar ( $\pi^0, \eta, \eta'$ ) pole dominance; this approach successfully predicts the decay rate (Ma and Pramudita, 1981). For the case of off-shell photons, there is an analogous contribution; information on this contribution can be obtained

(Barger *et al.*, 1982) from the dispersive contribution to the decay  $\eta \rightarrow \mu\mu$ . However, other contributions (Bergström *et al.*, 1984) to  $K_L^0 \rightarrow \gamma^* \gamma^*$  are also present. The current status of estimates for the long-distance dispersive  $K_L^0 \rightarrow \mu\mu$  amplitude leaves much to be desired. Two recent analyses have reached different conclusions; these will be discussed below. However, it is appropriate first to discuss the decay  $K_L^0 \rightarrow ee\gamma$ , which provides information on the  $K_L^0$ - $\gamma$ - $\gamma^*$  vertex. At present, this is the best source of guidance on the long-distance dispersive contribution to  $K_L^0 \rightarrow \mu\mu$  from the  $K_L^0$ - $\gamma^*$ - $\gamma^*$  vertex.

The decay  $K_L^0 \rightarrow ee\gamma$  plays a role for  $K_L^0 \rightarrow \mu\mu$  somewhat similar to that which  $K_L^0 \rightarrow \pi^0 \gamma \gamma$  plays for  $K_L^0 \rightarrow \pi^0 ee$ , namely, it provides information on a relatively less interesting contribution to the decay rate which needs to be understood in order to access the short-distance Standard Model information, which is our goal. Other  $K_L^0$  decay channels may eventually provide additional guidance concerning the long-distance dispersive  $K_L^0 \rightarrow \mu\mu$  rate, and these will be touched on briefly. The  $K_L^0 \rightarrow ee\gamma$  process, however, merits most of our attention because by now it has been relatively well measured by two experiments, and they provide consistent results.

The  $K_L^0 \rightarrow ee\gamma$  differential decay spectrum is given by the usual Kroll-Wada Dalitz decay expression (Kroll and Wada, 1955), which can be written

$$\frac{1}{\Gamma_{\gamma\gamma}} \frac{d\Gamma}{dx} = \frac{2\alpha}{3\pi} \frac{(1-x)^3}{x} \left[ 1 + \frac{2m_e^2}{xm_K^2} \right] \left[ 1 - \frac{4m_e^2}{xm_K^2} \right]^{1/2}, \quad (4.7)$$

where  $\Gamma_{\gamma\gamma}$  is the  $K_L^0 \rightarrow \gamma\gamma$  decay rate,  $x = m_{ee}^2/m_K^2$ , and radiative corrections are not included. This may be modified to account for the structure of the off-shell photon by multiplying by  $|f(x)|^2$ , where the function  $f(x)$  is a form factor that characterizes the deviation from the naive Dalitz decay form due to the structure of the  $K_L^0$ - $\gamma$ - $\gamma^*$  vertex. It is defined so that  $f(0)=1$ . In particular, it is a measurement of the form factor  $f(x)$ , in addition to the  $K_L^0 \rightarrow ee\gamma$  branching fraction, that has been the result of the two recent experiments. Each of these experiments, CERN NA31 and BNL E845, was previously discussed in the context of the  $K_L^0 \rightarrow \pi^0 ee$  mode, and we shall not repeat a discussion of the detectors here. The two measurements of  $K_L^0 \rightarrow ee\gamma$  are very similar. The CERN measurement (Barr *et al.*, 1990) is based on the observation of 1053  $K_L^0 \rightarrow ee\gamma$  decays. The BNL result (Ohl *et al.*, 1990b) is based on the observation of 919  $K_L^0 \rightarrow ee\gamma$  decays.

The potential background processes to a  $K_L^0 \rightarrow ee\gamma$  measurement are radiative  $K_{e3}$  decays ( $K_L^0 \rightarrow \pi e \nu \gamma$ ), where the pion is misidentified as an electron, and normal  $K_{e3}$  decays in which the pion shower develops in the electromagnetic calorimeter in such a way as to mimic two clusters. Such background events, however, were distinguished in both experiments by their low reconstructed  $ee\gamma$  mass. This is seen in Fig. 42, which shows a

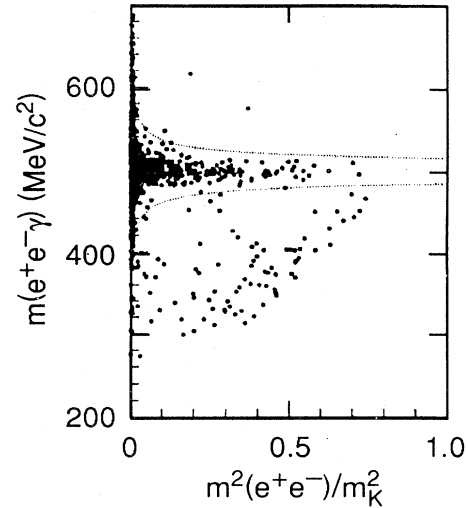


FIG. 42. Scatter plot of the  $ee\gamma$  mass vs  $x$  from the CERN experiment. The dashed lines are the  $4\sigma$  error contours (after Barr *et al.*, 1990).

scatter plot of  $ee\gamma$  mass versus the quantity  $x = m_{ee}^2/m_K^2$  for the CERN experiment. The events outside and principally below the signal region are due to these background sources. The CERN group estimated the background contribution within the signal region to be less than one event.

Both experimental groups used the same parametrization of the form factor, due to Bergström, Massó, and Singer (1983). The parametrization consists of two com-

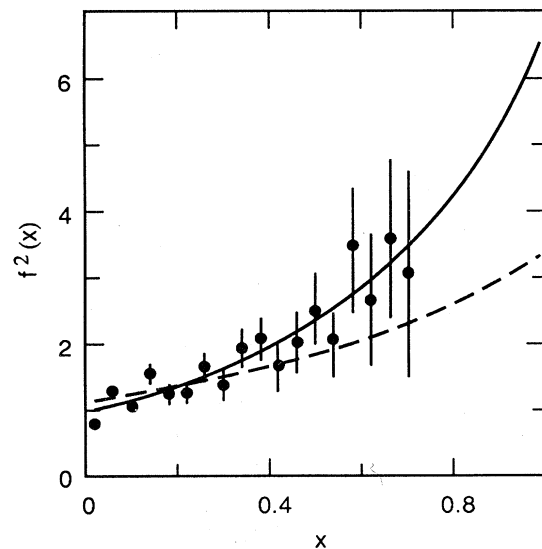


FIG. 43. Square of the form factor  $f(x)$  from the BNL experiment. Points are data. The solid line corresponds to the best-fit value  $\alpha_{K^*} = -0.28$  and the dotted line to  $\alpha_{K^*} = 0$  (after Ohl *et al.*, 1990b).

ponents, but has only one free parameter. The first component, due to the diagrams illustrated in Fig. 41(b), is motivated by  $\pi^0, \eta, \eta'$  pseudoscalar pole dominance. The relative weight of this term in the form factor is not free, since this term should reproduce the measured  $K_L^0 \rightarrow \gamma\gamma$  rate as the mass of the virtual photon goes to zero. The second component, illustrated in Fig. 41(c), represents a  $K_L^0 \rightarrow K^* \gamma$  transition, followed by a nonleptonic  $K^* \rightarrow \rho, \omega, \phi$  transition. The weight of this term is not fixed and depends on a parameter  $\alpha_{K^*}$ . Explicitly, the parametrization is

$$f(x) = \frac{1}{\left[1 - x \frac{m_K^2}{m_\rho^2}\right]} + \frac{\alpha_{K^*}}{\left[1 - x \frac{m_K^2}{m_{K^*}^2}\right]} A_{K^*}(x), \quad (4.8)$$

where

$$A_{K^*}(x) = \sqrt{8\pi\alpha} G_F f_{K^* K \gamma} \frac{m_\rho^2}{f_{K^*} f_\rho^2} \times \left[ \frac{4}{3} - \frac{1}{\left[1 - x \frac{m_K^2}{m_\rho^2}\right]} - \frac{1}{9} \left( \frac{1}{\left[1 - x \frac{m_K^2}{m_\omega^2}\right]} + \frac{2}{\left[1 - x \frac{m_K^2}{m_\phi^2}\right]} \right) \right]. \quad (4.9)$$

The coefficients  $f_{K^* K \gamma}$ ,  $f_{K^*}$ , and  $f_\rho$  are fixed by measured decay rates. We note that the first term in the expression for  $f(x)$  smoothly extrapolates to unity for the case of an on-shell photon, as required by the rate for  $K_L^0 \rightarrow \gamma\gamma$  for real photons. The second term vanishes for an on-shell photon, as required by gauge invariance.

Figure 43 shows the data for the form-factor determination from the Brookhaven experiment. The square of the form factor is plotted versus  $x$ . The solid line shows the form factor for the best-fit value of  $\alpha_{K^*}$ , and the dotted line shows the form factor for  $\alpha_{K^*} = 0$ . While the  $\alpha_{K^*} = 0$  curve is clearly inconsistent with the data, the errors are such that considerable freedom to vary  $\alpha_{K^*}$  still exists. In particular, the data do not extend above about  $x = 0.7$ , corresponding to  $m_{ee}$  values around 400 MeV. We shall return to this point when discussing the possible background the  $K_L^0 \rightarrow ee\gamma$  process may pose for  $K_L^0 \rightarrow ee$  searches. The best-fit value from the Brookhaven experiment was  $\alpha_{K^*} = -0.280^{+0.099}_{-0.090}$ . The CERN result was  $\alpha_{K^*} = -0.28 \pm 0.13$ . The experiments determined  $K_L^0 \rightarrow ee\gamma$  branching fractions to be  $(9.1 \pm 0.4^{+0.6}_{-0.5}) \times 10^{-6}$  (BNL) and  $(9.2 \pm 0.5 \pm 0.5) \times 10^{-6}$  (CERN), in obvious good agreement. Finally, we should remark that radiative corrections have been ignored in

our discussion, but are not negligible in practice. In the BNL experiment, the effect of ignoring radiative corrections on the best-fit value of the  $\alpha_{K^*}$  parameter was to change it to  $\alpha_{K^*} = -0.18$ .

Let us now resume our discussion of the dispersive  $K_L^0 \rightarrow \mu\mu$  contribution. An analysis by Bergström, Massó, and Singer (1990) relies on these recent measurements of the  $K_L^0 \rightarrow ee\gamma$  form factor, making use of the parametrization of  $f(x)$  for the  $K_L^0 - \gamma - \gamma^*$  vertex described above. A principal question is, given the form factor for the  $K_L^0 - \gamma - \gamma^*$  vertex, how to continue this to the  $K_L^0 - \gamma^* - \gamma^*$  case. Bergström, Massó, and Singer (1990) argue that by considering two alternatives, namely, saturating one photon by vector mesons or saturating both, one establishes bounds within which the true value must lie. They conclude that the long-distance dispersive contribution to  $K_L^0 \rightarrow \mu\mu$  is small and its contribution to the total decay rate is only  $2 \pm 2\%$  of the absorptive contribution.

This conclusion is not supported by an analysis by Ko (1992), which uses a chiral Lagrangian in the hidden-symmetry scheme (Ko, 1990, 1991; see also Bando *et al.*, 1988) with the Wess-Zumino anomaly. This model also includes a third contribution, shown in Fig. 41(d). The relative strengths of the three diagrams are fixed by the chiral Lagrangian, although other parameters appear which must be determined from data. The principal conclusions of Ko are that the magnitude of the long-distance dispersive amplitude is significant—roughly half that of the absorptive (unitarity) amplitude, but opposite in sign from the dispersive short-distance contribution. That is, the long- and short-distance dispersive amplitudes tend to cancel. If true, this complicates the situation with regard to using the value of  $K_L^0 \rightarrow \mu\mu$  as a probe for short-distance Standard Model physics. In view of these considerations, no definite conclusion can be drawn at the present time.

Several measurements are possible that will help to clarify the situation. For example, a measurement of  $K_L^0 \rightarrow \mu\mu\gamma$  has the potential to shed additional light on the  $K_L^0 - \gamma - \gamma^*$  form factor. It has been emphasized by Bergström, Massó, and Singer (1983) that this mode has considerable power to determine the parameter  $\alpha_{K^*}$ . In particular, the  $K_L^0 \rightarrow \mu\mu\gamma$  branching fraction is sensitive to  $\alpha_{K^*}$ , as shown in Fig. 44, in contrast to the  $K_L^0 \rightarrow ee\gamma$  case, in which the branching fraction is insensitive and a measurement of the  $m_{ee}$  spectrum is needed. The explanation of this is the  $1/q^2$  dependence ( $q^2 = m_{ee}^2$ ) of the decay rate, which peaks strongly near the threshold  $q^2 = 4m_e^2$  for the  $ee\gamma$  mode. For small values of  $q^2$  the contribution from the  $K^*$  transition term is small. For the  $\mu\mu\gamma$  mode the threshold ( $q^2 = 4m_\mu^2$ ) is much higher and is in the region where the  $K^*$  transition term has already become important. Ko (1991) has also emphasized the value of the  $\mu\mu\gamma$  mode for distinguishing between models. The branching fraction for  $K_L^0 \rightarrow \mu\mu\gamma$  is expected to be about  $4 \times 10^{-7}$  (Bergström, Massó, and Singer, 1990; Ko, 1991). Until recently, the only measurement of

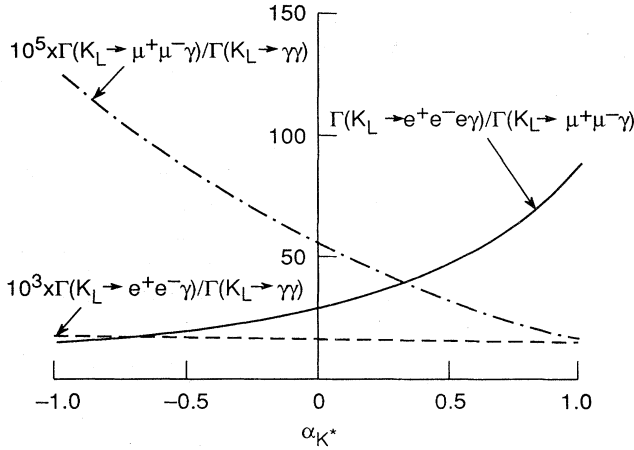


FIG. 44. Predicted branching fractions for  $K_L^0 \rightarrow ee\gamma$  and  $K_L^0 \rightarrow \mu\mu\gamma$  as a function of  $\alpha_{K^*}$ , after Bergström, Massó, and Singer (1983). Also shown is the ratio of predicted decay rates.

$K_L^0 \rightarrow \mu\mu\gamma$  was from a Brookhaven experiment (Carroll *et al.*, 1980), which observed one candidate and reported a branching fraction of  $(2.8 \pm 2.8) \times 10^{-7}$ . But in a significant step forward, the FNAL E799 experiment (a follow-on to E731 by the FNAL  $CP$  violation group) has reported (Tschirhart, 1992) the observation of 167 events with background at the 3–5 % level. The preliminary branching ratio  $K_L^0 \rightarrow \mu\mu\gamma$  from this experiment is  $(3.88 \pm 0.32) \times 10^{-7}$ , where the error is statistical only. Further analysis of systematic errors is underway. This result is clearly consistent with the theoretical expectations discussed above, but it would be premature at this time to draw definite conclusions.

Finally, the decay  $K_L^0 \rightarrow e^+e^-e^+e^-$  is a rather direct probe of the  $K_L^0\text{-}\gamma^*\text{-}\gamma^*$  vertex and has the clear advantage of not leaving the question of how to continue the  $K_L^0\text{-}\gamma\text{-}\gamma^*$  form factor to the region of interest. The current generation of experiments (CERN NA31, BNL 845, and FNAL E731/E799) have observed this process, but with insufficient statistics to probe the underlying matrix element. The future high-sensitivity searches for  $K_L^0 \rightarrow \pi^0 ee$  (FNAL E799 and KEK E162) may accumulate sufficiently large data samples to address this issue.

Having discussed the current situation with respect to the long-distance contributions to  $K_L^0 \rightarrow \mu\mu$ , we now turn to the short-distance dispersive contribution to  $K_L^0 \rightarrow \mu\mu$ . This has been discussed by several authors (Gaillard *et al.*, 1976; Shrock and Voloshin, 1979; Buras, 1981; Gilman and Hagelin, 1983; Bergström *et al.*, 1984; Geng and Ng, 1990; Buchalla *et al.*, 1991), with perhaps the most emphasis recently having been placed on the sensitivity of this contribution to the mass of the top quark. The process is due to the second-order weak diagrams shown in Figs. 41(e) and 41(f) and may be written (Inami and Lim, 1981).

$$B(K_L^0 \rightarrow \mu\mu)_{SD} = \frac{\alpha^2}{4\pi^2 \sin^4 \theta_W} \frac{\left[1 - \frac{4m_\mu^2}{m_K^2}\right]^{1/2}}{\left[1 - \frac{m_\mu^2}{m_K^2}\right]^2} \times \frac{\left| \text{Re} \sum_{i=c,t} \eta_i V_{is}^* V_{id} C_\mu(x_i) \right|^2}{|V_{us}|^2} \times B(K^+ \rightarrow \mu^+ \nu_\mu) \frac{\tau(K_L^0)}{\tau(K^+)}, \quad (4.10)$$

where the  $\eta_i$ 's are QCD correction factors,  $\tau(K_L^0)$  and  $\tau(K^+)$  are the  $K_L^0$  and  $K^+$  lifetimes,  $x_i = m_i^2/m_W^2$ , and

$$C_\mu(x_i) = \frac{4x_i - x_i^2}{4(1-x_i)} + \frac{3x_i^2 \ln x_i}{4(1-x_i)^2}. \quad (4.11)$$

The top quark dominates, and it is believed (Dib *et al.*, 1989) that  $\eta_i \approx 1$ , so it follows that to a good approximation

$$B(K_L^0 \rightarrow \mu\mu)_{SD} = 4.06 \times 10^{-10} A^4 |C_\mu(x_t)|^2 (1-\rho)^2. \quad (4.12)$$

Figure 45 shows  $|C_\mu(x_t)|^2$  as a function of  $m_t$ . If  $B(K_L^0 \rightarrow \mu\mu)_{SD}$  can be determined experimentally, Eq. (4.12) provides a means of constraining the Wolfenstein  $\rho$  parameter as a function of the top-quark mass. This is illustrated in Fig. 46, which shows  $\rho$  vs  $m_t$  for  $A = 1$  and three values of  $B(K_L^0 \rightarrow \mu\mu)_{SD}$ .

As in the case of  $K^+ \rightarrow \pi^+ \nu \bar{\nu}$  discussed in the previous section, Buchalla *et al.* (1991) have obtained the dependence of this rate on the mass of the top quark for the two allowable regions of the CKM parameter  $\delta$ . They obtain as rough analytic bounds

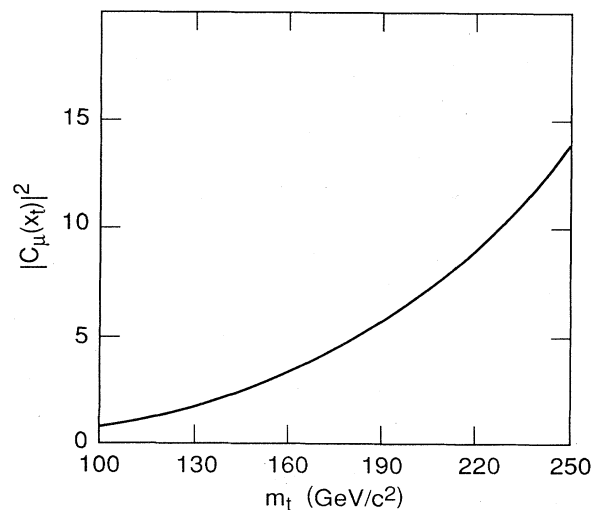


FIG. 45. The function  $|C_\mu(x_t)|^2$  vs the top-quark mass  $m_t$ .

$$\begin{aligned} \delta \text{ in first quadrant: } & 1.86 \times 10^{-10} x_t^{0.70} \leq B(K_L^0 \rightarrow \mu^+ \mu^-)_{\text{SD}} \leq 3.6 \times 10^{-10} x_t, \\ \delta \text{ in second quadrant: } & 2.4 \times 10^{-10} x_t^{1.17} \leq B(K_L^0 \rightarrow \mu^+ \mu^-)_{\text{SD}} \leq 5.88 \times 10^{-10} x_t^{1.41}. \end{aligned} \tag{4.13}$$

They also conclude that the most recent results from  $B^0-\bar{B}^0$  mixing imply that the most likely value for this branching fraction lies in the range  $(0.5-4) \times 10^{-9}$ . This range is well below the unitarity level and possibly of the same rough magnitude as the long-distance dispersive contributions discussed above, thereby making the short-distance contribution difficult to measure.

Extracting information on Standard Model parameters from  $K_L^0 \rightarrow \mu\mu$  depends on improvements in our understanding of the long-distance physics. However, it should be kept in mind that the mode is experimentally accessible, while the cleaner  $K^+ \rightarrow \pi^+ \nu\bar{\nu}$  has not been observed and relies on significant experimental advances before even a low-statistics sample will be available. Therefore it is certainly worthwhile both to make precise measurements of  $K_L^0 \rightarrow \mu\mu$  and to work to understand the long-distance physics.

## 2. Experimental status

The  $K_L^0 \rightarrow \mu\mu$  decay has enjoyed a lively history experimentally as well as theoretically. An early upper limit

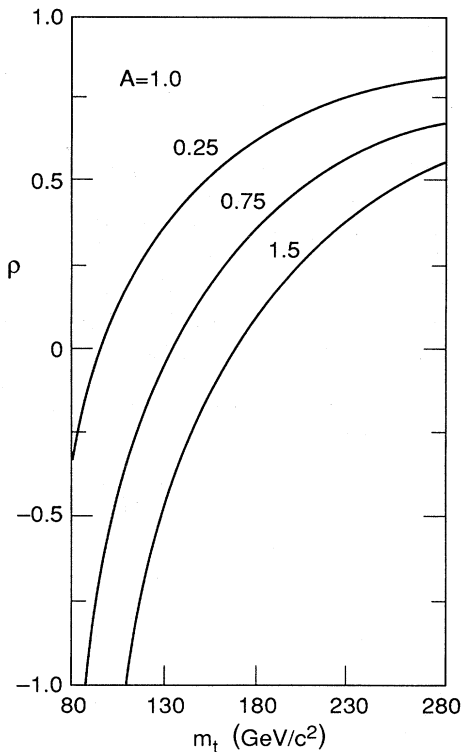


FIG. 46. The Wolfenstein  $\rho$  parameter as a function of top-quark mass  $m_t$  for three different values of  $B(K_L^0 \rightarrow \mu\mu)_{\text{SD}}$ , for  $A = 1$ . The three values of branching fraction are in units of  $10^{-9}$ .

from a Berkeley experiment (Clark *et al.*, 1971) was actually below the unitarity bound. This generated considerable interest at the time. Three subsequent experiments (Carithers *et al.*, 1973; Fukushima *et al.*, 1976; Shochet *et al.*, 1977 and 1979) in the 1970s observed a handful of  $K_L^0 \rightarrow \mu\mu$  events with branching fractions comfortably above the unitarity bound. Recent experiments have accumulated hundreds of events. Table VII lists the  $K_L^0 \rightarrow \mu\mu$  experiments to date.

The two recent experiments that have measured  $K_L^0 \rightarrow \mu\mu$  are BNL E791 and KEK E137 (Akagi *et al.*, 1991b). Both were discussed earlier in the context of  $K_L^0 \rightarrow \mu e$ . The two decays are so similar that detector issues are substantially the same. A spectrometer optimized for a  $K_L^0 \rightarrow \mu e$  search is well suited for  $K_L^0 \rightarrow \mu\mu$ . The backgrounds to  $K_L^0 \rightarrow \mu\mu$  arise from the  $K_L^0 \rightarrow \pi\mu\nu$  ( $K_{\mu 3}$ ) decay in ways that are analogous to the  $K_L^0 \rightarrow \mu e$  backgrounds from  $K_{e 3}$ . For example, if the pion decays in flight in the spectrometer, a  $\mu\mu$  pair will be observed, but will normally reconstruct below the  $K_L^0$  mass. An additional background under the  $K_{e 3}$  process can arise if the pion decays and the electron is misidentified as a muon; since the mass assignment error is on the high side, the event can reconstruct to the  $K_L^0$  mass. Suppression of this background depends on particle identification. Typically, the  $K_L^0 \rightarrow \mu\mu$  signal is large compared to the background, so that the experimental issue is subtracting a small background from under the  $K_L^0 \rightarrow \mu\mu$  mass peak. Figure 47 shows the  $K_L^0 \rightarrow \mu\mu$  signal for KEK E137 and Fig. 48 shows it for BNL E791. The BNL result listed in Table VII represents the preliminary result of combining the full three years' running of E791 and was recently reported (Schwartz, 1992). Final results remain to be published; final partial results from this experiment have been published (Mathiazhagan *et al.*, 1989; Heinson *et al.*, 1991; Kettell *et al.*, 1991; Schwartz, 1991).

The branching fraction in these experiments is normalized to the  $K_L^0 \rightarrow \pi^+ \pi^-$  decay. Large (heavily prescaled) samples of  $K_L^0 \rightarrow \pi^+ \pi^-$  decays were accumulated in both experiments. Owing to the similarity of the two decays,

TABLE VII. Summary of  $K_L^0 \rightarrow \mu\mu$  experiments.

Source	Year	Events	$B$ ( $10^{-9}$ )
Clark <i>et al.</i>	1971	0	< 1.8
Carithers <i>et al.</i>	1973	6	$14^{+13}$
Fukushima <i>et al.</i>	1976	3	$8.8^{+10.7}_{-5.5}$
Shochet <i>et al.</i>	1977	16	$8.1^{+2.8}_{-1.8}$
BNL E780 (Schaffner <i>et al.</i> )	1989	8	
KEK E137 (Akagi <i>et al.</i> )	1991b	179	$7.9 \pm 0.7$
BNL E791 (Preliminary)	1992	708	$6.9 \pm 0.4$
Unitarity bound			$\sim 6.8$

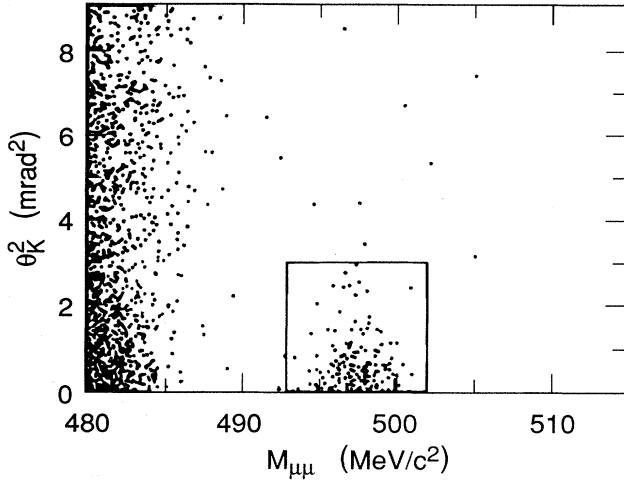


FIG. 47.  $K_L^0 \rightarrow \mu\mu$  events from KEK E137 (after Akagi *et al.*, 1991b).

the detector response and acceptance were very similar for the two decays, and only small corrections for a relative acceptance difference were needed. This was a 16% correction in KEK E137 and a 15% correction in BNL E791. Systematic errors arise from a number of sources, including the uncertainty in the relative acceptance correction, the uncertainty in the subtraction of background under the  $K_L^0 \rightarrow \mu\mu$  peak, the error in counting  $K_L^0 \rightarrow \pi^+\pi^-$  events, the uncertainty in the muon particle identification efficiency, and the uncertainty in the  $K_L^0 \rightarrow \pi^+\pi^-$  branching fraction. In both experiments, systematic errors were reduced to a level below the statistical errors, so that the precision of these experiments was ultimately statistically limited. The branching fraction results of BNL E791 and KEK E137 are consistent within errors.

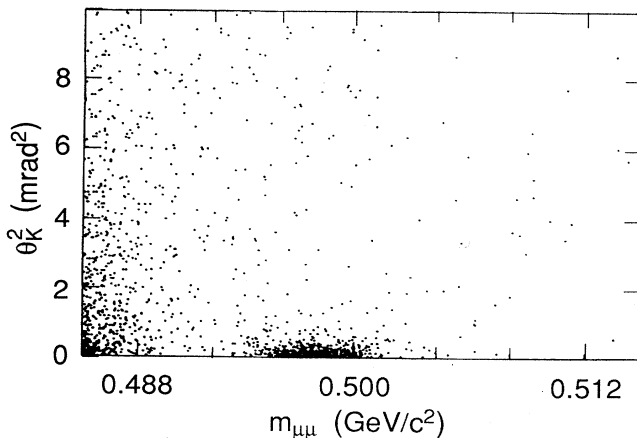


FIG. 48.  $K_L^0 \rightarrow \mu\mu$  events from BNL E791.

### 3. Future prospects

The only currently planned experiment that will measure  $K_L^0 \rightarrow \mu\mu$  is BNL E871, which also plans to search for the  $K_L^0 \rightarrow \mu e$  decay at the  $10^{-12}$  level. The experiment should accumulate a sample of approximately 10 000  $K_L^0 \rightarrow \mu\mu$  events. This will almost certainly shift the situation so that systematic errors dominate the branching-fraction error. The spectrometer improvements planned for E871, as compared to the E791 experiment, will favor improvements in the  $K_L^0 \rightarrow \mu\mu$  systematics, with one significant exception. E871 will rely on the parallelism with respect to the beam direction of two-body decay products downstream of the spectrometer magnets for the trigger. This will tend to increase the difference in the acceptance for  $K_L^0 \rightarrow \mu\mu$  and  $K_L^0 \rightarrow \pi\pi$  decays. It will be difficult to understand all systematic effects at the 1% level. Nonetheless, E871 promises to make a substantial improvement in the precision with which the  $K_L^0 \rightarrow \mu\mu$  branching ratio is measured. It remains to be seen whether theoretical improvements are possible, particularly in the understanding of the long-distance dispersive contribution to this decay, to fully exploit the anticipated improvement in experimental precision.

### C. $K_L^0 \rightarrow ee$

#### 1. Phenomenology

The physics of the decay  $K_L^0 \rightarrow ee$  is the same as that of the decay  $K_L^0 \rightarrow \mu\mu$ , under the assumption of  $\mu e$  universality. Standard Model physics, however, is suppressed in this channel by a factor of order  $O(m_e^2/m_\mu^2)$ , leaving open the possibility that some non-Standard-Model contribution, which would have to be a pseudoscalar interaction to avoid helicity suppression, might be observable above the Standard Model level.

As with the  $K_L^0 \rightarrow \mu\mu$  decay, the  $K_L^0 \rightarrow ee$  amplitude will have an absorptive and dispersive part. The absorptive part will again be dominated by the real two-photon intermediate state. The rate for this process is given by Eq. (4.5) if the electron mass replaces the muon mass in the equation. Therefore it follows that

$$\frac{B(K_L^0 \rightarrow ee)_{2\gamma}}{B(K_L^0 \rightarrow \mu\mu)_{2\gamma}} = \left(\frac{m_e}{m_\mu}\right)^2 \frac{\beta_\mu}{\beta_e} \frac{\left[\ln \frac{1+\beta_e}{1-\beta_e}\right]^2}{\left[\ln \frac{1+\beta_\mu}{1-\beta_\mu}\right]^2}, \quad (4.14)$$

where  $\beta_\mu = \sqrt{1-4m_\mu^2/m_K^2}$  and  $\beta_e = \sqrt{1-4m_e^2/m_K^2}$ . Numerically,  $\beta_\mu$  is about 0.9, but  $\beta_e$  is very close to unity ( $1-\beta_e \approx 2 \times 10^{-6}$ ). Plugging in the  $\beta$ 's and evaluating the logarithms indicates that the ratio in Eq. (4.14) is a factor of 17 higher than it would be if given by  $m_e^2/m_\mu^2$  alone. Physically, this enhancement results because there is a logarithmic singularity as  $m_l \rightarrow 0$  in the total electro-

dynamic cross section for  $\gamma\gamma \rightarrow l^+l^-$ . The unitarity bound for this mode is then given by

$$B(K_L^0 \rightarrow ee)_{2\gamma} \approx 3 \times 10^{-12}. \quad (4.15)$$

The dispersive amplitude does not receive the same enhancement discussed above. For example, the short-distance contribution to  $K_L^0 \rightarrow ee$  is given by Eq. (4.10) if appropriate substitutions of the electron mass for muon mass are made. It follows that

$$\frac{B(K_L^0 \rightarrow ee)_{SD}}{B(K_L^0 \rightarrow \mu\mu)_{SD}} \approx \frac{B(K^+ \rightarrow e\nu)}{B(K^+ \rightarrow \mu\nu)}. \quad (4.16)$$

The short-distance part, then, receives full helicity suppression from the  $m_e^2/m_\mu^2$  factor. That is, the short-distance contribution is more suppressed than the absorptive two-photon contribution. Therefore it is unlikely that the  $K_L^0 \rightarrow ee$  can teach us anything about Standard Model short-distance physics.

A new interaction outside the Standard Model could induce  $K_L^0 \rightarrow ee$  above the expected  $3 \times 10^{-12}$  level. Such an interaction would have to escape the helicity suppression factor, implying a pseudoscalar coupling, and would have to depend on a mechanism that avoids the constraint on strangeness-changing neutral-current interactions from the  $K_L^0$ - $K_S^0$  mass difference discussed earlier in the context of  $K_L^0 \rightarrow \mu e$ . These requirements restrict the possibilities. Nonetheless, until  $K_L^0 \rightarrow ee$  is observed at the Standard Model level, a window for new physics remains open.

## 2. Experimental considerations and status

KEK E137 and BNL E791 have recently set new upper limits on  $K_L^0 \rightarrow ee$ . The KEK experiment (Akagi *et al.*, 1991a) observed one event in its signal box, shown in Fig. 49, and set a 90%-confidence-level upper limit of  $1.6 \times 10^{-10}$ . The candidate event is near the edge of the signal box and does not appear plausible as a genuine  $K_L^0 \rightarrow ee$  event. The BNL E791 experiment has set a preliminary limit of  $4.1 \times 10^{-11}$  on this mode using the full (three-year) data set (Belz, 1992). No events appear inside the E791 signal box, as shown in Fig. 50.

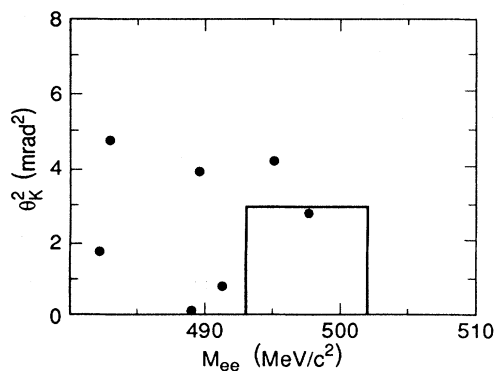


FIG. 49.  $K_L^0 \rightarrow ee$  candidates from KEK E137 (after Akagi *et al.*, 1991b).

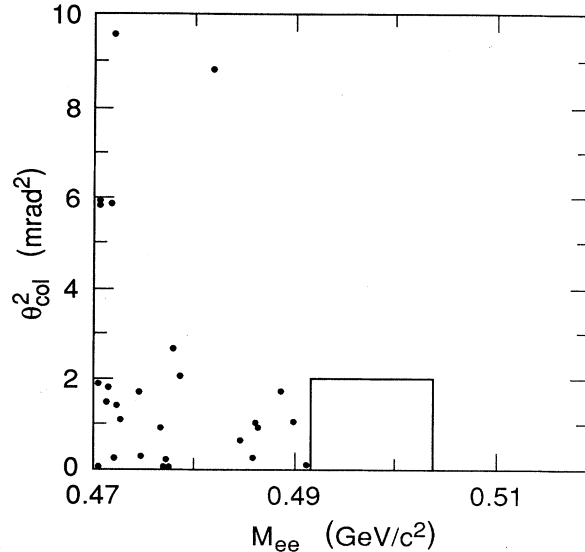


FIG. 50.  $K_L^0 \rightarrow ee$  candidates from BNL E791.

Potential background sources for  $K_L^0 \rightarrow ee$  include the decay modes  $K_L^0 \rightarrow \pi e \nu$ ,  $K_L^0 \rightarrow ee \gamma$ , and  $K_L^0 \rightarrow e^+ e^- e^+ e^-$ , as well as accidentals (i.e., electrons from two different  $K_L^0$  decays). The  $K_L^0 \rightarrow \pi e \nu$  decay, in which the pion is misidentified as an electron, results in a reconstructed mass well below the  $K_L^0$  mass and is not likely to pose a serious problem. Accidentals can be suppressed through good timing and have not been a problem for the current generation of experiments. The decays  $K_L^0 \rightarrow ee \gamma$  and  $K_L^0 \rightarrow e^+ e^- e^+ e^-$  pose a different set of problems (the electrons are both real and from the same decay, so events cannot be rejected via particle identification or timing) and deserve additional attention.

The  $K_L^0 \rightarrow ee \gamma$  branching ratio has recently been measured by BNL E845 (Ohl *et al.*, 1990b) to be  $(9.1 \pm 0.4_{-0.5}^{+0.6}) \times 10^{-6}$  and by CERN NA31 (Barr *et al.*, 1990b) to be  $(9.2 \pm 0.5 \pm 0.5) \times 10^{-6}$ . Both experiments measured the distribution of the  $ee$  invariant mass  $m_{ee}$ , from which the form factor was determined. (See the discussion in Sec. IV.B.1.) However, the data did not extend to values of  $m_{ee}$  above about 400 MeV, so that a significant extrapolation is needed to estimate the effective branching ratio for  $K_L^0 \rightarrow ee \gamma$  decays with  $m_{ee}$  close enough to the  $K_L^0$  mass to fall within the  $K_L^0 \rightarrow ee$  signal region. An extrapolation using the Bergström, Massó, and Singer (1983, 1990) form factor with the parameter  $\alpha_{K^*} = -0.28$ , as favored by both experiments, yields an effective branching ratio for  $K_L^0 \rightarrow ee \gamma$  with  $m_{ee} > 492$  MeV of about  $2 \times 10^{-13}$ . This is significantly below the sensitivity of the BNL E791 or KEK E137 experiments, but is uncertain by at least a factor of 2 or 3 due to the uncertainty in the form factor as  $m_{ee}$  approaches  $M_K$ .

The  $K_L^0 \rightarrow e^+ e^- e^+ e^-$  decay is more complicated to consider. The process can occur via the transition

$K_L^0 \rightarrow \gamma^* \gamma^*$ , where each virtual photon couples to a real  $e^+e^-$  pair. Fully reconstructed  $K_L^0 \rightarrow e^+e^-e^+e^-$  events have been reported by three groups. The mode has been observed in the CERN NA31 experiment [Barr *et al.*, 1991; two events, yielding a branching fraction of  $(4 \pm 3) \times 10^{-8}$ ] and BNL E845 [Vagins *et al.*, 1993; six events, yielding a branching fraction of  $(3.07 \pm 1.25 \pm 0.26) \times 10^{-8}$ ]. More recently, FNAL E799 (performed by the group active in  $CP$  studies at Fermilab with substantially the same apparatus) has reported (Gu, 1992) the observation of 31 events (of which two are estimated to be background). The branching ratio from these events is  $(4.47 \pm 0.85) \times 10^{-8}$ , where the error is statistical only; this result is preliminary, and the analysis of systematic errors is still underway.<sup>3</sup>

The decay  $K_L^0 \rightarrow e^+e^-e^+e^-$  can fake  $K_L^0 \rightarrow ee$  when both  $ee$  pairs are highly asymmetric and opposite-sign members receive most of the energy. If the low-energy electron and positron go unobserved and those with high energy reconstruct to a mass close to the  $K_L^0$  mass, the event can be confused with  $K_L^0 \rightarrow ee$ . It is not simple to estimate the effective branching fraction of this background source. An estimate by the E791 collaboration, using the E791 detector Monte Carlo and relying on the theoretical  $K_L^0 \rightarrow e^+e^-e^+e^-$  branching fraction ( $3.36 \times 10^{-8}$ ) and its matrix element (Miyazaki and Takasugi, 1973), yielded an effective branching fraction of  $11 \times 10^{-12}$  for such events to reconstruct with  $m_{ee} > 492$  MeV. The  $K_L^0 \rightarrow e^+e^-e^+e^-$  decay is very likely the source of the event in the  $K_L^0 \rightarrow ee$  signal box in KEK E137. In fact, the KEK E137 group has analyzed (Akagi *et al.*, 1993) 18  $K_L^0 \rightarrow ee$  candidates with  $m_{ee} > 470$  MeV and interpreted them as coming from the  $K_L^0 \rightarrow e^+e^-e^+e^-$  decay. The branching fraction they infer,  $(6 \pm 2 \pm 1) \times 10^{-8}$ , is consistent with the measurements of CERN NA31, BNL E845, and FNAL E799 cited above.

### 3. Future prospects

A new experiment, E871, is planned at BNL to begin running in 1994. E871 is expected to reach a single-event sensitivity slightly below  $10^{-12}$  for the  $K_L^0 \rightarrow ee$  decay. Since this is below the unitarity bound ( $3 \times 10^{-12}$ ) for this mode, at least a few events should be observed. This would rank as the rarest decay mode ever observed in particle physics. However, it is not *a priori* clear that backgrounds will not obscure the result. The  $K_L^0 \rightarrow e^+e^-e^+e^-$  background appears to be potentially the most troublesome and may appear at a similar or somewhat higher level. The background events will not cluster at the  $K_L^0$  mass, of course, so it may be possible to distinguish signal and background.

<sup>3</sup>See Addendum at end of this article.

## V. DECAYS INTO NEW PARTICLES

### A. Theoretical background

In addition to testing various features of the Standard Model,  $K$  decays offer a potentially fruitful way to look for new particles that might arise naturally in some of the extensions of the Standard Model. These generally fall into two broad categories:

(a) Stable (or long-lived) and noninteracting particles, which would escape detection in the apparatus. Their signature in charged  $K$  decays would be the presence of a charged track unaccompanied by other particles and having unique energy if only one additional particle were emitted.

(b) Unstable and relatively short-lived particles, which could decay into  $\gamma$ 's,  $e$ 's, or  $\mu$ 's. Their presence would then be identified by a mass peak in the appropriate spectra.

In the last several years, a variety of extensions of the Standard Model have been proposed, most of which require the presence of new particles. If these particles are massless or relatively light, then they might be detected in  $K$ -decay processes. The limits on their production in  $e^+e^-$  collisions at the  $Z^0$  mass have made the relevance of some of these models much less likely. However, one can make a case for complementary searches in the  $K$  decays, and thus we enumerate below some of the better known models that might be tested in  $K$  decays:

(a) A light Higgs boson (Higgs, 1964, 1966; Guralnik *et al.*, 1965) in the minimal Standard Model. Depending on its mass, its decay modes and lifetime are predictable (Ellis *et al.*, 1976). This was a very exciting possibility several years ago, but the most recent LEP results (Decamp *et al.*, 1990) appear to have ruled out the possibility that a standard Higgs particle exists with a mass accessible to being observed in  $K$  decays.

(b) A familon particle  $f^0$ , which was postulated (Wilczek, 1982) as a Goldstone boson that arises naturally as a by-product of spontaneous breakdown of family symmetry. It would be expected to be massless. Because the postulated familons couple to divergences of flavor-changing currents, they can be emitted in flavor-changing decays. The expected rate would depend on the energy scale at which the flavor symmetry was spontaneously broken, and branching fractions for  $K^+ \rightarrow \pi^+ f^0$  of about  $10^{-10}$  or higher do not appear *a priori* impossible.

(c) An axion, a very light pseudoscalar Goldstone boson that arises (Weinberg, 1978; Wilczek, 1978) as a consequence of breaking the  $U(1)$  symmetry postulated by Peccei and Quinn (1977a, 1977b) to solve the puzzle of  $P$  and  $T$  conservation in strong interactions. Such a particle might be expected (Goldman and Hoffman, 1978; Frère *et al.*, 1981) to show up in the decay  $K^+ \rightarrow \pi^+ h$ ,  $h$  being the axion, with a branching fraction of about  $10^{-8}$ .

(d) Majorons, Goldstone bosons that arise in theories in which lepton number is spontaneously broken globally (Chikashige *et al.*, 1981). The doublet majoron model,

containing a massless majoron  $J$  and its light partner  $\rho_L$  has been analyzed by Bertolini and Santamaria (1989) and shown to be capable of contributing to the decay  $K^+ \rightarrow \pi^+ + (\text{nothing})$ , at a level comparable to one  $\nu\bar{\nu}$  family. An alternative triplet model of Gelmini and Roncadelli (1989) could give an effect a few times larger.

(e) Supersymmetric particles, postulated within the framework of various supersymmetric theories (Fayet, 1977), that represent a minimal variant on the Standard Model. For example, one would expect such spin- $\frac{1}{2}$  light particles as a photino  $\tilde{\gamma}$ , goldstino  $\tilde{G}$ , or neutral shiggs  $\tilde{H}$ . For sufficiently low masses these particles could provide  $K$ -decay channels like

$$K^+ \rightarrow \pi^+ X^0 X^0, \quad (5.1)$$

where  $X^0$  stands for any of the particles mentioned above. The decay into two photinos has been studied by Gaillard *et al.* (1983) and Ellis and Hagelin (1983), who showed that this channel is suppressed significantly with respect to the  $\pi^+ \nu\bar{\nu}$  mode. On the other hand, it was shown (Ellis and Hagelin, 1983) that decays into  $\tilde{H}$  particles should be comparable to that into a  $\nu\bar{\nu}$  pair of a single flavor.

(f) Heavy neutrinos, which would give rise to mixing among the three neutrino flavors:  $e$ ,  $\mu$ , and  $\tau$ . If the neutrino weak and mass eigenstates are not identical, in analogy with the quark sector, then the two-body  $K$  (and  $\pi$ ) decays could exhibit one or two additional monochromatic peaks in the energy spectra of electrons and/or muons, corresponding to a small admixture of a massive neutrino of a different flavor. Detection of such an additional peak is feasible experimentally only if the mass of the heavy neutrino is in the few-MeV range or higher, so that the corresponding peak in the charged lepton energy spectrum is well separated from the dominant peak corresponding to the light neutrino.

The importance of such searches has been stressed by Shrock (1980), who has also emphasized the significantly enhanced sensitivity to heavy neutrinos in  $\pi_{12}$  and  $K_{12}$  searches due to the fact that the standard mode with a light (or zero) -mass neutrino is greatly suppressed by the helicity arguments coming from the  $V - A$  theory.

For completeness, we should mention two other possibilities that have been discussed in the literature, even though it is highly unlikely that they may contribute to  $K$ -decay channels.

(g) An "invisible" axion, originally suggested by Dine *et al.* (1971), which solves the strong- $CP$  puzzle and whose couplings and mass are suppressed by an inverse power of a large mass. If this mass were taken large enough, the axion would effectively be invisible. Later, this idea was elaborated on by Wise *et al.* (1981), who related it to  $SU(5)$  symmetry breaking.

(h) A hyperphoton, i.e., the quantum of a massive vector field coupled to the hypercharge current. This would be a quantum of a new interaction proposed by Fischbach *et al.* (1986) to explain the results from their reanalysis of the Eötvös experiment and some possible in-

consistencies in  $K^0 - \bar{K}^0$  regeneration experiments at different energies. If the latter connection is relevant and the inconsistencies are real, then according to Lusignoli and Pugliese (1986) such a hyperphoton should be seen in the  $K^+ \rightarrow \pi^+ + (\text{nothing})$  experiments with a branching ratio greater than  $6 \times 10^{-5}$ . Thus it seems to be safely excluded already by the experiment of Asano *et al.* (1981).

An additional interesting possibility (Gaillard *et al.*, 1983) is the decay chain

$$K^+ \rightarrow \pi^+ \pi^0, \quad \pi^0 \rightarrow X^0 X^0, \quad (5.2)$$

which would result in a monoenergetic  $\pi^+$  in the  $K^+$  rest frame but no other visible particles in the detector if  $X^0$  belonged to a category of long-lived, weakly interacting particles.

## B. Experimental results

Several of the rare- $K$ -decay experiments, discussed in more detail in the previous sections, have also reported limits on possible decays into new particles. In this section, we briefly summarize the results relevant to new particle searches.

(a) The in-flight  $K^+$  experiment at BNL (E777), designed originally to search for the decay mode  $K^+ \rightarrow \pi^+ \mu^+ e^-$ , has also studied the process  $K^+ \rightarrow \pi^+ e^+ e^-$ . Simultaneously, the experiment is sensitive to the decay chain

$$K^+ \rightarrow \pi^+ X^0, \quad X^0 \rightarrow e^+ e^-. \quad (5.3)$$

No evidence for such an  $X^0$  particle was seen and a 90%-confidence-level limit of  $1.1 \times 10^{-8}$  ( $1.5 \times 10^{-8}$  for 99% C.L.) was obtained for a product of the two relevant branching fractions over an  $X^0$  mass range 150–340 MeV (Alliegro *et al.*, 1992). The authors point out that this limit, for the mass range of 160–212 MeV ( $2m_\mu$ ), corresponds to less than one-tenth of the predicted rate for the decay into a standard Higgs particle.

(b) The stopped  $K^+$  experiment at BNL (E787), designed to look for

$$K^+ \rightarrow \pi^+ + (\text{nothing}), \quad (5.4)$$

reported several results relevant to new light-particle searches. One search (Atiya *et al.*, 1989b), motivated by the possible existence of a light Higgs particle, addressed the possibility of the decay chain

$$K^+ \rightarrow \pi^+ H, \quad H \rightarrow \mu^+ \mu^-. \quad (5.5)$$

Three events were observed, and they are consistent with the expected decay rate for  $K^+ \rightarrow \pi^+ \mu^+ \mu^-$  without an intermediate state. They can be used to set a 90%-confidence-level limit on the product of the two branching fractions of  $1.5 \times 10^{-7}$  for the mass range  $220 < m_H < 320$  MeV. The explicit dependence of this limit as a function of  $m_H$  is shown in Fig. 51. For this mass range, the  $\mu^+ \mu^-$  channel represents the dominant decay mode for the Higgs particle.

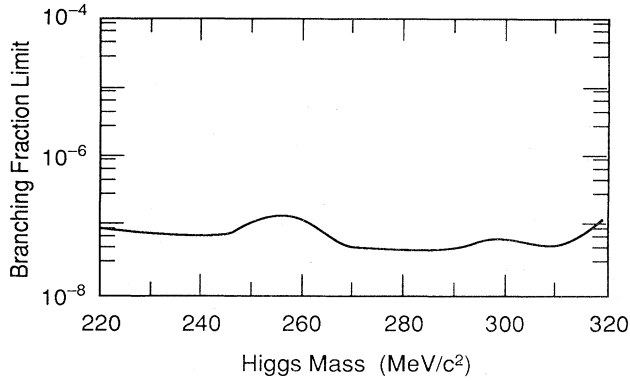


FIG. 51. The 90%-confidence-level upper limits on the branching fraction for the decay  $K^+ \rightarrow \pi^+ H, H \rightarrow \mu^+ \mu^-$  as a function of  $m_H$  (after Atiya *et al.*, 1989b).

(c) The same experiment also took data with a trigger optimized for detection of the mode  $K^+ \rightarrow \pi^+ \gamma \gamma$  (Atiya *et al.*, 1990b). This reaction is relevant to the topic discussed in this section because of a possible decay chain

$$K^+ \rightarrow \pi^+ X^0, X^0 \rightarrow \gamma \gamma, \quad (5.6)$$

which would form a subset of the accepted events. The region of sensitivity lies in the range  $0 < m_{X^0} < 100$  MeV; the upper limit is due to the overwhelming background from the dominant  $K^+ \rightarrow \pi^+ \pi^0$  decay mode. Other, more manageable sources of background are the decay modes  $K^+ \rightarrow \mu^+ \pi^0 \nu$  and  $K^+ \rightarrow \mu^+ \gamma \nu$  with an accidental photon. They were rejected by unambiguous identification of the pion and the kinematical constraints. In addition, possible feed-down from the  $\pi^+ \pi^0$  decay mode due to poor measurements was eliminated by requiring self-consistency of the charged track's range, momentum, and energy measurement.

No events consistent with the  $\pi^+ \gamma \gamma$  final state were found in the defined  $m_{\gamma \gamma}$  mass range (corresponding to  $117 < T_{\pi^+} < 127$  MeV), yielding a 90%-confidence-level limit on  $B(K^+ \rightarrow \pi^+ \gamma \gamma) \leq 1.0 \times 10^{-6}$ . The limit was calculated on the assumption of phase-space distribution for the pion momentum. The data were also used to set upper limits for the decay chain in Eq. (5.6), as a function of  $X^0$  mass and lifetime. These limits are displayed in Fig. 52.

(d) The same collaboration also sets limits on the exclusive process (Atiya *et al.*, 1990a)

$$K^+ \rightarrow \pi^+ X^0, \quad (5.7)$$

where  $X^0$  is a light, weakly interacting particle. The analysis is essentially identical to that for the general decay mode  $K^+ \rightarrow \pi^+ + (\text{nothing})$  (e.g.,  $K^+ \rightarrow \pi^+ \nu \bar{\nu}$ ) and has been described previously. The 90%-confidence-level limit for a zero-mass particle is  $6.4 \times 10^{-9}$ . For other masses, the limits are a function of lifetime, and they can be calculated on the assumption that  $X^0$  decays into

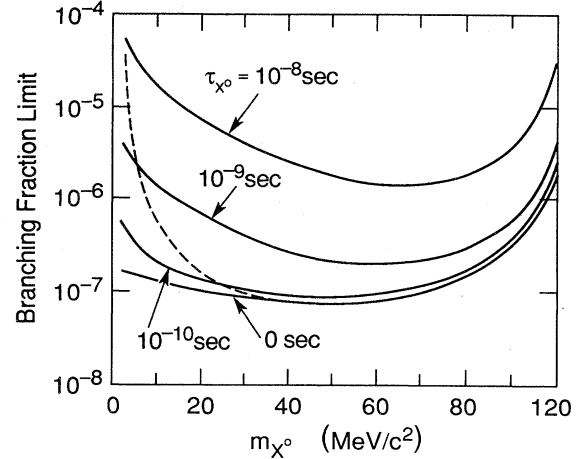


FIG. 52. The 90%-confidence-level upper limits for the branching fraction of  $K^+ \rightarrow \pi^+ X^0, X^0 \rightarrow \gamma \gamma$  for different  $X^0$  lifetimes ( $\tau_{X^0}$ ) as a function of mass ( $m_{X^0}$ ). The dashed curve shows the upper limit for the combined branching ratio for the Higgs-boson decay  $K^+ \rightarrow \pi^+ H^0, H^0 \rightarrow \gamma \gamma$  (after Atiya *et al.*, 1990b).

detectable daughters, e.g.,  $\gamma$ 's or  $e$ 's, which would veto the event. The limits are displayed in Fig. 53.

(e) Finally, the same group also looked for a possible decay of a  $\pi^0$  into weakly interacting neutrals (Atiya *et al.*, 1991). The analysis is similar to that discussed above except that tighter photon cuts are required, since the background from the decay chain

$$K^+ \rightarrow \pi^+ \pi^0, \pi^0 \rightarrow \gamma \gamma \quad (5.8)$$

is now much more severe. After all the cuts, 27 candidate events survive. They correspond to a branching fraction for  $K^+ \rightarrow \pi^+ \pi^0$  with no observed photons of  $6.3 \times 10^{-7}$ . This is consistent with the calculated frac-

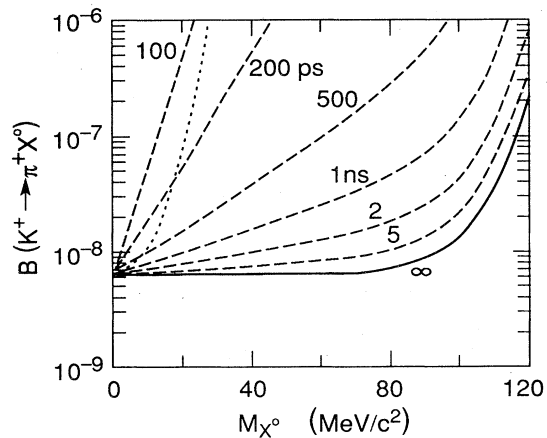


FIG. 53. 90%-confidence-level upper limits: solid curve, limit on the branching fraction for  $K^+ \rightarrow \pi^+ X^0$  as a function of  $M_{X^0}$  on the assumption of infinite  $X^0$  lifetime; dashed curves, limits for cases in which  $X^0$  has a finite lifetime; dotted curve, limit on  $B(K^+ \rightarrow \pi^+ H^0)$  (after Atiya *et al.*, 1990a).

tion of missed  $\pi^0 \rightarrow \gamma\gamma$  events of  $(1.2 \pm 0.3) \times 10^{-6}$ . The quoted error is statistical; systematic uncertainty could be an order of magnitude higher than the calculated rate. The dominant  $\pi^0$  loss mechanism appears to be an asymmetric  $\pi^0$  decay with loss of the low-energy  $\gamma$  due to sampling fluctuations and a photonuclear capture of the higher-energy  $\gamma$  without yielding any detected reaction products. To quote a branching-ratio limit the authors convert the observed 27 events into a 90%-confidence-level limit, on the grounds that they are consistent with background but that the background calculation is too uncertain to allow subtraction. The final number is

$$B(\pi^0 \rightarrow X^0 X^0) < 8.3 \times 10^{-7} \text{ (90\% C.L.)}, \quad (5.9)$$

where  $X^0$  is any weakly interacting neutral light particle.

(f) The  $\epsilon'/\epsilon$  collaboration at CERN has analyzed their data (Barr *et al.*, 1990a) for the possible presence of the decay chain

$$K_L^0 \rightarrow \pi^0 + H^0, \quad H^0 \rightarrow e^+ e^-, \quad (5.10)$$

again being motivated by the possible existence of a light Higgs scalar. The topology is identical to  $K_L^0 \rightarrow \pi^0 e^+ e^-$  and the analysis is quite similar except for the fact that the  $e^+ e^-$  pair is allowed to originate from a different point in space than the  $\pi^0$ , thus allowing a finite  $H^0$  lifetime. The main backgrounds are due to  $K_L^0 \rightarrow \pi^0 \pi^0$  events with a decay of one of the  $\pi^0$ 's via the Dalitz mode  $e^+ e^- \gamma$  and simultaneous loss of the photon or conversion of both  $\gamma$ 's from one  $\pi^0$  in the 0.004 radiation length of material upstream from the first wire chamber. In that situation the  $\gamma$ 's will appear as electrons in the tracking chambers. The calculated number of background events from those two sources are  $0.7 \pm 0.3$  and 2.6, respectively. Three candidate events were seen, consistent with their being due to background. The 90%-confidence-level limits were computed based on those results as a function of the  $H^0$  mass and lifetime, and are displayed in Fig. 54 together with the Standard Model prediction of the Higgs particle lifetime as a function of its mass.

(g) The most recent dedicated search for heavy neutrinos (or any other heavy neutral noninteracting particles) was performed at KEK by Hayano *et al.* (1982), who used a high-resolution magnetic spectrometer to measure the muon momentum spectrum in  $K_{\mu 2}$  decay. NaI counters around the stopping target were used to suppress the continuum background. No distinct peaks were seen, allowing one to set an upper bound on the strength of the mixing between the muon neutrino and a massive neutrino of  $10^{-4}$ – $10^{-6}$  in the mass range of 70–300 MeV/ $c^2$ . Their results are summarized graphically in Fig. 55, which also shows the previously obtained limits from  $\pi_{\mu 2}$  decay (Abela *et al.*, 1981) and from an earlier Bevatron experiment searching for the decay  $K^+ \rightarrow \mu^+ \nu \bar{\nu}$  (Pang *et al.*, 1973).

For completeness, we also present the status of similar information in the electron sector. Even though no dedicated peak-searching experiments have been done in  $K_{e 2}$

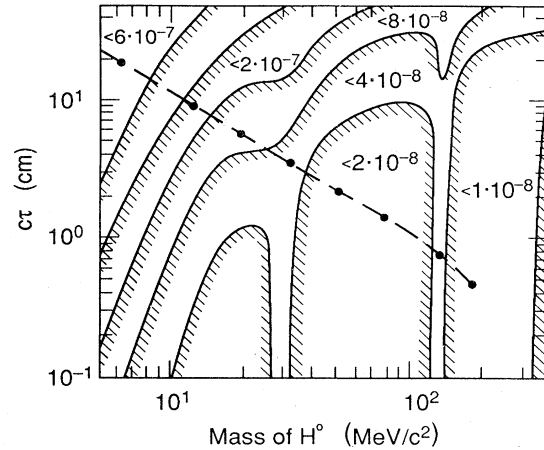


FIG. 54. The 90% confidence limits on the product of the branching fractions  $B(K_L^0 \rightarrow \pi^0 H^0) \times B(H^0 \rightarrow ee)$  as a function of the  $H^0$  mass and lifetime. Contour lines of equal limit, as a function of mean lifetime and  $m_{ee}$  are shown. Also shown (dot-dashed line) are values for the lifetime as a function of mass for the single neutral standard model Higgs (after Barr *et al.*, 1990a).

decay, the data from experiments measuring that branching ratio (Heintze *et al.*, 1976) and from experiments looking for  $K^+ \rightarrow e \nu \gamma$  and  $K^+ \rightarrow e^+ \nu \bar{\nu}$  (Heintze *et al.*, 1979) could be used to set limits on mixing strength for relatively high neutrino masses. Limits at lower neutrino mass values have been set from studies of electron energy spectra from  $\pi_{e 2}$  decay (Berghofer *et al.*, 1982) and from comparison of the measured  $\pi_{e 2}/\pi_{\mu 2}$  branching-fraction ratio with the theoretical prediction (Shrock, 1981). This last ratio would increase dramatically even with a small

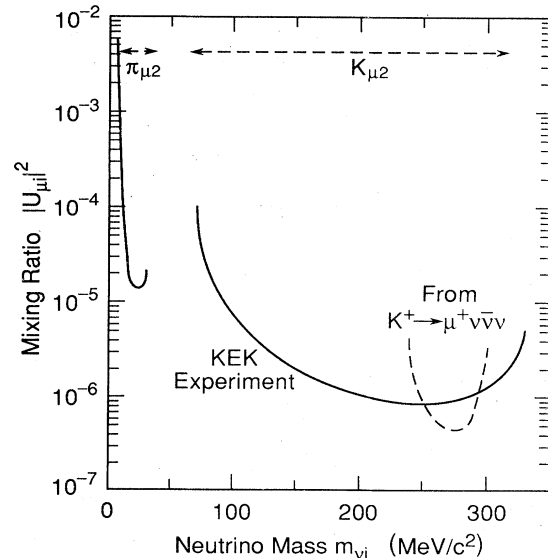


FIG. 55. 90% confidence limits on mixing ratio between  $\nu_\mu$  and heavier neutrinos as a function of heavy neutrino mass (after Hayano *et al.*, 1982).

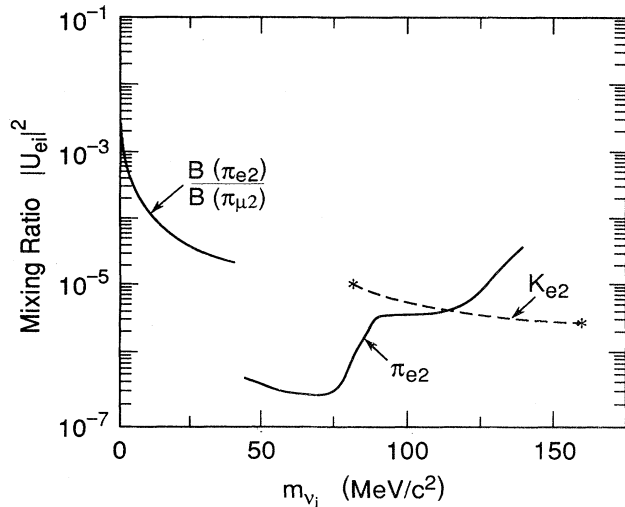


FIG. 56. 90% confidence limits on mixing ratio between  $\nu_e$  and heavier neutrinos as a function of heavy neutrino mass (after Berghofer *et al.*, 1982).

admixture of a heavy neutrino, due to strong suppression of the  $\pi_{e2}$  decay mode with a massless neutrino. Figure 56 shows the compilations of all the relevant results from Berghofer *et al.* (1982).<sup>4</sup>

#### ADDENDUM

Since the completion of this article in October 1992, the first phase of the FNAL E799 experiment has produced several new results. These include a new and somewhat improved upper limit on branching fraction for the decay  $K_L^0 \rightarrow \pi^0 e^+ e^-$  (less than  $4.2 \times 10^{-9}$ ), a considerably improved upper limit on  $K_L^0 \rightarrow \pi^0 \mu^+ \mu^-$  (less than  $5.1 \times 10^{-9}$ ), and a new measurement of the  $K_L^0 \rightarrow e^+ e^- e^+ e^-$  branching fraction,  $(3.29 \pm 0.64 \pm 0.19) \times 10^{-8}$ . These results are unpublished, but have been described in various conference settings (Wah, 1993).

Finally, more recent results on the  $\pi_{e2}$  decay than those discussed in the last section of the article are available (Britton *et al.*, 1992a, 1992b; Czapek *et al.*, 1993). Consequently, Fig. 56 is no longer up to date. For an updated figure and a review of these new experiments, see Bryman (1993).

#### ACKNOWLEDGMENTS

The authors would like to acknowledge our collaborators on BNL experiments 791 and 871. The mutual interactions over the past years and numerous conversations have contributed greatly to our understanding of the field. We should also like to thank many of our colleagues working on other experiments in the field for their willingness to discuss their work and to share information about unpublished results. We owe special

<sup>4</sup>See Addendum, which follows.

thanks to D. Bryman, T. Inagaki, L. Littenberg, Y. Wah, B. Winstein, and M. Zeller. This work was supported in part by DOE Grant No. DE-FG05-85ER40200 and NSF Grant No. PHY 88-18444.

#### REFERENCES

- Abe, F., *et al.* (CDF Collaboration), 1992a, Phys. Rev. Lett. **68**, 447.  
 Abe, F., *et al.* (CDF Collaboration), 1992b, Phys. Rev. D **45**, 3921.  
 Abela, R., M. Daum, G. H. Eaton, R. Frosch, B. Jost, P. R. Kettle, and E. Steiner, 1981, Phys. Lett. B **105**, 263.  
 Acker, A., and S. Pakvasa, 1992, Mod. Phys. Lett. A **7**, 1219.  
 Akagi, T., *et al.*, 1991a, Phys. Rev. Lett. **67**, 2614.  
 Akagi, T., *et al.*, 1991b, Phys. Rev. Lett. **67**, 2618.  
 Akagi, T., *et al.*, 1993, Phys. Rev. D **47**, 2644.  
 Albrecht, H., *et al.*, 1988, Phys. Lett. B **209**, 380.  
 Alexandrou, C., S. Gsken, F. Jegerlehner, K. Schilling, and R. Sommer, 1992, Paul Scherrer Institute Preprint PSI-PR-92-27.  
 Alexandrou, C., F. Jergerlehner, S. Gsken, K. Schilling, and R. Sommer, 1991, Phys. Lett. B **256**, 60.  
 Alliegro, C., *et al.*, 1992, Phys. Rev. Lett. **68**, 278.  
 Allton, C., C. T. Sachrajda, V. Lubicz, L. Maiani, and G. Martinelli, 1991, Nucl. Phys. B **349**, 598.  
 Altarelli, G., 1987, in *Proceedings of International Europhysics Conference on High Energy Physics*, Uppsala, Sweden, edited by O. Botner (European Physical Society, Geneva, Switzerland) Published in Uppsala EPS HEP 1987:1002.  
 Appelquist, T., R. M. Barnett, and K. Lane, 1978, Annu. Rev. Nucl. Part. Sci. **28**, 387.  
 Appelquist, T., D. Karabali, and L. C. R. Wijewardhana, 1986, Phys. Rev. Lett. **57**, 957.  
 Appelquist, T., and L. C. R. Wijewardhana, 1987, Phys. Rev. D **36**, 568.  
 Arisaka, K., *et al.*, 1993, Phys. Rev. Lett. **70**, 1049.  
 Asano, Y., *et al.*, 1981, Phys. Lett. B **107**, 159.  
 Atiya, M. S., *et al.* (presented by Y. Kuno), 1989a, in *Rare Decay Symposium . . . 1988*, Vancouver, Canada, edited by D. Bryman, J. Ng, T. Numau, and J.-M. Poutissou (World Scientific, Singapore), p. 61.  
 Atiya, M. S., *et al.*, 1989b, Phys. Rev. Lett. **63**, 2177.  
 Atiya, M. S., *et al.*, 1990a, Phys. Rev. Lett. **64**, 21.  
 Atiya, M. S., *et al.*, 1990b, Phys. Rev. Lett. **65**, 1188.  
 Atiya, M. S., *et al.*, 1991, Phys. Rev. Lett. **66**, 2189.  
 Atiya, M. S., *et al.*, 1992, Nucl. Instrum. Methods A **321**, 129.  
 Atiya, M. S., *et al.*, 1993a, Phys. Rev. Lett. **70**, 2521.  
 Atiya, M. S., *et al.*, 1993b, Phys. Rev. D **48**, R1.  
 Avery, P., *et al.*, 1989, Phys. Lett. B **223**, 470.  
 Baker, M., and S. L. Glashow, 1962, Nuovo Cimento **25**, 857.  
 Bando, M., T. Kugo, and K. Yamawaki, 1988, Phys. Rep. **164**, 217.  
 Barbieri, R., S. Ferrara, and C. A. Savoy, 1982, Phys. Lett. B **119**, 343.  
 Barger, V., G. F. Giudice, and T. Han, 1989, Phys. Rev. D **40**, 2987.  
 Barger, V., J. L. Hewett, and R. J. N. Phillips, 1990, Phys. Rev. D **41**, 3421.  
 Barger, V., W. F. Long, E. Ma, and A. Pramudita, 1982, Phys. Rev. D **25**, 1860.  
 Barker, A., *et al.*, 1990, Phys. Rev. D **41**, 3546.  
 Barker, T., *et al.*, Fermi National Accelerator Laboratory Pro-

- posal E799.
- Barr, G., 1992, in *Joint International Lepton Photon Symposium at High Energies (15th) and European Physical Society Conference on High Energy Proceedings*, CERN, Geneva, Switzerland, 1991, edited by S. Hegarty, K. Potter, and E. Quercigh (World Scientific, Singapore) Vol. I, p. 179.
- Barr, G. D., *et al.*, 1988, Phys. Lett. B **214**, 303.
- Barr, G. D., *et al.*, 1990a, Phys. Lett. B **235**, 356.
- Barr, G. D., *et al.*, 1990b, Phys. Lett. B **240**, 283.
- Barr, G. D., *et al.*, 1991, Phys. Lett. B **259**, 389.
- Barr, G. D., *et al.*, 1992, Phys. Lett. B **284**, 440.
- Barroso, A., G. C. Branco, and M. C. Bento, 1984, Phys. Lett. B **134**, 123.
- Beall, G., M. Bander, and A. Soni, 1982, Phys. Rev. Lett. **48**, 848.
- Bean, A., *et al.*, 1993, Phys. Rev. Lett. **70**, 138.
- Bélanger, G., and C. Q. Geng, 1991, Phys. Rev. D **43**, 140.
- Bellgardt, U., *et al.*, 1988, Nucl. Phys. B **299**, 1.
- Belz, J., 1992, Ph.D. thesis (Temple University).
- Berghofer, D., *et al.*, 1982, in *Proceedings of the International Conference on Neutrino Physics and Astrophysics: Neutrino 81*, Maui, Hawaii, 1981, edited by R. J. Cence, E. Ma, and A. Roberts (University of Hawaii, Honolulu) Vol. II, p. 67.
- Bergström, L., E. Massó, and P. Singer, 1983, Phys. Lett. B **131**, 229.
- Bergström, L., E. Massó, and P. Singer, 1990, Phys. Lett. B **249**, 141.
- Bergström, L., E. Massó, P. Singer, and D. Wyler, 1984, Phys. Lett. B **134**, 373.
- Bernard, C. W., Y. Shen, and A. Soni, 1992, presented at the *International Symposium on Lattice Field Theory: Lattice '92*, Amsterdam, Netherlands, 15–19 September, 1992, available as Washington University Preprint UW-PT-92-21.
- Bertolini, S., and A. Santamaria, 1989, Nucl. Phys. B **315**, 558.
- Bigi, I. I., and F. Gabbiani, 1991, Nucl. Phys. B **367**, 3.
- Bijnens, J., S. Dawson, and G. Valencia, 1991, Phys. Rev. D **44**, 3555.
- Bolton, R. D., *et al.*, 1988, Phys. Rev. D **38**, 2077.
- Botella, F. J., and C. S. Lim, 1986, Phys. Rev. Lett. **56**, 1651.
- Britton, D. I., *et al.*, 1992a, Phys. Rev. Lett. **68**, 3000.
- Britton, D. I., *et al.*, 1992b, Phys. Rev. D **46**, R885.
- Brown, R. H., U. Camerini, P. Fowler, H. Muirhead, C. Powell, and D. M. Ritson, 1949, Nature **163**, 82.
- Bryman, D. A., 1993, Comments Nucl. Part. Phys. **21**, 101.
- Buchalla, G., A. J. Buras, and M. K. Harlander, 1991, Nucl. Phys. B **349**, 1.
- Buras, A. J., 1981, Phys. Rev. Lett. **46**, 1354.
- Buras, A. J., P. Krawczyk, M. E. Lautenbacher, and C. Salazar, 1990, Nucl. Phys. B **337**, 284.
- Burkhardt, H., *et al.*, 1988, Phys. Lett. B **206**, 169.
- Cabibbo, N., 1963, Phys. Rev. Lett. **10**, 531.
- Cable, G. D., R. H. Hildebrand, C. Y. Pang, and R. Stiening, 1973, Phys. Rev. D **8**, 3807.
- Cahn, R. N., and H. Harari, 1980, Nucl. Phys. B **176**, 135.
- Carithers, W. C., T. Modis, D. R. Nygren, T. P. Pun, E. L. Schwartz, H. Sticker, J. Steinberger, P. Weilhammer, and J. H. Christenson, 1973, Phys. Rev. Lett. **30**, 1336.
- Carithers, W. C., D. R. Nygren, H. A. Gordon, M. L. Ioffredo, K.-W. Lai, and P. Weilhammer, 1973, Phys. Rev. Lett. **31**, 1025.
- Carroll, A., I-H. Chiang, T. F. Kycia, K. K. Li, L. Littenberg, M. Marx, P. O. Mazur, J. P. de Brion, and W. C. Carithers, 1980, Phys. Rev. Lett. **44**, 525.
- Carroll, A. S., *et al.*, 1980, Phys. Rev. Lett. **44**, 525.
- Cheng, H.-Y., 1990, Phys. Rev. D **42**, 72.
- Cheng, T. P., 1967, Phys. Rev. **162**, 1734.
- Cheng, T. P., and L. F. Li, 1977, Phys. Rev. D **16**, 1425.
- Chikashige, Y., R. N. Mohapatra, and R. D. Peccei, 1981, Phys. Lett. B **98**, 265.
- Christenson, J. H., J. W. Cronin, V. L. Fitch, and R. Turley, 1964, Phys. Rev. Lett. **13**, 138.
- Clark, A., T. Elioff, R. C. Field, H. J. Frisch, R. P. Johnson, L. T. Kerth, and A. Wenzel, 1971, Phys. Rev. Lett. **26**, 1667.
- Colić, P., B. Gubernina, D. Tadić, and J. Trampetić, 1983, Nucl. Phys. B **221**, 141.
- Cousins, R., *et al.*, 1984, Brookhaven National Laboratory Proposal E791.
- Cronin, J. W., P. F. Kunz, W. S. Risk, and P. C. Wheeler, 1967, Phys. Rev. Lett. **18**, 25.
- Czapek, G., *et al.*, 1993, Phys. Rev. Lett. **70**, 17.
- Dalitz, R. H., 1954, Phys. Rev. **94**, 1046.
- Decamp, D., *et al.*, 1990, Phys. Lett. B **236**, 233.
- De Rújula, A., H. Georgi, and S. L. Glashow, 1975, Phys. Rev. D **12**, 147.
- Deshpande, N. G., and R. J. Johnson, 1983, Phys. Rev. D **27**, 1193.
- Diamant-Berger, A. M., *et al.*, 1976, Phys. Lett. B **62**, 485.
- Dib, C. O., 1992, Phys. Lett. B **282**, 201.
- Dib, C. O., I. Dunietz, and F. J. Gilman, 1989, Phys. Rev. D **39**, 2639.
- Dib, C. O., I. Dunietz, and F. J. Gilman, 1991, Mod. Phys. Lett. A **6**, 3573.
- Dimopoulos, S., and J. Ellis, 1981, Nucl. Phys. B **182**, 505.
- Dimopoulos, S., S. Raby, and G. L. Kane, 1981, Nucl. Phys. B **182**, 77.
- Dimopoulos, S., and L. Susskind, 1979, Nucl. Phys. B **155**, 237.
- Dine, M., W. Fischler, H. Georgi, S. L. Glashow, and M. Srodnicki, 1971, Phys. Lett. B **104**, 199.
- Donoghue, J. F., E. Golowich, and B. R. Holstein, 1982, Phys. Lett. B **119**, 412.
- Donoghue, J. F., B. R. Holstein, and G. Valencia, 1987, Phys. Rev. D **35**, 2769.
- Ecker, G., and W. Grimus, 1985, Nucl. Phys. B **258**, 328.
- Ecker, G., A. Pich, and E. de Rafael, 1987a, Phys. Lett. B **189**, 363.
- Ecker, G., A. Pich, and E. de Rafael, 1987b, Nucl. Phys. B **291**, 692.
- Ecker, G., A. Pich, and E. de Rafael, 1988, Nucl. Phys. B **303**, 665.
- Ecker, G., A. Pich, and E. de Rafael, 1990, Phys. Lett. B **237**, 481.
- Eichten, E., I. Hinchliffe, K. D. Lane, and C. Quigg, 1986, Phys. Rev. D **34**, 1547.
- Eichten, E., and K. Lane, 1980, Phys. Lett. B **90**, 125.
- Eilam, G., J. L. Hewett, and T. G. Rizzo, 1987, Phys. Lett. B **193**, 533.
- Ellis, J., M. K. Gaillard, and D. V. Nanopoulos, 1976, Nucl. Phys. B **106**, 292.
- Ellis, J., and J. S. Hagelin, 1983, Nucl. Phys. B **217**, 189.
- Ellis, J., J. Hagelin, S. Rudaz, and D.-D. Wu, 1988, Nucl. Phys. B **304**, 205.
- Farhi, E., and L. Susskind, 1981, Phys. Rep. **74**, 277.
- Fayet, P., 1977, Phys. Lett. B **69**, 489.
- Feinberg, G., and S. Weinberg, 1961, Phys. Rev. Lett. **6**, 381.
- Fischbach, E., D. Sudarsky, A. Szafer, C. Talmadge, and S. H. Aronson, 1986, Phys. Rev. Lett. **56**, 3.
- Flynn, J., and L. Randall, 1989a, Nucl. Phys. B **326**, 31.
- Flynn, J., and L. Randall, 1989b, Phys. Lett. B **216**, 221.

- Fowler, W. B., R. P. Shutt, A. M. Thorndike, and W. L. Whittemore, 1954, *Phys. Rev.* **93**, 861.
- Frère, J. M., J. A. M. Vermaseren, and M. B. Gavela, 1981, *Phys. Lett. B* **103**, 129.
- Fukushima, Y., D. A. Jensen, M. N. Kreisler, A. M. Lopez, P. Shah, P. Surko, and J. J. Thaler, 1976, *Phys. Rev. Lett.* **36**, 348.
- Gaillard, M. K., Y.-C. Kao, I-H. Lee, and M. Suzuki, 1983, *Phys. Lett. B* **123**, 241.
- Gaillard, M. K., and B. W. Lee, 1974, *Phys. Rev. D* **10**, 897.
- Gaillard, M. K., B. W. Lee, and R. E. Shrock, 1976, *Phys. Rev. D* **13**, 2674.
- Gasser, J., and H. Leutwyler, 1985, *Nucl. Phys. B* **250**, 465.
- Gell-Mann, M., 1953, *Phys. Rev.* **92**, 833.
- Gell-Mann, M., and A. Pais, 1955, *Phys. Rev.* **97**, 1387.
- Gell-Mann, M., P. Raymond, and R. Slansky, 1979, in *Supergravity*, edited by P. van Nieuwenhuizen and D. Freeman (North-Holland, Amsterdam), p. 315.
- Gelmini, G. B., and M. Roncadelli, 1989, *Phys. Lett. B* **99**, 411.
- Geng, C. Q., and J. N. Ng, 1989, *Phys. Rev. D* **39**, 3330.
- Geng, C. Q., and J. N. Ng, 1990, *Phys. Rev. D* **41**, 2351.
- Geng, C. Q., and P. Turcotte, 1991, "Impacts of a large  $f_B$  on rare kaon decays," Université de Montreal preprint, UdeM-LPN-TH-66.
- Georgi, H., and S. L. Glashow, 1974, *Phys. Rev. Lett.* **32**, 438.
- Gibbons, L. K., *et al.*, 1988, *Phys. Rev. Lett.* **61**, 2661.
- Gibbons, L. K., *et al.*, 1993, *Phys. Rev. Lett.* **70**, 1203.
- Gilman, F. J., and J. S. Hagelin, 1983, *Phys. Lett. B* **126**, 111.
- Gilman, F., and M. B. Wise, 1980, *Phys. Rev. D* **21**, 3150.
- Giudice, G. F., 1987, *Z. Phys. C* **34**, 57.
- Glashow, S. L., J. Iliopoulos, and L. Maiani, 1970, *Phys. Rev. D* **2**, 1285.
- Godfrey, S. 1986, *Phys. Rev. D* **33**, 1391.
- Godfrey, S., and N. Isgur, 1985, *Phys. Rev. D* **32**, 189.
- Goldman, T., and C. M. Hoffman, 1978, *Phys. Rev. Lett.* **40**, 220.
- Good, M. L., 1957, *Phys. Rev.* **106**, 591.
- Good, R. H., R. P. Matsen, F. Muller, O. Piccioni, W. M. Powell, H. S. White, W. B. Fowler, and R. W. Birge, 1961, *Phys. Rev.* **124**, 1223.
- Graham, G. E., *et al.*, 1992, *Phys. Lett. B* **295**, 169.
- Greenberg, O. W., R. N. Mohapatra, and S. Nussinov, 1984, *Phys. Lett. B* **148**, 465.
- Greenlee, H. B., 1990, *Phys. Rev. D* **42**, 3724.
- Gu, P., 1992, in *The Fermilab Meeting, DPF '92*, edited by C. H. Albright, P. H. Kasper, R. Raja, and J. Yoh (World Scientific, River Edge, NJ), p. 809.
- Guralnik, G. S., C. R. Hagen, and T. W. B. Kibble, 1965, *Phys. Rev. Lett.* **13**, 585.
- Hagelin, J. S., and L. S. Littenberg, 1989, *Prog. Part. Nucl. Phys.* **23**, 1.
- Harris, G. R., and J. L. Rosner, 1992, *Phys. Rev. D* **45**, 946.
- Hayano, R. S., *et al.*, 1982, *Phys. Rev. Lett.* **49**, 1305.
- Heinson, A. P., *et al.*, 1991, *Phys. Rev. D* **44**, 1.
- Heintze, J., *et al.*, 1976, *Phys. Lett. B* **60**, 302.
- Heintze, J., *et al.*, 1979, *Nucl. Phys. B* **149**, 365.
- Herczeg, P., 1983, *Phys. Rev. D* **27**, 1512.
- Higgs, P. W., 1964, *Phys. Lett.* **12**, 132.
- Higgs, P. W., 1966, *Phys. Rev.* **145**, 1156.
- Holdom, B., 1984, *Phys. Lett. B* **143**, 227.
- Hou, W. S., and A. Soni, 1985, *Phys. Rev. Lett.* **54**, 2083.
- Hou, W. S., and A. Soni, 1987, *Phys. Rev. D* **35**, 2776.
- Iconomidou-Fayard, L., 1992, in *Proceedings of the XXVI International Conference on High Energy Physics*, AIP Conf. Proc. No. 272, edited by J. R. Sanford (AIP, New York), p. 516.
- Inami, T., and C. S. Lim, 1981, *Prog. Theor. Phys.* **65**, 297.
- Ivanov, A. N., 1992, *Phys. Lett. B* **275**, 450.
- Jastrzembki, E., *et al.*, 1988, *Phys. Rev. Lett.* **61**, 2300.
- Kane, G. L., and R. Thun, 1980, *Phys. Lett. B* **94**, 513.
- Kelly, R. L., *et al.*, 1980, *Rev. Mod. Phys.* **52**, No. 2, Part II, S1.
- Kernan, A., and G. VanDalen, 1984, *Phys. Rep.* **106**, 297.
- Kibble, T. W. B., 1967, *Phys. Rev.* **155**, 1554.
- Kilcup, G. W., S. R. Sharpe, R. Gupta, and A. Patel, 1990, *Phys. Rev. Lett.* **64**, 25.
- Kim, C. S., J. L. Rosner, and C.-P. Yuan, 1990, *Phys. Rev. D* **42**, 96.
- Kim, P. C., 1989, in *Proceedings of the Tau-Charm Factory Workshop*, Stanford, California, edited by Lydia V. Beers, Stanford Linear Accelerator Center report SLAC-343, p. 671.
- King, S. F., 1987, *Phys. Lett. B* **195**, 66.
- King, S. F., 1989, *Nucl. Phys. B* **320**, 487.
- King, S. F., and D. A. Ross, 1989, *Phys. Lett. B* **228**, 363.
- Klems, J. H., R. H. Hildebrand, and R. Stiening, 1970, *Phys. Rev. Lett.* **24**, 1086.
- Klems, J. H., R. H. Hildebrand, and R. Stiening, 1971, *Phys. Rev. D* **4**, 66.
- Kleinknecht, K., 1976, *Annu. Rev. Nucl. Part. Sci.* **26**, 1.
- Ko, P., 1990, *Phys. Rev. D* **41**, 1531.
- Ko, P., 1991, *Phys. Rev. D* **44**, 139.
- Ko, P., 1992, *Phys. Rev. D* **45**, 174.
- Ko, P., and J. L. Rosner, 1989, *Phys. Rev. D* **40**, 3775.
- Ko, P., and T. N. Truong, 1991, *Phys. Rev. D* **44**, 1616.
- Kobayashi, M., and T. Maskawa, 1973, *Prog. Theor. Phys.* **49**, 652.
- Kroll, N. M., and W. Wada, 1955, *Phys. Rev.* **98**, 1355.
- KTeV Design Report, 1992, "Physics at the Main Injector," Fermilab FN-580, January, 1992.
- Lande, K., E. T. Booth, J. Impeduglia, L. M. Lederman, and W. Chinowsky, 1956, *Phys. Rev.* **103**, 1901.
- Langacker, P., 1992, in *Research Directions for the Decade, Snoumass, 1990*, edited by E. L. Berger (World Scientific, Singapore), p. 270.
- Langacker, P., S. U. Sankar, and K. Schilcher, 1988, *Phys. Rev. D* **38**, 2841.
- Lee, A. M., *et al.*, 1990, *Phys. Rev. Lett.* **64**, 165.
- Lee, B. W., and R. E. Shrock, 1977, *Phys. Rev. D* **16**, 1444.
- Lee, T. D., and C. N. Yang, 1955, *Phys. Rev.* **98**, 1501.
- Lee, T. D., and C. N. Yang, 1956, *Phys. Rev.* **104**, 254.
- LEP Collaborations: ALEPH, DELPHI, L3 and OPAL, 1992, *Phys. Lett. B* **276**, 247.
- Littenberg, L. S., 1989, *Phys. Rev. D* **39**, 3322.
- Littenberg, L. S., 1992, private communication.
- Littenberg, L. S., and R. E. Shrock, 1992, *Phys. Rev. Lett.* **68**, 443.
- Lusignoli, M., and A. Pugliese, 1986, *Phys. Lett. B* **171**, 468.
- Ma, E., and A. Pramudita, 1981, *Phys. Rev. D* **24**, 2476.
- Mainland, G. B., and K. Tanaka, 1979, *Phys. Rev. D* **20**, 1241.
- Marciano, W. J., and Z. Parsa, 1986, *Annu. Rev. Nucl. Part. Sci.* **36**, 171.
- Martin, B. R., E. de Rafael, and J. Smith, 1970, *Phys. Rev. D* **2**, 179.
- Mathiazhagan, C., *et al.*, 1989, *Phys. Rev. Lett.* **63**, 2185.
- McWilliams, B., and L. F. Li, 1981, *Nucl. Phys. B* **179**, 62.
- Melese, P. L., 1989, *Comments Nucl. Part. Phys. A* **19**, 117.
- Miyake, N., *et al.*, 1988, KEK Proposal E799, August 1988.
- Miyazaki, T., and E. Takasugi, 1973, *Phys. Rev. D* **8**, 2051.
- Mohapatra, R. N., and J. C. Pati, 1975, *Phys. Rev. D* **11**, 566.

- Morozumi, T., and H. Iwasaki, 1989, *Prog. Theor. Phys.* **82**, 371.
- Morse, W. M., *et al.*, 1992, *Phys. Rev. D* **45**, 36.
- Mukhopadhyaya, B., and A. Raychaudhuri, 1990, *Phys. Rev. D* **42**, 3215.
- Nishijima, K., 1957, *Phys. Rev.* **108**, 907.
- Novikov, V. A., M. A. Shifman, A. I. Vainshtein, and V. I. Zakharov, 1977, *Phys. Rev. D* **16**, 223.
- Ohl, K. E., *et al.*, 1990a, *Phys. Rev. Lett.* **64**, 2755.
- Ohl, K. E., *et al.*, 1990b, *Phys. Rev. Lett.* **65**, 1407.
- Pais, A., 1952, *Phys. Rev.* **86**, 663.
- Pais, A., and O. Piccioni, 1955, *Phys. Rev.* **100**, 1487.
- Pais, A., and S. B. Treiman, 1968, *Phys. Rev.* **176**, 1974.
- Pang, C. Y., R. H. Hildebrand, G. D. Cable, and R. Stiening, 1973, *Phys. Rev. D* **8**, 1989.
- Papadimitriou, V., *et al.*, 1991, *Phys. Rev. D* **44**, R573.
- Particle Data Group, 1992, *Phys. Rev. D* **45**, Part II, I.1.
- Pati, J. C., 1984, *Phys. Rev. D* **30**, 1144.
- Pati, J. C., and A. Salam, 1974, *Phys. Rev. D* **10**, 275.
- Pati, J. C., and H. Stremnitzer, 1986, *Phys. Lett. B* **172**, 441.
- Patterson, J. R., *et al.*, 1990, *Phys. Rev. Lett.* **64**, 1491.
- Peccei, R. D., and H. R. Quinn, 1977a, *Phys. Rev. Lett.* **38**, 1440.
- Peccei, R. D., and H. R. Quinn, 1977b, *Phys. Rev. D* **16**, 1791.
- Pirogov, Y. F., 1983, *Sov. J. Nucl. Phys.* **38**, 921.
- Rein, D., and L. M. Sehgal, 1989, *Phys. Rev. D* **39**, 3325.
- Reinders, L. J., 1988, *Phys. Rev. D* **38**, 947.
- Sakurai, J. J., 1964, *Invariance Principles and Elementary Particles* (Princeton University, Princeton, NJ), p. 177.
- Salam, A., and J. Strathdee, 1974, *Nucl. Phys. B* **80**, 499.
- Schaffner, S. F., *et al.*, 1989, *Phys. Rev. D* **39**, 990.
- Schwartz, A., 1991, in *Fourth Conference on the Intersections between Particle and Nuclear Physics*, Tucson, Arizona, AIP Conf. Proc. No. 243, edited by Willem T. H. Van Oers (AIP, New York), p. 609.
- Schwartz, A. J., 1992, in *The Fermilab Meeting DPF '92*, edited by C. H. Albright, P. H. Kasper, R. Raja, and J. Yoh (World Scientific, River Edge, NJ), p. 816.
- Sehgal, L. M., 1969a, *Phys. Rev.* **181**, 2151.
- Sehgal, L. M., 1969b, *Phys. Rev.* **183**, 1511.
- Sehgal, L. M., 1972, *Phys. Rev. D* **6**, 367.
- Sehgal, L. M., 1988, *Phys. Rev. D* **38**, 808.
- Sehgal, L. M., 1990, *Phys. Rev. D* **41**, 161.
- Senjanovic, G., and R. N. Mohapatra, 1975, *Phys. Rev. D* **12**, 1502.
- Shanker, O., 1981, *Nucl. Phys. B* **185**, 382.
- Shochet, M. J., P. Linsay, C. Grosso-Pilcher, H. J. Frisch, R. DeVoe, J. W. Cronin, and D. R. Moffett, 1977, *Phys. Rev. Lett.* **39**, 59.
- Shochet, M. J., P. Linsay, C. Grosso-Pilcher, H. J. Frisch, R. DeVoe, J. W. Cronin, and D. R. Moffett, 1979, *Phys. Rev. D* **19**, 1965.
- Shrock, R. E., 1980, *Phys. Lett. B* **96**, 159.
- Shrock, R. E., 1981, *Phys. Rev. D* **24**, 1232.
- Shrock, R. E., and S. B. Treiman, 1979, *Phys. Rev. D* **19**, 2148.
- Shrock, R. E., and M. B. Voloshin, 1979, *Phys. Lett. B* **87**, 375.
- Smith, J., and Z. E. S. Uy, 1973, *Phys. Rev. D* **7**, 2738.
- Susskind, L., 1979, *Phys. Rev. D* **20**, 2619.
- Swallow, E., 1992, in *The Vancouver Meeting: Particles and Fields '91: Proceedings, . . .*, Vancouver, Canada, edited by D. Axen, D. Bryman, and M. Comyn (World Scientific, River Edge, NJ).
- Tschirhart, R. S., 1992, in *The Fermilab Meeting DPF '92*, edited by C. H. Albright, P. H. Kasper, R. Raja, and J. Yoh (World Scientific, River Edge, NJ), p. 813.
- Türke, U., 1986, *Phys. Lett. B* **168**, 296.
- Vagins, M. R., *et al.*, 1993, *Phys. Rev. Lett.* **71**, 35.
- Vysotskii, M. I., 1980, *Sov. J. Nucl. Phys.* **31**, 797.
- Wah, Y., 1993, private communication.
- Weinberg, S., 1976, *Phys. Rev. D* **13**, 974.
- Weinberg, S., 1978, *Phys. Rev. Lett.* **40**, 223.
- Weinberg, S., 1979a, *Phys. Rev. Lett.* **43**, 1566.
- Weinberg, S., 1979b, *Phys. Rev. D* **19**, 1277.
- Weinberg, S., 1979c, *Physica A* **96**, 327.
- Weyl, H., 1950, *The Theory of Groups and Quantum Mechanics* (Dover, New York), p. 100.
- Wess, J., and B. Zumino, 1974, *Nucl. Phys. B* **7**, 39.
- Wheeler, P. C., 1968, Ph.D. thesis (Princeton University).
- Wilczek, F., 1978, *Phys. Rev. Lett.* **40**, 279.
- Wilczek, F., 1982, *Phys. Rev. Lett.* **49**, 1549.
- Wise, M. B., H. Georgi, and S. Glashow, 1981, *Phys. Rev. Lett.* **47**, 402.
- Wolfenstein, L., 1964, *Phys. Rev. Lett.* **13**, 562.
- Wolfenstein, L., 1983, *Phys. Rev. Lett.* **51**, 1945.